UNIVERSIDADE DE LISBOA

FACULDADE DE MEDICINA DE LISBOA

What is the role of the cell adhesion protein N-cadherin in the molecular and morphological asymmetries of the Hensen's node

Raquel Valente Mendes

Supervisor | Leonor Saúde, PhD

Doutoramento em Ciências Biomédicas

Especialidade | Ciências Morfológicas

A impressão desta dissertação foi aprovada pelo Conselho Cientifico da Faculdade de Medicina de Lisboa em reunião de (*22 de Julho de 2014*).

TABLE OF CONTENTS

AGRADECIMENTOS		i
ABSTRACT		iii
RESUMO		vi
ABBREVIATIONS		ix
INDEX OF FIGURES		xi
INDEX OF TABLES		xiv
INDEX OF MOVIE LEGENDS		xv

CHAPTER I GENERAL INTRODUCTION

I.1	LEFT-RIGHT ASYMMETRY IN VERTEBRATES	2
I.2	STEPS IN LEFT-RIGHT ASYMMETRY ESTABLISHMENT	5
I.3	BREAKING THE INITIAL SYMMETRY	7
I.3.1	The conceptual F-molecule model	7
I.3.2	Different mechanisms to break symmetry	8
I.3.2.1	Motile cilia in the node	8
I.3.2.1.1	Directional Nodal Flow	10
I.3.2.1.2	Two Models for generating Left-Right asymmetric gene expression by Nodal Flow	11
I.3.2.2	Other players in Left-Right patterning prior to the formation of cilia	13
I.3.2.2.1	Gap junction communication (GJC)	16
I.3.2.2.2	Ion Flux	17
I.3.2.2.3	Motor Proteins/Cytoskeleton	19
I.3.2.2.4	Serotonin (5HT)	20
I.3.2.3	Putting it all together - Intracellular Model	22
I.3.2.4	Planar cell polarity (PCP)	25
I.4	CHICKEN EMBRYO AS A MODEL SYSTEM	27
I.4.1	Early development of the chick	28
I.4.1.1	Cleavage	28
I.4.1.2	Gastrulation	30
I.4.1.2.1	Primitive Streak formation	30

I.4.1.2.2	Hensen's node	33
I.4.1.2.3	Primitive streak and Hensen's node regression	35
I.4.2	Hensen's node, a Left-Right inducer	37
I.4.2.1	Left side gene expression in the node	40
I.4.2.2	Right side gene expression in the node	42
I.4.3	Left-Right asymmetry, downstream of the Node	43
I.4.3.1	Nodal in the left Lateral Plate Mesoderm and asymmetric gene expression	45
I.4.3.2	Right Lateral Plate Mesoderm and asymmetric gene expression	46
I.4.4	Stabilization of side-specific gene expression – – Midline Barrier Model	47
I.5	LATE STEPS: ASYMMETRIC ORGAN MORPHOGENESIS	51
I.6	EVOLUTIONARY CONSERVATION	55
I.7	CADHERINS	57
I.7.1	Cadherins are involved in multiple Biological Processes	60
I.7.2	Structural and functional organization of the cytoplasmic domain	61
I.7.3	Interactions with the Actin Cytoskeleton	64
I.8	CADHERIN EXPRESSION AND FUNCTION IN DEVELOPMENT	65
I.8.1	Cadherins and morphogenetic movements	65
I.8.1.1	Convergent and Extension movements	65
I.8.1.2	Border Cell Migration	66
I.8.2	Classical cadherins in cell sorting	67
I.9	N-CADHERIN	70
I.9.1	N-cadherin in development	71
I.9.1.1	N-cadherin and Left-Right asymmetries	74
I.9.1.2	N-cadherin and collective cell migration	75
I.9.2	N-cadherin and cancer	77
I.10	AIMS AND SCOPES OF THIS THESIS	80

CHAPTER II MATERIAL AND METHODS

II.1 PREPARATION AND TRANSFORMATION OF COMPETENT *E. COLI* BACTERIA 86

II.2 ANTI-SENSE RNA PROBE SYNTHESIS 88

II.3 OLIGONUCLEOTIDES 90

II.4 POLYMERASE CHAIN REACTION (PCR) 90

II.5 DNA CONSTRUCTS 91

II.6 EMBRYOLOGICAL METHODS 93

II.7 DRUG TREATMENT 93

II.8 BEAD IMPLANTATION 93

II.9 *IN VITRO* CHICK EMBRYO ELECTROPORATION IN NEW CULTURE 95

II.10 CELL LABELLING IN THE HENSEN'S NODE WITH THE LIPOPHILIC DYES DII AND DIO 95

II.11 WHOLE-MOUNT *IN SITU* HYBRIDIZATION 96

II.12 TISSUE EMBEDDING AND PREPARATION OF CRYOSTAT SECTIONS 96

II.13 IMUNOFLUORESCENCE 98

II.14 FLUORESCENCE IMAGING 98

II.15 LIVE IMAGING 98

II.16 STATISTICAL ANALYSIS 99

CHAPTER III N-CADHERIN LOCKS LEFT-RIGHT ASYMMETRY BY ENDING THE LEFTWARD MOVEMENT OF HENSEN'S NODE CELLS

ABSTRACT 102

INTRODUCTION 103

III.1 RESULTS 104

III.1.1 N-cadherin asymmetric expression in Hensen's node is generated by the leftward cell movements downstream of the H^+/K^+-ATPase pump 105

III.1.2 N-cadherin asymmetric activity halts the leftward cell movements in Hensen's node 106
III.1.3 Blocking N-cadherin activity perturbs Left-Right asymmetry establishment 110
III.1.4 Inhibition of Fgf signalling on the left side of the node, rescues normal gene expression in the left Lateral Plate Mesoderm 114
III.1.5 Overexpression of N-cadherin on the right side of the node does not affect Left-Right gene expression in the node and Lateral Plate Mesoderm 116
III.2 DISCUSSION 118

SUPPLEMENTARY DATA
SI.I MNCD2 recognizes chicken N-cadherin and weakly blocks cell-cell adhesion 124
SI.2 N-cadherin asymmetric activity halts the leftward cell movements in Hensen's node 128
SI.3 Blocking N-cadherin activity perturbs Left-Right asymmetry establishment 129

CHAPTER IV N-CADHERIN PRESERVES THE ASYMMETRIC MORPHOLOGY OF THE NODE AND ITS LEFT-RIGHT CELL IDENTITY
ABSTRACT 136
INTRODUCTION 137
IV.1 RESULTS 139
IV.1.1 N-cadherin preserves the asymmetric morphology of the Hensen's node 139
IV.1.2 Asymmetric number of cells between both sides of Hensen's node underlies its morphological asymmetry 140
IV.1.3 N-cadherin prevents cell mixing in the Hensen's 145
IV.2 DISCUSSION 149
IV.2.1 Asymmetric morphology of the Hensen's node is attributed to differences in cell numbers 149

IV.2.2 N-cadherin prevents cell mixing in the Hensen's node during gastrulation 151

CHAPTER V NOTCH TARGET GENE – c*HES6-1*, A NOVEL PLAYER IN LEFT-RIGHT ASYMMETRY

ABSTRACT 156

INTRODUCTION 157

V.1 RESULTS 164

V.1.1 c*Hes6-1* asymmetric expression is downstream of the H^+/K^+ATPase pump 164

V.1.2 c*Hes6-1* asymmetric expression requires Nodal signalling 165

V.1.3 c*Hes6-1* asymmetric expression seems to be conserved between chicken and mouse but not in quail embryos 167

V.2 DISCUSSION 170

V.2.1 Asymmetric expression of c*Hes6-1* is H^+/K^+-ATPase pump dependent 170

V.2.2 Nodal signalling activates c*Hes6-1* on the left mesoderm lateral to the primitive streak 171

V.2.3 c*Hes6-1* asymmetric expression seems to be conserved between chicken and mouse but not in quail embryos 172

V.2.4 A fate map of the c*Hes6-1*-expressing region is needed 173

CHAPTER VI CONCLUSIONS AND FUTURE DIRECTIONS

CONCLUSIONS 178

FUTURE WORK 182

VI.1 What directs cell movements towards the left side of the node during stage HH4? 186

VI.2 What is inhibiting *fgf8* expression in the rostral region of the node? 185

VI.3 Find out what causes the asymmetric morphology of the node 185

VI.4 Investigate the functional relevance of asymmetric levels of N-cadherin in the node 186

VI.5 Is the activation of c*Hes6-1* expression by Nodal dependent on the Notch signalling pathway? 187
VI.6 Fate mapping c*Hes6-1*-expressing region 188

References 192

AGRADECIMENTOS

Gostaria de agradecer a todas as pessoas que, directa ou indirectamente me permitiram chegar até aqui, que aumentaram os meus conhecimentos e me aperfeiçoaram.

Em primeiro lugar gostaria de agradecer à Leonor, a minha orientadora, por me ter guiado durante todo este percurso, por todo o apoio, ensinamentos e porque sempre acreditou e depositou confiança no meu trabalho. MUITO OBRIGADA LEONOR!

A todas as pessoas que fizeram e fazem parte do nosso grupo (SD, UDEV e L. Saúde lab.), que permitiram que o ambiente fosse sempre descontraído, animado e estimulante.

Obrigada Rita Fior pelos teus conselhos, as tuas ideias, a tua energia e a tua boa disposição (mesmo quando havia ABBA a acompanhar...). Obrigada Susaninha, por seres uma Amiga, vou ter saudades tuas! Obrigada às minhas colegas de doutoramento, Sofia Azevedo, Rita Pinto e Sara Fernandes. Sara, obrigada pela companhia da noite e pelos lanchinhos partilhados.

Ana Ribeiro, obrigada por seres tão simples e boa colega de trabalho. Obrigada Ana Margarida, por me teres ajudado na etapa final do meu trabalho. Obrigada às duas pelos cafézinhos depois de almoço e pelas conversas que ajudaram tanto a descontrair.

Raquel Lourenço, obrigada por me teres ensinado e partilhado os teus conhecimentos de galinha. Obrigada também à Susana Lopes.

Joaninha, obrigada pela tua amizade e pelos momentos de distracção.

João Pereira, mesmo que por pouco tempo que tenhas estado no nosso grupo, obrigada.

Muito obrigada Gabriel, por me teres ensinado tudo o que sei em BioImaging e por toda a ajuda que me prestaste desde o início do meu estágio até agora.
Flipe V. Boas, obrigada pelas discussões sobre o Hes.
Agradeço também ao Joaquin, por me ter ensinado a pôr as "beads", pela troca de ideias e por ser tão prestável.

Agradeço também ao meu comité de tese, Ana Tavares, Domingos Henrique e António Jacinto, pelas reuniões e discussões construtivas.

Obrigada à equipa do BioImaging, José Rino, António Temudo e Ana Nascimento, pela ajuda sempre presente e por serem tão profissionais.

Obrigada às minhas amigas, Joana Tato e Andreia Pinto pelos lanches, almoços de Natal, amigos secretos e conversas que nos ajudaram a esquecer os momentos difíceis.

Finalmente, um OBRIGADA aos meus pais e à minha mana, por todo o encorajamento e por se terem sempre preocupado.

E ao Pedro, OBRIGADA! Por seres o meu companheiro em tudo, no meu trabalho e na minha vida. Por teres estado sempre lá! Por me teres SEMPRE incentivado, apoiado, ajudado e por me teres acompanhado nesta luta (de noite e de dia).

ABSTRACT

In contrast to the symmetric appearance from the outside, the vertebrate body is asymmetric on the inside, if we consider the distribution of the internal organs. Problems in the correct establishment of the internal organs may give rise to several human developmental disorders. Therefore, it is imperative to understand how left-right (LR) asymmetry is initiated and moreover, how it is maintained. One of the symmetry breaking mechanisms in vertebrates is the leftward fluid flow generated by cilia in the embryonic node. However, the chicken embryo is an exception, since the establishment of asymmetry occurs much earlier than the appearance of cilia. Indeed, the asymmetric expression of *shh* and *fgf8* is established by a leftward cell movement around the Hensen's node at stage HH4. It was also uncovered that the activity of the H^+/K^+ATPase pump is upstream of this leftward cell movement. In the chicken embryo, one of the earliest molecules asymmetrically expressed in the node is the cell adhesion N-cadherin. Both, mRNA and protein show a preferential localization on its right side. It has been shown that inhibition of N-cadherin function at early stages leads to a LR mispositioning of the chicken heart, suggesting that N-cadherin plays a role in LR patterning.

The main objective of this thesis was to uncover what is the role of N-cadherin in the establishment/maintenance of the molecular and morphological asymmetries of Hensen's node. I show that asymmetric N-cadherin is under the control of both, the H^+/K^+ATPase activity and the leftward cell movements. I also show that when N-cadherin's function is blocked, the node cells on the right side instead of stopping the leftward

movements at stage HH4 persist to be displaced to the left side until late stage HH6. This continuous leftward cell displacement altered the asymmetric expression of *fgf8* and *nodal* in the node, becoming symmetric and severely reduced, respectively. Consequently, an incorrect expression of *cer1* and *snai1* is translated to the left lateral plate mesoderm (LPM). On the basis of these results, the information that is given by the LPM for the heart formation is distorted, resulting in a range of abnormal heart looping phenotypes. Conversely, the inhibition of Fgf signalling on the left side of the node rescued the normal expression of *cer1* and *snai1* in the LPM and the correct looping of the heart. This work shows that N-cadherin's asymmetric localization in the chicken's node is crucial to terminate the leftward cell movements, and therefore, it is an essential step in the establishment of LR asymmetry.

I also evaluated the role of N-cadherin in the maintenance of the node's morphological asymmetry. Blocking N-cadherin's function compromised the asymmetric morphology of the node, not through cell shape changes but by changing the difference in the number of cells between both sides of the node. In addition, I propose that different levels of N-cadherin between the right and the left side of the node are important to avoid cell mixing in the node region. As a consequence, cells on the left and on the right side of the node are kept unmixed so they can preserve their molecular identity.

Finally, I also demonstrate that in the chicken embryo the novel asymmetrically expressed gene c*Hes6-1* is downstream of the ion exchanger H^+/K^+-ATPase and the Nodal signalling pathway. Unexpectedly, the asymmetric localization of c*Hes6-1* in the mesoderm lateral to the primitive streak is not shared with the quail. Instead, this asymmetric

expression is shared with the mouse m*Hes6*. Overall, these results reveal a new possible player in the LR asymmetry cascade. However, what is the functional relevance of this asymmetric expression in the mesoderm lateral to the primitive streak, and moreover to which asymmetric structure(s) will this particular territory give rise to, is still an unanswered question.

KEYWORDS: left-right asymmetry, Hensen's node, leftward cell movement, N-cadherin, cell-sorting, Notch signalling, Hes6-1, cell fate.

RESUMO

Embora externamente os vertebrados se apresentem como organismos simétricos, o seu interior é assimétrico, tendo em conta a distribuição dos órgãos internos. O incorrecto estabelecimento da assimetria dos órgãos internos pode originar vários distúrbios no desenvolvimento humano. Como tal, é necessário não só compreender como é que a assimetria esquerda-direita (ED) é estabelecida, mas também como é mantida. Um dos mecanismos de quebra de simetria conhecido nos vertebrados é feito por cílios que geram um fluído para o lado esquerdo no nó embrionário. No entanto, o embrião de galinha é uma excepção, uma vez que o estabelecimento da assimetria ocorre muito antes do aparecimento de cílios. Na galinha, a expressão assimétrica de *shh* e *fgf8* é estabelecida por um movimento de células que ocorre para o lado esquerdo no nó de Hensen durante o estadio HH4. Sabe-se ainda, que a actividade da bomba H^+/K^+-ATPase está a juzante destes movimentos celulares. No embrião de galinha, uma das primeiras moléculas expressas assimetricamente no nó é a molécula de adesão celular N-caderina. Tanto o seu mRNA como proteína, estão localizados preferencialmente no lado direito do nó. Demonstrou-se que a inibição da N-caderina no início do desenvolvimento da galinha promove a incorrecta localização do coração, sugerindo que a N-caderina desempenha um papel na padronização da assimetria ED.

O principal objectivo desta tese foi descobrir qual o papel da N-caderina na criação/manutenção das assimetrias moleculares e morfológicas do nó de Hensen. É aqui demonstrado, que a localização assimétrica da N-caderina não só está sob o controlo da actividade da bomba protónica - H^+/K^+-

ATPase, como também depende dos movimentos celulares. Aquando a inibição da função da proteína de adesão N-caderina, verificou-se que as células do lado direito do nó em vez de cessarem a sua migração para o lado esquerdo no final do estadio HH4, continuavam a executar este tipo de movimento, até ao final do estadio HH6. Este deslocamento contínuo das células para o lado esquerdo do nó, altera a expressão normal do *fgf8* e do *nodal* no nó, tornando-se simétrica e reduzida, respectivamente. Consequentemente, a expressão do *cer1* e do *snai1* é incorrectamente transferida para o lado esquerdo da mesoderme da placa lateral (MPL). Como efeito dos resultados anteriores, a informação dada pela MPL para a formação do coração é incorrecta, resultando na formação de corações com diversos fenótipos anormais. No entanto, se inibirmos a sinalização Fgf do lado esquerdo do nó, conseguimos não só recuperar a expressão normal do *cer1* e *snai1* na MPL, como a correcta posição do coração. Este trabalho, mostra que a localização assimétrica da N-caderina no nó de Hensen é crucial para parar os movimentos das células do nó para o lado esquerdo, tratando-se assim, de um ponto crítico para o estabelecimento da assimetria ED.

No sentido de promover um entendimento mais abrangente acerca da função da N-caderina no nó, fui ainda avaliar qual o seu papel na conservação da assimetria morfológica no nó de Hensen. Verificou-se, que quando a função da N-caderina é bloqueada, a morfologia assimétrica do nó é comprometida, não porque as suas células mudam de forma, mas porque é alterada a diferença no número de células entre os dois lados do nó. Observámos ainda, que a acumulação N-caderina do lado direito do nó poderá estar envolvida no processo de segregação celular entre os seus dois lados. Ou seja, a N-caderina poderá estar a garantir que as células do

lado esquerdo e do lado direito do nó não se misturem, de forma a conservar a sua identidade molecular.

Por fim, demonstro ainda que o gene c*Hes6-1* está expresso assimetricamente no embrião da galinha, é dependente da via de sinalização da bomba H^+/K^+-ATPase e da via de sinalização Nodal. Surpreendentemente, a sua localização assimétrica na mesoderme lateral à linha primitiva não está conservada entre a galinha e a codorniz. No entanto, esta assimetria é partilhada entre a galinha e o m*Hes6* no ratinho. No geral, estes resultados revelam um possível novo candidato na cascata da assimetria ED. No entanto, porque é que este gene está assimetricamente localizado na mesoderme lateral à linha primitiva ou qual(ais) a(s) estrutura(s) assimétrica(s) a que poderá dar origem, é ainda uma questão por responder.

PALAVRAS-CHAVE: assimetria esquerda-direita, nó de Hensen, movimento celular para o lado esquerdo, N-caderina, segregação celular, sinalização Notch, Hes6-1, destino celular.

ABBREVIATIONS

cAct-RIIa	**c**hicken **Act**ivin type **IIa r**eceptor
AJ	**A**dherens **J**unction
AP	**A**nterior **P**osterior
ASE	side-specific enhancer
bHLH	**b**asic **H**elix **L**oop **H**elix
BMP	**B**one **M**orphogenetic **P**rotein
BBR	**B**oeringer **B**locking **R**eagent
BSA	**B**ovine **S**erum **A**lbumin
CAMs	**C**ell **A**dhesion **M**olecules
C. elegans	***C****aenorhabditis* ***e****legans*
cDNA	**c**omplementary **DNA**
CSL	mammalian **C**BF-1, Drosophila **S**upressor of Hairless and *C. elegans* **L**ag-1
DIG	**Dig**oxigenin
DiI	1,1'-dioctadecyl-3,3,3'-tetramethylindocarbocyamine perchlorate
DiO	3,3'-dioctadecyloxacarbocyanine perchlorate
DV	**D**orso **V**entral
DNA	**D**eoxyribo**n**ucleic **A**cid
EMT	**E**pithelial-to-**M**esenchymal **T**ransition
FGF	**F**ibroblast **G**rowth **F**actor
GFP	**G**reen **F**luorescent **P**rotein
GJC	**G**ap **J**unction **C**omunication
GRP	**G**astrocoel **R**oof **P**late
her	Zebrafish **he**s-**r**elated genes
hes	**H**airy **E**nhancer of **S**plit genes
HH	**H**amburguer and **H**amilton stage
H^+/K^+/ATPase	**H**ydrogen-potassium **a**denosine **t**ri**p**hosphatase
H^+-V-ATPase	**V**acuolar **H(+)-ATPase** subunit A
Iv	**I**nversus **v**iscerum
KV	**K**upffer's **V**esicle

LB	**L**uria **B**ertani bacterial medium
Lfng	**L**unatic **f**ri**ng**e
LPM	**L**ateral **P**late **M**esoderm
LR	**L**eft-**R**ight
Lrd	**L**eft-**r**ight **d**ynein
MAM	**Ma**ster**m**ind
Min	**min**utes
mRNA	**m**essenger **RNA**
NICD	**N**otch **I**ntra-**C**ellular **D**omain
NLS	**N**uclear **L**ocalization **S**equence
NVP	**N**odal **V**esicular **P**article
OD	**O**ptical **D**ensity
o.n	**o**ver**n**ight
PCP	**P**lanar **C**ell **P**olarity
PS	**P**rimitive **S**treak
PSM	**P**re-**S**omitic **M**esoderm
RA	**R**etinoic **A**cid
Raldh2	**R**etin**aldeh**yde dehydrogenase **2**
RNA	**R**ibo**n**ucleic **A**cid
sec	**sec**onds
SELI	**S**elf-**E**nhancement and **L**ateral **I**nhibition
SHH	**S**onic **h**edge**h**og
YFP	**Y**ellow **F**luorescent **P**rotein
ZO-1	**Z**onula **O**ccludens

Index of Figures

CHAPTER I

Figure 1	Human laterality disorders	3
Figure 2	Left–right axis determination in a vertebrate embryo	5
Figure 3	The F-molecule model.	6
Figure 4	Leftward flow is generated by the posterior tilt of nodal cilia	8
Figure 5	Establishment of LR asymmetry in the mouse embryo	12
Figure 6	Conserved mechanisms of LR patterning among phyla over developmental stages	21
Figure 7	A model of the LR pathway based on cytoplasmic motor protein movement	23
Figure 8	Early gastrulation stages in chick development	28
Figure 9	Schematic representation of a transversal section from the blastoderm of a chicken embryo at stage HH4.	32
Figure 10	Mesodermal cell fates during vertebrate gastrulation	36
Figure 11	Leftward cell movements generates asymmetry in the chicken Hensen's node	38
Figure 12	Schematic representation of the genes involved in chick left-right asymmetry pathway	46
Figure 13	The classic cadherin–catenin protein complex	63
Figure 14	Cadherin in morphogenetic movements.	65
Figure 15	The role of cadherin in cell sorting and positioning	69

CHAPTER III

Figure 1	*cdh2* asymmetric expression in Hensen's node is promoted by leftward cell movements downstream of the H^+/K^+-ATPase pump	106
Figure 2	Transient leftward cell movements in Hensen's node are promoted by asymmetric N-cadherin activity	108
Figure 3	Loss of N-cadherin activity affects asymmetric gene expression in Hensen's node and Lateral Plate Mesoderm	113
Figure 4	N-cadherin controls *cer1* and *snai1* expression in the Lateral Plate Mesoderm by controlling Fgf signalling	115
Figure 5	N-cadherin overexpression on the right side of the node does not affect asymmetric gene	117
Figure 6	Proposed model for N-cadherin function in the establishment of Left-Right asymmetry in the chick embryo	120
Figure S1	MNCD2 recognizes chicken N-cadherin and weakly blocks cell-cell adhesion.	126
Figure S2	Transient leftward cell movements in Hensen's node are promoted by asymmetric N-cadherin activity.	129
Figure S3	Loss of N-cadherin activity affects asymmetric gene expression in Hensen's node and Lateral Plate Mesoderm	130

CHAPTER IV

Figure 1	Blocking N-cadherin activity impacts on Hensen's node asymmetric morphology	140
Figure 2	Blocking N-cadherin activity does not affect cell shape in the Hensen's node	144
Figure 3	Cell mixing in the Hensen's node at different stages of development	148

CHAPTER V

Figure V.1	The core pathway of Notch signalling	160
Figure 1	The H^+/K^+ATPase pump activity modulates the expression of c*Hes6-1*	165
Figure 2	Nodal induces c*Hes6-1* expression	167
Figure 3	*hes6* expression pattern in different organisms	169

Index of Tables

CHAPTER I

Table 1	Some of the asymmetrically expressed genes in the chicken embryo	50

CHAPTER II

Table 1	Appropriate restriction enzyme and RNA polymerase for each probe	90
Table 2	Oligonucleotides	91

CHAPTER III

Table 1	Number of cells that crossed the midline at different stages of development in control versus Anti-N-cad treated embryos	109

Index of Movie Legends

Movie 1	Time-lapse movie of a chicken embryo electroporated on the right side with Kaede-NLS photoconvertible fluorescent protein and treated with IgG2a control antibody.	121
Movie 2	Time-lapse movie of a chicken embryo electroporated on the right side with Kaede-NLS photoconvertible fluorescent protein and treated with anti-N-cad antibody.	121
Movie 3	Time-lapse movie of a chicken embryo electroporated on the right side with full-length N-cadherinYFP	121
Movie S1	Time-lapse movie of a chicken embryo electroporated with Kaede-NLS photo-convertible fluorescent protein on the right side.	132
Movie S2	Time-lapse movie of a chicken embryo electroporated with Kaede-NLS photo-convertible fluorescent protein on the right side and treated with the N-cadherin blocking MNCD2 antibody.	132

Chapter

INTRODUCTION

INTRODUCTION

In this Chapter, I will start by presenting a general overview on left-right (LR) asymmetry establishment, which is the central topic of this thesis. I will begin by describing its components and its regulators in different model systems, and then I will focus in one specific model - the chicken embryo. I will give a brief summary of the initial steps of chicken embryo development, and I will describe how its left-right (LR) asymmetry is initiated, stabilized, propagated and lastly, translated into the asymmetric positioning of the heart. Finally, I will briefly review the function of a major family of cell adhesion proteins, the cadherins, during development and, in particular, the role of in N-cadherin role during embryonic development, LR asymmetries, and its relation to abnormal cell migration.

I.1 Left-Right Asymmetry in Vertebrates

The vertebrate body plan exhibits outwardly a bilateral symmetry along the mediolateral axis. Internally, however, the distribution of the organs such as the heart, stomach, and intestines has both an asymmetric structure and asymmetric position. The same general pattern of LR asymmetry is conserved in vertebrates and the LR patterning is remarkably similar (reviewed in (Fujinaga 1997)), suggesting that the asymmetric structure and arrangement of organs is required for their normal function.

The orientation of the LR axis is not by chance, with a predisposition of nearly 100% for a precise handedness (*situs solitus*) (Fig. 1a), which implies

the existence of genetic mechanisms that tightly regulate patterning along the LR axis. The failure to properly pattern the LR axis results in distinct classes of laterality defects: *situs inversus* corresponds to a situation where the position of the internal organs is completely reverted as a mirror-image (Fig. 1b), left or right isomerism are situations where bilateral symmetry is not broken and two left or right sides will form (Figs. 1c, d) (Fliegauf, Benzing et al. 2007).

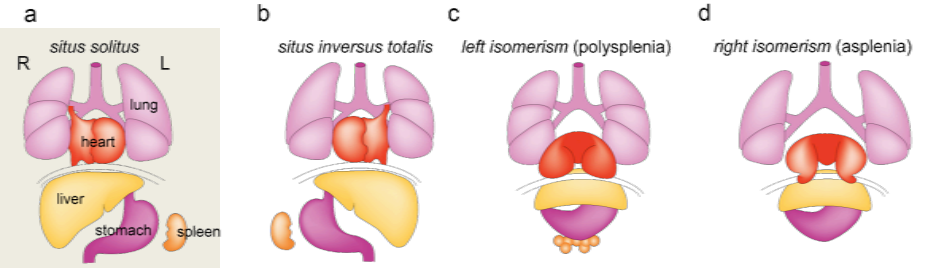

Figure 1| Human laterality disorders. (**a**) Schematic illustration of normal left–right body asymmetry (*situs solitus*). (**b-d**) Three laterality defects that affect the lungs, heart, liver, stomach and spleen. (**b**) *Situs inversus totalis* is a complete mirror-image reversal of organ asymmetry. (**c**) Left isomerism: two left sides are formed. (**d**) Right isomerism: two right sides are formed. R-Right; L-Left. Adapted from (Fliegauf, Benzing et al. 2007).

Over the last 20 years, there was an effort to understand LR axis patterning and to identify the molecular and cellular mechanisms that regulate the asymmetric development. These regulatory mechanisms have been revealed through the identification of asymmetrically expressed genes and the characterization of targeted mutations that lead to LR problems. Several discoveries have helped to build a model on how LR asymmetry is initiated, stabilized, propagated, and translated into asymmetric organogenesis during development of vertebrate embryos.

I.2 Steps in Left-Right asymmetry establishment

In general terms, the establishment of LR asymmetry can be divided into four steps: 1) initial breaking of LR symmetry in or near the organizer (node) (Figs. 2a-d); 2) transfer of LR signals from the node to the lateral plate mesoderm (LPM) (Fig. 2e); 3) LR asymmetric expression of signalling molecules to the left side in the lateral plate and (Fig. 2f) and 4) LR morphogenesis of the visceral organs induced by these signalling molecules (Fig. 2h). Studies on different vertebrates, such as zebrafish, frog, chick and mouse have contributed for this view of the establishment of LR asymmetry.

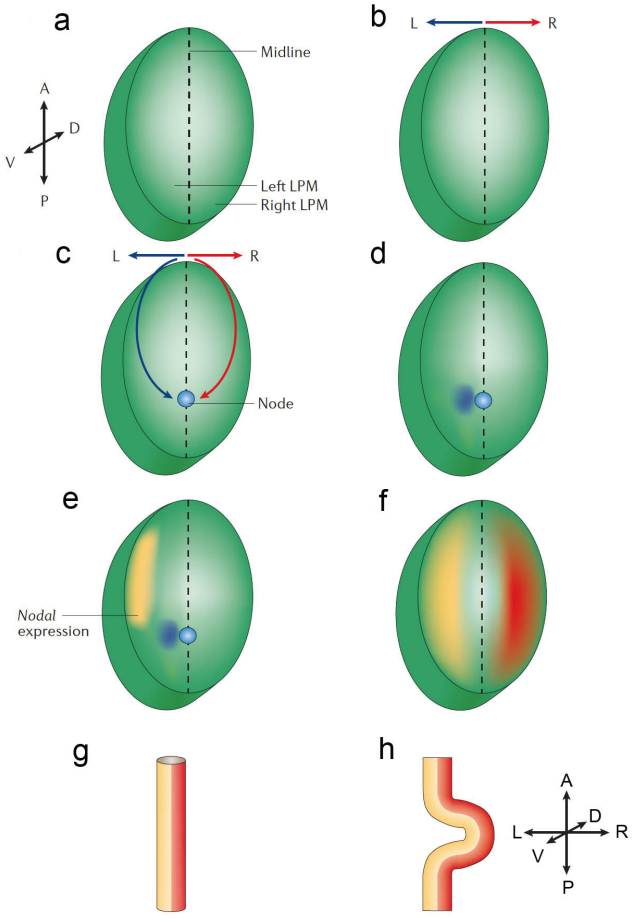

Figure 2| Left–right axis determination in a vertebrate embryo. Early embryo that is already patterned along the AP and DV axes is bilaterally symmetrical (**a**). A symmetry-breaking step generates initial left–right information (**b**), although the nature of this event is unknown. The initial left–right information is then transferred to the embryo node (shown as a blue circle) (**c**). The node generates a directional output in the form of a discrete perinodal domain of Nodal expression and/or lateralized hedgehog signalling (**d**), which results in local left–right asymmetries (shown as dark-blue shading). These local asymmetries around the node are conveyed to the left lateral plate mesoderm (LPM) in the form of side-specific Nodal expression (**e**). Broad domains of expression of left- and right-side specific genes (yellow and red, respectively) are then established (**f**), transferring laterality information to the organ primordia (a structure that represents a single primordium is shown in (**g**), which, in turn, execute LR asymmetrical morphogenetic programs (illustrated as the directional looping of the organ primordium in (**h**). Adapted from (Raya and Izpisua Belmonte 2006).

However, a unifying mechanism that that breaks symmetry has not yet been found and different strategies seem to be used by different vertebrates.

I.3 Breaking the initial symmetry

I.3.1 The conceptual F-molecule model

The vertebrate body plan is progressively organized according to the establishment of three body axes during embryonic morphogenesis: antero-posterior (AP), dorso-ventral (DV) and finally left-right (LR). Since the LR axis is the last to be determined during development, it could be assumed that using the pre-existing positional cues the LR polarity could be generated.

In the early 1990s, Wolpert and colleagues postulated a model called the F-molecule model (Brown and Wolpert 1990). This hypothetical molecule of F-shape would have three arms. When two arms are aligned with the AP and DV axes, the third arm would be automatically aligned along the future LR axis. If the third arm has intrinsic polarity, like the plus and minus ends of microtubules, cells on the left and right sides of the embryo would be polarized asymmetrically with regard to the LR orientation (Fig. 3). This model turns out to be correct in principle: as later studies revealed, the cilium of the node cells and its cytoskeletal structure could fill the role of the F-molecule (see below).

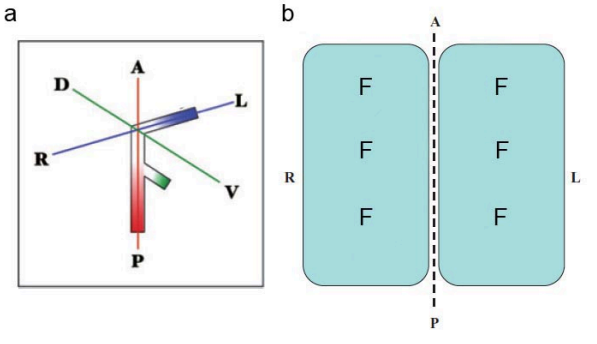

Figure 3| The F-molecule model. (**a**) Hypothetical F-molecule with three arms. The upper arm (the one aligned with the LR axis) is polarized. (**b**) Two cells facing the midline (dotted line) contain F molecules. Two cells are asymmetric with regard to the midline. A-anterior; P-posterior, L-left; R-right; D-dorsal; V-ventral. Adapted from (Hamada 2008).

I.3.2 Different mechanisms to break symmetry

The fact that the first asymmetrically expressed genes are found at the LR organizer (node in mice, Hensen's node in the chick, the gastrocoel roof plate in *Xenopus*, and Kupffer's vesicle (KV) in zebrafish) (Levin, 2005) drew attention to this structure as the place where the initial LR decisions might be taken. Evidence from various experimental approaches and model organisms demonstrates that the embryo node has a crucial role for LR asymmetrical patterning in all vertebrates (Capdevila, Vogan et al. 2000; Mercola and Levin 2001; Palmer 2004). Nevertheless, compelling evidence from several model organisms support the possibility that LR symmetry breaking events might occur prior to gastrulation and therefore prior to node formation.

I.3.2.1 Motile cilia in the node

The role of cilia in the establishment of LR asymmetries has been best studied in the mouse embryo. An elegant series of experiments done in the mouse node provided the first experimental evidence for the role of cilia in LR axis determination (Nonaka, Tanaka et al. 1998; Okada, Nonaka et al. 1999; Takeda, Yonekawa et al. 1999). Interestingly, this model is completely consistent with a previously observed correlation between *situs* abnormalities and ciliary dysfunction in humans, the so called Kartagener's syndrome (Afzelius 1976). In these affected individuals a reversion of the localization of the organs is associated with immotile sperm and defective cilia in their airways (Afzelius 1976). Thus, this association indicated that motile cilia might control LR asymmetry.

This conclusion was later supported by the analysis of the *inversus viscerum* (*iv*) mutant mice (Okada, Nonaka et al. 1999). *Iv* mutant mice,

which have randomized LR patterning, were shown to have a mutation in the *left-right dynein* (*lrd*) (Supp et al. 1997), an important component of the ciliary motion motor. And in fact, it was then shown that human patients with Kartagener's syndrome present mutations in this motor protein.

Equally important, was the discovery that cells in the murine ventral node are monociliated. These cilia are composed of 9 + 0 microtubules arrangement, rather than the 9 + 2 conventional motile cilia arrangement in normal ciliated cells. Therefore, based on their structure, these monocilia were thought to lack motility (Bellomo, Lander et al. 1996). However, it was later discovered that the nodal monocilia 9 + 0 have an accelerated movement and that this generates a leftward extracellular fluid flow (nodal flow) around the node (Hirokawa, Tanaka et al. 2006). This leftward nodal flow is able to determine laterality by a yet unknown mechanism (Fig. 4b) (Nonaka, Tanaka et al. 1998; Nonaka, Yoshiba et al. 2005).

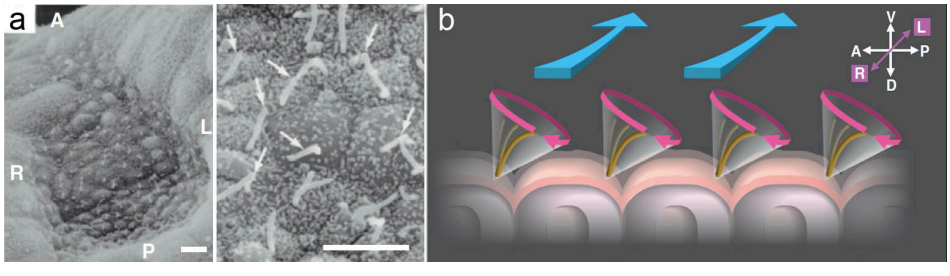

Figure 4| Leftward flow is generated by the posterior tilt of nodal cilia. (**a**) Scanning electron micrographs of wild-type mouse nodes in ventral view. (**b**) Generation of leftward flow by tilted cilia rotation in the node. Arrows-monocilia. Upper, anterior (A); lower, posterior (P); left of the figure, right (R); right of the figure, left (L). Bars, 5 mm. Adapted from (Hirokawa, Tanaka et al. 2012).

I.3.2.1.1 DIRECTIONAL NODAL FLOW

The discovery of nodal flow generated by the rotation of cilia was based on studies of molecular motors like the kinesin superfamily proteins (KIFs) KIF3 motor. KIFs are the main motor proteins involved in the transport along microtubules. They transport various cargoes, such as membranous organelles, protein complexes and mRNA, along the network of intracellular microtubules within cells (Aizawa, Sekine et al. 1992; Hirokawa 1998).

Studies with knockout mice for Kif3a and Kif3b (subunits of the heterotrimeric motor protein, kinesin2) revealed that around 50% of both Kif3a deficient and Kif3b deficient mice showed reversed heart loops. Observation of the nodes then surprisingly revealed that nodal cilia were lacking in $Kif3^{-/-}$ mutants and, as a consequence, there was no generation of nodal flow (Marszalek, Ruiz-Lozano et al. 1999; Takeda, Yonekawa et al. 1999).

The implication of the nodal flow in the determination of LR asymmetric patterning was further supported by a series of elegant experiments in which mouse embryos in culture were subjected to an artificial rightward flow. This manipulation, of the intensity and/or direction of the flow, was sufficient to reverse LR *situs*. These results provided the first direct evidence of the fluid flow role in LR patterning (Nonaka, Shiratori et al. 2002).

Despite the initial description of this fluid flow in the mouse node, it is not exclusive to the mouse embryo. Zebrafish and medaka fish also share the same mechanism, promoted by motile cilia inside the Kupffer's vesicle. In the rabbit's node, a homologue structure called posterior notochord, as well as the gastrocoel roof plane in *Xenopus*, also has motile cilia capable

to create a leftward fluid flow (Essner, Amack et al. 2005; Okada, Takeda et al. 2005; Schweickert, Weber et al. 2007; Basu and Brueckner 2008).

In the zebrafish KV it was previously though that the rotating cilia moved in a counter-clockwise manner (when viewed from the apical side) (Kramer-Zucker, Olale et al. 2005; Shu, Huang et al. 2007), differing from the mouse model (Fig. 3). This contradictory result was puzzling, since it suggested that the mechanism for LR determination, which depends on the initial leftward transport of a molecule, was not conserved in zebrafish. However, it was found out later that all cilia in the KV actually rotate in a clockwise manner if observed from ventrally, similar to what is observed in the mouse node (Nonaka, Shiratori et al. 2002; Okada, Takeda et al. 2005).

I.3.2.1.2 Two Models for generating Left-Right asymmetric gene expression by Nodal Flow

After bilateral symmetry is disrupted in or near the node and LR asymmetry is initiated, it is necessary to transfer the LR signals from the node to the LPM to enable the asymmetrical development of the body. Although the nodal flow has been widely accepted to be the mechanism for breaking symmetry in the majority of vertebrates, it is not yet fully understood how the nodal flow directs LR asymmetry.

There are two current models, which are not mutually exclusive, and have both been proposed to explain how the information generated by leftward nodal flow is interpreted.

The first model is based on the formation of chemical gradients and it assumes that the directional flow will produce a concentration gradient of a secreted morphogen in the cavity of the ventral node (Nonaka, Tanaka et

al. 1998; Okada, Takeda et al. 2005). The resulting asymmetric morphogen distribution would initiate downstream molecular events that then establish LR asymmetries in the LPM (Nonaka, Tanaka et al. 1998).

More recently, it was reported the presence of membrane-sheathed vesicles in the node that could correspond to the chemical morphogen. These Nodal Vesicular Particles (NVPs), containing Sonic hedgehog (SHH) and Retinoic acid (RA), two molecules involved in LR asymmetry determination (Schilling, Concordet et al. 1999; Tsukui, Capdevila et al. 1999), were shown to be secreted and transported to the left side by the nodal flow. This release of NVPs was shown to be dependent on FGF signalling, and they are transported to the left edge of the node where they fragment and release their contents (Tanaka, Okada et al. 2005) (Fig. 5a).

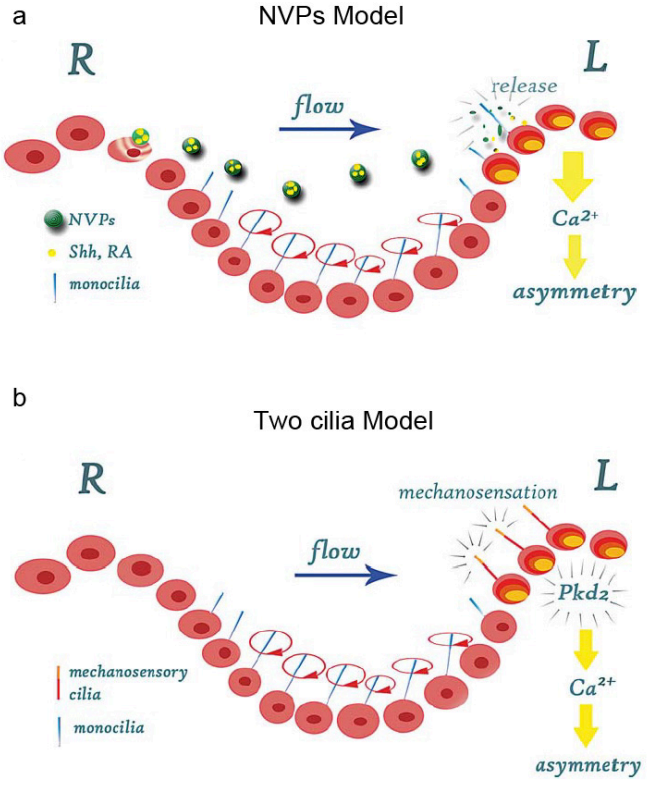

Figure 5| Establishment of Left-Rigth asymmetry in the mouse embryo. In the mouse embryo two versions of the nodal flow model have been proposed. (**a**) The NVPs model. NVPs are released from the node cells in an FGF8-dependent manner. They are transported to the left side of the node by means of a nodal flow, which is generated by cilia on the ventral surface of the node cells. The content of the NVPs (RA and Shh) is released on the left side of the node inducing an intracellular Ca^{2+} signal. (**b**) The two cilia model. Two types of cilia (monocilia and mechanocilia) were found to be present in the ventral node cells. Monocilia, which show co-expression of Pkd2 and Lrd, are motile cilia that drive the nodal flow. In the periphery of the node, mechanosensory cilia are present that express the calcium channel Pkd2 but not Lrd. These cilia are immotile and it is proposed that they are involved in detecting the nodal flow resulting in the generation of an asymmetric intracellular Ca^{2+} signal that is transduced into asymmetric gene expression. Adapted from (Schlueter and Brand 2007).

The second model, called physical stimulation, was proposed as a critique of the chemical gradient model. It establishes that there is a second population of nodal cilia that are immotile and can mechanically sense the physical stimulation produced by the nodal flow, the so-called

"mechanosensory cilia" (McGrath, Somlo et al. 2003). This model is now commonly known as the "two-cilia" model, since one type of cilia generates the flow and the other senses it (Tabin and Vogan 2003).

One class of cilia, found throughout the center of the node, is associated with both Lrd and Polycystin-2 protein, while a second class of cilia, present on the node periphery, contains only Polycystin-2. Polycystin-2 is encoded by the gene Pkd2 and functions as a calcium release channel and it was observed that Pkd2 mouse mutants display LR asymmetry defects (Fig. 5b) (Pennekamp et al., 2002).

It has been proposed that immotile mechanosensory cilia sense the fluid flow pressure on the left side of the node triggering an asymmetric intracellular Ca^{2+} flux which creates a left-sided elevation of intracellular of Ca^{2+} culminating with the left-sided *nodal* expression (McGrath, Somlo et al. 2003). Propagation of the increased Ca^{2+} concentration through the LPM then breaks LR symmetry, establishing the "leftness" of the LPM and inducing left-side specific gene cascades (McGrath, Somlo et al. 2003).

However, the validity of this model was recently questioned (Cartwright, Piro et al. 2004), due to the observation that, even in the presence of directional flow, the magnitude of the shear stresses and flow velocities generated in the mice node would lead to an overall symmetrical effect, and therefore would be unable to asymmetrically bend monocilia.

I.3.2.2 Other players in Left-Right patterning prior to the formation of cilia

Although the monocilia in the ventral murine node or its equivalent structures seem to be evolutionarily conserved (reviewed in (Hamada,

Meno et al. 2002), the leftward nodal flow they generate might not be the initial determinant for the LR asymmetry in some other vertebrates such as amphibians, chick and fish.

Various early requirements for correct LR asymmetrical patterning have been identified in different vertebrate species. Currently, none of these mechanisms have been found to be conserved in all main vertebrate models: *Xenopus*, chick, zebrafish and mice. Similarly, the requirement for all these mechanisms in any one model has not been shown/analysed.

The *Xenopus* embryo has allowed the discovery of a number of mechanisms, which underlie asymmetry at the earliest stages known in any species. Experiments done in this model suggested that the LR axis might be established extremely early, long before the onset of cilia and it is linked to the formation of the DV axis (Yost 1991). The DV axis is initiated by sperm entry during fertilization, followed by a cytoplasmic rotation during the first cell cycle and is driven by a microtubule array at the vegetal cortex (Gerhart, Danilchik et al. 1989). Thus, laterality is generated 2 hours after fertilization in frog eggs.

The appearance of LR asymmetry between fertilization and the first cell divisions is consistent with the recent work showing asymmetric mRNA and protein localization during the first few cleavages (Levin, Thorlin et al. 2002; Bunney, De Boer et al. 2003). Randomly distributed maternal mRNAs and ion-transporter proteins in the egg (e.g. H^+ and K^+ transporters) become asymmetrically distributed by the activity of intracellular motor proteins.

As ion channels and pumps become asymmetrically distributed, they create a LR gradient in membrane voltage that, in turn, shifts small molecules determinants such as serotonin (5HT) to one specific side of the

embryo (Fukumoto, Blakely et al. 2005). This asymmetric shift is promoted by an electrophoretic mechanism through a system of gap junctions. The accumulation of these small molecule determinants on one side of the embryo eventually induces unilateral gene expression of a key signalling molecules and consequently organ *situs* (Levin, 2006).

While this has been studied in most detail in *Xenopus* embryos, analysis of a wide variety of phyla reveals surprising conservation in the pathways involved (Levin 2006; Oviedo and Levin 2007) long before ciliogenesis.

I.3.2.2.1 GAP JUNCTION COMUNICATION (GJC)

One of the earliest mechanisms involved in LR patterning is the gap junction communication system that connects adjacent cells through channels allowing the direct transfer of small molecule signals. A large family of connexins (or gap junction proteins) exists and many contain a large cytoplasmic region postulated to confer conductance regulation by intracellular pH, voltage, and phosphorylation (Bruzzone, White et al. 1996; White and Bruzzone 1996).

Specific expression patterns as well as functional studies contributed to the idea that GJC is involved in diverse processes such as embryogenesis and tumour progression (reviewed in (Levin 2007)). Analysis of 16 to 64-cell *Xenopus* embryos revealed that dorsal blastomeres have more GJC than ventral blastomeres and that subtle differences in GJC exist between blastomeres on the left and right sides (Guthrie 1984; Guthrie, Turin et al. 1988). This supports the idea that these channels may be involved in coordinating global DV and LR polarity in the early embryo.

Based on a report that shows that several unrelated patients with

visceroatrial heterotaxia (congenital disorder characterized by complex heart malformations and disturbance of viscera asymmetry) contain potential mutations within Connexin43 (Cx43) (gap junction protein) (Britz-Cunningham, Shah et al. 1995) and data from frog embryos that indicated asymmetric patterns of GJC in early blastomeres (Britz-Cunningham, Shah et al. 1995), lead Levin *et al* (1998) to test the hypothesis that gap junctional path is a mechanism by which LR information was communicated across large cell fields (Levin and Mercola 1998).

Recently, Hatler *et al*; (2009) discovered that Cx43 is also required for the LR patterning in zebrafish through the development of a functional KV with normal cilia (Hatler, Essner et al. 2009). It was proposed (Levin and Nascone 1997; Levin and Mercola 1998) that small molecule determinants are initially randomly distributed, but go trough the circumferential GJC path unidirectionally, accumulate on one side of the midline, and then induce asymmetric gene expression. Thus, GJC may propagate signals throughout the epiblast but not across an insulating zone at the streak.

I.3.2.2.2 ION FLUX

Another mechanism that controls LR asymmetry has been proposed by Levin *et al.* on the basis of the observation that ion-pump and ion-channel gene products become asymmetrically expressed at cleavage stages in *Xenopus* embryos (Levin, Thorlin et al. 2002) (Fig. 6). This polarized expression would result in the formation of an asymmetric ion flux that would produce a LR gradient of pH and membrane potential over the midline, on the left side of chick (Levin, Thorlin et al. 2002) and right side of *Xenopus* (Levin, Thorlin et al. 2002; Adams, Robinson et al. 2006).

The electrophoretic forces that would result could actively transport small LR determinants such as serotonin (5HT) (Fukumoto, Blakely et al. 2005; Fukumoto, Kema et al. 2005), Ca^{2+} (McGrath, Somlo et al. 2003; Raya and Izpisua Belmonte 2004; Tanaka, Okada et al. 2005), inositol phosphates (Sarmah, Latimer et al. 2005) or RA, through the gap junctions, specifically to one side where they would, in turn, initiate asymmetric gene expression of *nodal*. It is worth mentioning that treatments with specific ion-pump inhibiting drugs directed against H^+/K^+-ATPase channels cause heterotaxia in *Xenopus* and chick embryos (Levin, Thorlin et al. 2002), suggesting that the ion flows may have a functional role in LR asymmetry.
In drug inactivation experiments or molecular genetics approaches, several different ion pumps have now been found, in species ranging from echinoderms to vertebrates, to be involved in early LR asymmetry determination: H^+/K^+-ATPases in tunicates (Shimeld and Levin 2006), sea urchin (Duboc, Rottinger et al. 2005; Hibino, Ishii et al. 2006), frog (Levin, Thorlin et al. 2002; Adams, Robinson et al. 2006) and chicken (Levin, Thorlin et al. 2002); H^+-V-ATPases in frog, chicken and fish (Adams, Robinson et al. 2006); Na^+/K^+-ATPase in fish (Shu, Huang et al. 2007).

Until now, there have been no reports of ion transporters being involved in LR asymmetry determination in mammals, although there is a lack of specific studies. A different type of ion channel, the murine calcium Ca^{2+}-activated ion channel polycystin-2 (Pkd2) is, however, implicated in the transduction of the leftward nodal flow information into a transient intracellular increase of Ca^{2+} concentration at the left margin of the node, (as it was mentioned in section I.2.2.3) (Pennekamp, Karcher et al. 2002; Tanaka, Okada et al. 2005). An increase in intracellular Ca^{2+} on the left side of KV is also observed in zebrafish (Sarmah, Latimer et al. 2005).

Interestingly, it was also reported on the left side of Hensen's node in the chicken embryo a transiently up-regulated extracellular Ca^{2+} levels that seemed to depend on H^+/K^+-ATPase activity that consequently will activate Notch signalling on that side (Raya, Kawakami et al. 2003). These findings might indicate a conserved role for a calcium-dependent mechanism in LR asymmetry establishment in vertebrates during gastrulation, although some species might have developed different strategies according to their embryonic development.

I.3.2.2.3 MOTOR PROTEINS/CYTOSKELETON

The LR asymmetries in mRNA localization may plausibly be driven by cytoplasmic motor proteins such as dynein and kinesin, which is analogous to the animal-vegetal asymmetries in mRNA localization in the frog oocyte and many other cell types (Tekotte and Davis, 2002). During the first few cell cleavages in *Xenopus,* many mRNAs and proteins were found to be asymmetrically localized (e.g., Bunney et al., 2003). These phenomena may reflect potential non-ciliary functions of motors in the LR pathway and asymmetric cargo transport is the answer.

The possibility of cytoplasmic transport functions of motor proteins which might be relevant to LR patterning has been suggested in several reviews (Levin and Nascone, 1997; Tamura et al., 1999; Hobert et al., 2002; Robinson and Messerli, 2003) and primary papers (Supp et al., 1997; Levin et al., 2002), because the ciliary and cytoplasmic roles have not yet been experimentally distinguished.

Succinctly, cytoplasmic motor movement results in an asymmetric distribution of specific ion pump mRNA and protein cargo in a key group of early cells. The presence of electrogenic proteins on the cell surface on

one side of the midline allows those cells to carry out an ion exchange with the extracellular space, which is not replicated on the contra-lateral side. This ion flux results in differential membrane voltage and pH among cells on either side of the midline (Levin and Mercola 1998; Levin, Thorlin et al. 2002).

Together, the systems of cytoplasmic motor transport, ion flux, and gap junctional paths offer a way to solve the question of how LR orientation information on the level of a single cell (given by an oriented F-molecule) is converted into global information on LR position in relation to the midline of the embryo (which in turns will specify the asymmetric gene expression in cell fields) (Levin and Palmer 2007). By establishing localized ion gradients across the midline which can control the movement of LR determinants through embryo-wide gap junctional paths, motor proteins can initiate the cascade by which oriented intracellular movement is transduced into large fields of gene expression (Fig. 7).

I.3.2.2.4 SEROTONIN (5HT)

The recent findings that indicated that LR axis was patterned at early stages by flows of small molecules and ions (Levin and Mercola 1998; Levin and Mercola 1999; Levin, Thorlin et al. 2002) made it necessary to examine the involvement of non-protein signalling molecules in mechanisms upstream of the known LR cascade. This led to two main questions that needed to be answered: what could be controlling the unidirectional (chiral) flow of LR information through the GJ (Levin, Thorlin et al. 2002); and what is the molecular nature of the LR small-molecule signals that are exchanged between cells on the left and right sides.

The ideal candidate molecule would be smaller than a GJ, water-

soluble (signalling molecules such as retinoic acid do not need GJ to move between cells), and charged (to enable regulation of movement via ion pump-dependent voltage gradients (Levin and Nascone 1997). Serotonin, a key neurotransmitter with crucial roles in physiology and cognition, fits these criteria, and it has already been demonstrated to go through gap junctions in other contexts such as, growth control, pattern formation, tissue differentiation and LR asymmetry (Wolszon, Rehder et al. 1994). Analysing the endogenous localization of 5HT and related proteins, and using functional experiments designed to probe 5HT function, Levin *et al.* showed that 5HT signalling is upstream of early asymmetric gene expression in both chick and frog species, and revealed novel developmental aspects of this versatile signalling molecule (Levin, Thorlin et al. 2002).

During early *Xenopus* development, 5HT was distributed in a striking radial pattern, eventually forming a gradient. It was shown that the ability of 5HT to localize asymmetrically through the GJC-connected blastomeres was dependent upon open GJ and upon the function of the H^+/K^+-ATPase and V-ATPase ion pumps (Wolszon, Rehder et al. 1994; Fukumoto, Kema et al. 2005; Adams, Robinson et al. 2006) (Fig. 6).

Taken together, these data suggested a model that provides a possible answer to the chirality of the morphogen movement through gap junctions in LR patterning (Esser, Smith et al. 2006): that 5HT moves asymmetrically through the field of GJC-connected cells under an electrophoretic force provided by differential membrane voltages (Fukumoto, Kema et al. 2005).

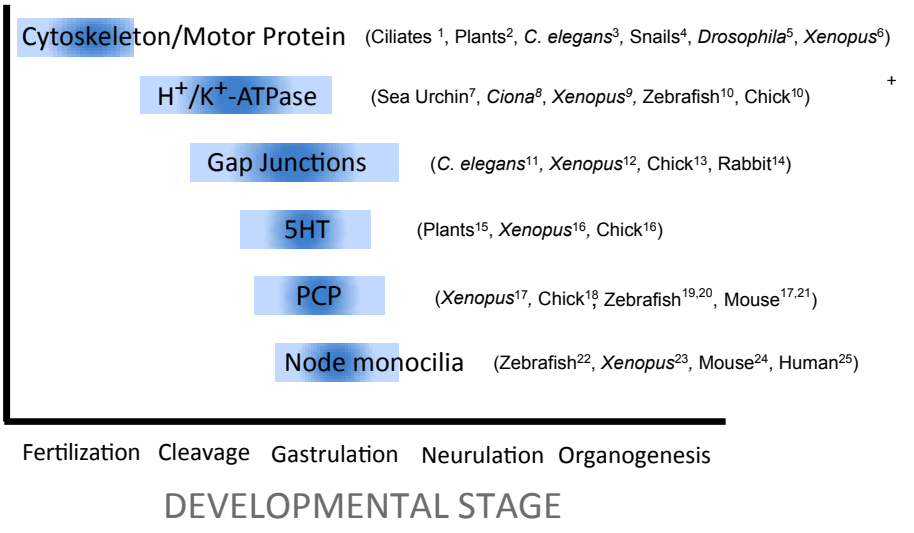

Figure 6| Conserved mechanisms of Left-Right patterning among phyla over developmental stages. The various proteins and structures likely to contribute to LR asymmetry determination. Animal species for which the components have been examined are listed in parentheses. 5HT- Serotonin (auxin in plants). 1-(Frankel 1991); 2-(Hashimoto 2002); 3-(Wood and Kershaw 1991; Hashimoto 2002); 4-(Shibazaki, Shimizu et al. 2004); 5-(Speder, Adam et al. 2006); 6-(Qiu, Cheng et al. 2005); 7-(Hibino, Ishii et al. 2006); 8-(Shimeld and Levin 2006); 9-(Levin, Thorlin et al. 2002); 10-(Adams, Robinson et al. 2006); 11-(Chuang, Vanhoven et al. 2007); 12-(Levin and Mercola 1998); 13-(Levin and Mercola 1999); 14-(Muders, K. et al; 2006); 15-(Pekker, Alvarez et al. 2005); 16-(Fukumoto, Blakely et al. 2005); 17-(Antic, Stubbs et al. 2010) ; 18-(Song, Hu et al. 2010); 19-(Wang, Cadwallader et al. 2011); 20-(Borovina, Superina et al. 2010); 22-(Essner, Amack et al. 2005); 23-(Qiu, Cheng et al. 2005); 24-(Nonaka, Shiratori et al. 2002); 25-(Afzelius 1976).

I.3.2.3 Putting it all together - Intracellular Model

The earliest evidence for the intracellular model (Fig. 7) came from *Xenopus* studies (reviewed in (Levin 2004)), where the asymmetry was shown to be imposed on cell fields through the steps outlined (maternal mRNAs for key ion transporters; cytoskeletal re-arrangements; motor proteins; ion flux; gradients of pH and voltage; unidirectional net movement; accumulation of small molecules on one side of the midline; excess 5HT; asymmetric expression of *nodal* on the left side) (Figs. 7a-g).

Although the details of this pathway have only been worked out in *Xenopus* it was also observed, to a lesser extent, in chick (Levin and Mercola 1999; Levin, Thorlin et al. 2002), zebrafish (Kawakami, Raya et al. 2005; Adams, Robinson et al. 2006) and sea urchin (Hibino, Ishii et al. 2006).

The intracellular model proposes that asymmetry arises at very early stages inside cells, and oriented cytoskeletal elements assume the ‘‘F-molecule’’ function. In addition, this model predicts a connection between cellular polarity and ion flux. In the intracellular model, an early component of the cell-polarity system (likely involving the cytoskeleton) orients the transport of key molecules within cells that in the end creates an LR difference in the embryo. Randomly distributed maternal mRNAs and ion-transporter proteins in the egg (like for instance H^+ and K^+ transporters), become asymmetrically distributed by the activity of intracellular motor proteins (Figs. 7a–c).

The motor proteins move these ion transporters in only one direction, along asymmetric cytoskeletal elements that derive their chirality from a basal body or other oriented ‘‘F-molecule’’ (Fig. 7c). As ion channels and pumps become asymmetrically distributed, a LR gradient in membrane voltage is generated (Figs. 7d, e) that, in turn, moves small molecule determinants such as 5HT through a system of GJ by an electrophoretic mechanism (Figs. 7g, i).

The accumulation of these small molecules on one side of the embryo eventually induces unilateral gene expression of a key signalling molecule such as *nodal* (Fig. 7h). This intracellular model shows how physiological mechanisms integrate to produce large-scale LR gradients from initial subcellular polarities. Although the orienting cytoskeletal element is not yet known, this model provides a comprehensive summary of all the

molecular and biophysical steps leading from LR orientation within single cells to asymmetric gene expression in the early embryo, independently on ciliary motion.

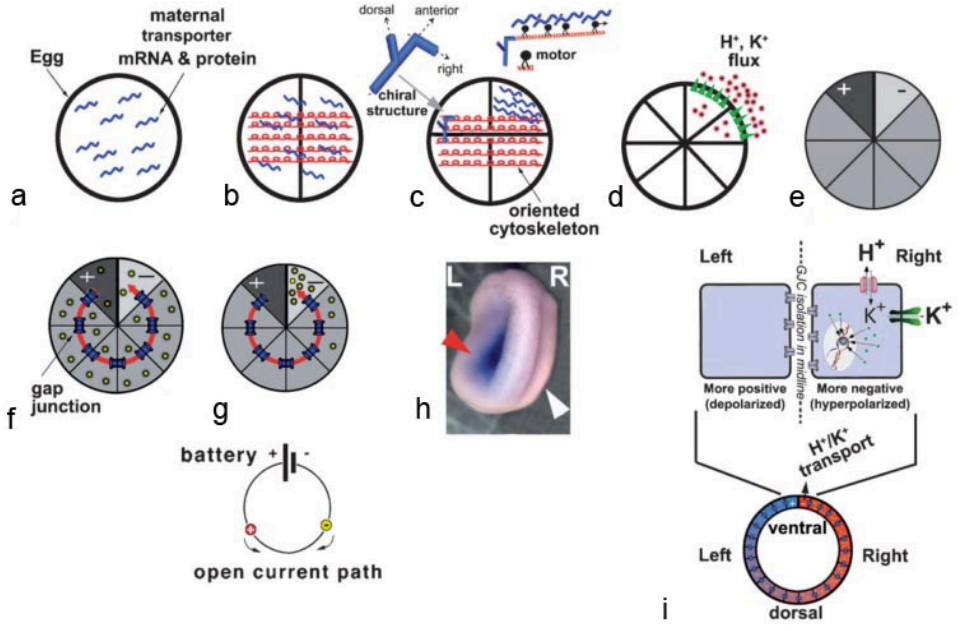

Figure 7| A model of the Left-Right pathway based on cytoplasmic motor protein movement. (**a**) In the unfertilized egg maternal mRNAs for key ion transporters are evenly distributed. (**b**) Cytoskeletal re-arrangements following fertilization set up microfilaments or microtubules which are oriented along the newly established LR axis. (**c**) Motor proteins (such as dynein (LRD) and kinesin (KIF3B) translocate along these tracks and result in an asymmetric localization of certain mRNAs. (**d**) These mRNAs are translated and thus initiate ion flux. (**e**) The differential ion flux results in LR asymmetric gradients of pH and voltage. (**f**) The system of gap-junctional communication is set up, featuring junctional isolation across the ventral midline and a path of GJC circumferentially around it. (**g**) The voltage gradient between the L and R sides imposes a unidirectional net movement of as-yet-uncharacterized small signalling molecules. This results in an accumulation of these molecules on one side of the midline from an initially random (homogenous) distribution. (**h**) Excess 5HT (and perhaps other long-distance signalling molecules) initiate asymmetric gene expression of *nodal* on the left side (red arrow); white arrow indicates lack of *nodal* expression on the right side. (**i**) The accumulation of these small molecule morphogens on one side induces gene expression in conventional ways. From (Levin and Palmer 2007).

The hallmarks of this model are that LR asymmetry is established extremely early (long before nodal cilia appear); that asymmetry originates in the orientation of a cytoplasmic structure; that components of this system might be very widely conserved, and that intracellular physiological signals and cell-cell interactions are important in transmitting LR information across cell fields (Fig. 7).

Another pathway now emerges as a fascinating candidate for a well-conserved role in amplifying LR patterning: planar cell polarity (PCP). It may also provide a link between the intracellular and the cilia model, as it seems to operate in the initial steps of both (Aw and Levin 2009).

I.3.2.4 PLANAR CELL POLARITY (PCP)

Proper development and functioning of tissues require, among many other things, the establishment of common orientation in a sheet of cells. Planar cell polarity (PCP) signalling refers to the mechanism or mechanisms responsible for providing the cells with the information on this polarity.

This mechanism is described to occur in three steps. First, a directional cue initiates polarity, which will orient the field with respect to the rest of the embryo; the second step involves the cell-autonomous response that promotes asymmetry in each cell and the amplification of that asymmetry through an intercellular feedback loop; the third step involves controlling the localized activation within cells of specific proteins, by the PCP pathway (Wang and Nathans 2007).

Several studies have shown that PCP pathway is necessary for cilia posterior displacement within the node cells. Mice lacking *dishevelled* (*dvl2* and *dvl3*) genes (cytoplasmic PCP core proteins) were shown not to

be able to correctly locate the basal bodies (from which cilia elongate) to the posterior region of the node cells, and were unable to generate a unidirectional leftward flow (Hashimoto, Shinohara et al. 2010). Also, in mouse conditional mutants for *vangl1* and *vangl2* (which encode PCP transmembrane proteins homologues of the *Drosophila* gene *van gogh* (*vang*)), the basal bodies do not acquire a posterior localization within the cells and consequently cilia also do not acquire a posterior localization or a posterior tilt orientation. Further, the unidirectional leftward flow is compromised, left side specific genes become randomized and internal organs acquire laterality problems (Song, Hu et al. 2010).

It was also shown in zebrafish and *Xenopus* that the PCP gene *vangl2* also regulates the posterior position and tilt of cilia in the KV and gastrocoel roof plate, respectively (Antic, Stubbs et al. 2010; Borovina, Superina et al. 2010). Given this, the PCP mediated polarity in ciliated cells is clearly a conserved approach in mouse, zebrafish and *Xenopus.*

Recently, it was also shown that in the chicken embryo, the subcellular localization of Vangl2 is consistently polarized, giving the cells in the blastoderm a vector pointing towards the primitive streak (PS). Experiments where this protein was non-functional led to a randomized left-sided expression of *shh* (*sonic hedgehog* - one of the first asymmetric genes to be expressed in the chick organizer and a key left-sided determinant) in the Hensen's node (Zhang and Levin 2009).

One of the most attractive features of PCP for understanding LR patterning throughout phyla is its scale of conservation. By setting up alignment of polarization on the cellular level, PCP mechanisms allow embryos to achieve large-scale polarization from intracellular events.

It is not known whether any of the above mentioned events (motor proteins/cytoskeleton, gap junction communications, H^+/K^+-ATPase activity and monocilium function) occur in the same or parallel LR developmental pathways. Thus, the field currently has a series of isolated islands of knowledge about the earliest steps in LR development that precede monocilium function.

Divergent chick, frog, fish and mouse evolution might have provided selective advantages that favoured the orientation of LR asymmetry as early as the first cell cycle in animals such as the frog. Similarly, whether the node functions to initiate LR patterning, as monociliary motion might do in mouse, or respond to early cues, as might occur in chick, could reflect divergent architectures of the node (Dathe, Gamel et al. 2002).

While the node may not be the structure where the initial symmetry of chick or frog embryos is broken, it certainly plays key role for the establishment of LR asymmetries in all vertebrates species analysed so far.

I.4 Chicken embryo as a model system

The chick embryo has played a major role in ground-breaking advances of our understanding on embryonic development and in the LR asymmetry establishment.

This is particularly true for early stages of development, such as gastrulation, when embryos from other species display more complicated geometries (as in the case of the mouse, which gastrulates as a cylinder) or develop on top of comparatively huge yolks (as in the case of zebrafish), thus complicating or obscuring the visualization of gene expression patterns. Instead, the chicken embryo develops as a flat disk, is physically

separated (and easily removed) from the egg yolk, and is large enough in size to allow straightforward identification of the different structures and tissue layers present at early stages of development. It is, therefore, not surprising that the first clues into LR asymmetric gene expression were obtained using the chick embryo.

I.4.1 Early development of the chick

I.4.1.1 CLEAVAGE

The chicken embryo develops in the blastodisc, a small region with a disc shape on top of the yolk. After the egg is fertilized, the cells divide repeatedly (cleavage), giving rise to a multicellular structure called blastula, that in the case of the chicken embryos, is stratified and is therefore called blastoderm (Khaner 1993). After this, morphogenetic movements starts to occur between stages VII-X, at which the center cells of the blastodisc (area pellucida) (Figs. 8a, b) split from the yolk and will give rise to a region beneath the disc, called the sub-germinal cavity (Khaner 1993). The area pellucida remains surrounded by a peripheral region rich in yolk cells (area opaca) (Figs. 8a, b) (Lemaire and Kessel 1997). The most important event for the cleaving embryo is the establishment of the axes polarity.

First, a dorsal and ventral sides become apparent and then the antero-posterior (AP). The establishment of the dorso-ventral (DV) axis is directly associated with the relationship between the yolk and the cytoplasm as those cells in the direct contact with the yolk become ventral and those immediately beneath the vitelline membrane become dorsal and thereafter known as the epiblast. The establishment of the AP axis is

brought about by interaction with the periblast, whose components become shifted by gravity.

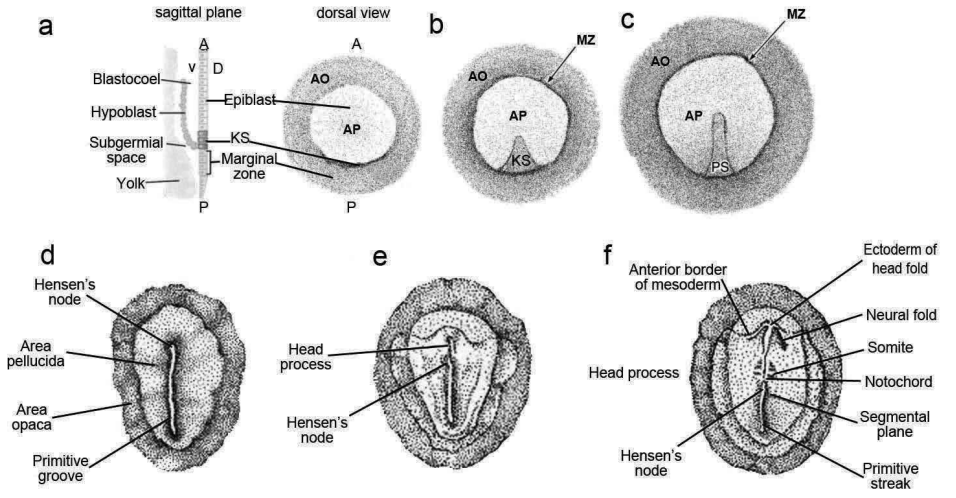

Figure 8| Early gastrulation stages in chick development. Schematic diagram representing the onset of gastrulation in the chick embryo. (**a**) Dorsal surface of the chick embryo at stage XIII. (**b**) A posterior accumulation of cells from the posterior margin of the blastoderm migrates anteriorly to the Koller's sickle. (**c**) Gastrulation initiates with the appearance of the PS. (**d**) When the PS reaches its full extension the Hensen's node is formed. (**e**,**f**) After this, the Hensen's node and PS regresses leaving behind cells that will contribute to the notochord and mesodermic derivatives. AO- Area Opaca; AP- Area Pellucida; MZ- Marginal Zone; KS- Koller's sickle; PS- Primitive Streak; A- anterior; P- posterior; D- dorsal; V- ventral. Adapted from (Bodenstein and Stern 2005) and (Gilbert, 2000).

The majority of the cells from the area pellucida remain at the surface forming the epiblast, while others delaminate and migrate individually into the subgerminal cavity forming the primary hypoblast. Shortly thereafter, a sheet of cells from the posterior margin of the blastoderm (Koller's sickle) migrates anteriorly and pushes the primary hypoblast cells anteriorly to form the secondary hypoblast (Lemaire and Kessel 1997; Bertocchini and Stern 2002).

During these pre-streak stages, the cells from Koller's sickle express genes that codify signalling molecules of growth factor families, like FGF

and TGF-β, while also expressing genes of the Wnt family (Skromne and Stern 2001). This set of genes play important roles in the control of later development (Lawson and Schoenwolf 2001; Chapman, Schubert et al. 2002). The shape of the expression domain of these genes changes from a sickle-shaped domain into an elongated domain along the midline of the embryo, stretching in an anterior direction from the posterior marginal zone.

In the chicken embryo, once the cleavage process is finished, the embryo presents two layers of cells: the epiblast, that originates the proper embryo and the hypoblast from which the extra-embryonic structures are derived (Rosenquist 1972).

I.4.1.2 GASTRULATION

Gastrulation is a critical stage in the development of all higher organisms, since it is the stage where the three germ layers, the ectoderm, the mesoderm and the endoderm are formed (Stern 2004). In avian and mammalian embryos, key events of gastrulation include the formation and progression of the primitive streak (PS), and the ingression of cells through it to form the three germ layers; ectoderm, mesoderm and endoderm (reviewed in (Bellairs 1986; Lemaire and Kessel 1997; Schoenwolf and Smith 2000)).

I.4.1.2.1 PRIMITIVE STREAK FORMATION

Gastrulation is a phase of extensive cellular convergence movements towards the midline of the epiblast (Khaner 1993) and its beginning is indicated by a local thickening close to Koller's sickle, the PS primordium.

The PS in avian embryos is first identified morphologically at stage HH3 (Hamburger and Hamilton 1992), in the caudal third of the area pellucida. It subsequently undergoes progression, during which it elongates and defines the midline of the embryo and the rostro-caudal axis. In parallel, epiblast cells fated to form mesoderm and endoderm, ingress through the PS.

The cells that initiate the PS formation migrate bilaterally and anteriorly from the marginal zone, giving rise to the antero-lateral endoderm and mesoderm (Mikawa, Poh et al. 2004; Cui, Yang et al. 2005). When this migration reaches half of its full extension, the deeper cells of the streak start to move radially away from the midline, as they are replaced by epiblast cells that ingress into the streak after undergoing an epithelial-to-mesenchymal transition (EMT). Epiblast cells undergo intercalations, reminiscent of convergent and extension movements, that contribute to the elongation of the PS (Lawson and Schoenwolf 2001; Voiculescu, Bertocchini et al. 2007).

The movement pattern of the cells in the epiblast then changes and cells in the lateral epiblast start to move medially towards the streak to replace the cells that the streak loses to ingression. The first cells to ingress form the definitive endoderm, which replaces the secondary hypoblast (Bertocchini and Stern 2002).

Streak formation is concurrent with large vortical flows of cells in the epiblast. These vortices rotate in opposite directions, away from the midline in the anterior and towards the midline in the posterior (Cui, Yang et al. 2005; Chuai and Weijer 2008; Chuai and Weijer 2009). The streak extends progressively in the anterior direction until it reaches ~80% of the length of the area opaca reaching the stage HH4.

The formation of the PS relies on a complex network of signalling pathways that work together to ensure that this process is highly-regulated. Activation of various secreted factors (Vg1, Nodal, Wnt8C, Fgf8 and Chordin) (Shah, Skromne et al. 1997; Bachvarova, Skromne et al. 1998; Skromne and Stern 2001; Bertocchini and Stern 2002) and transcription factors (Brachyury and Goosecoid) (Izpisua-Belmonte, De Robertis et al. 1993; Kispert, Ortner et al. 1995) adjacent to the site of streak formation are required for this process. In addition, structures, such as the hypoblast, also play an important role in the regulation of streak formation.

Removal of the hypoblast in the chick results in correctly patterned ectopic streaks, suggesting that the hypoblast serves to inhibit formation of the PS (Bertocchini and Stern 2002).

The formation and elongation of the PS gives rise to two of the three germinative layers: the endoderm (which substitutes the hypoblast) and the mesoderm. The cells that remain in the epiblast will form the ectoderm, the third germinative layer (Bellairs 1986) (Fig. 9).

Finally, purely on theoretical grounds, it as been proposed that streak formation might involve chemotaxis (Painter, Maini et al. 2000; Mikawa, Poh et al. 2004). Cells in the epiblast could secrete an attractant for streak cells or a combination of attractants and repellents as proposed for the migration of mesoderm cells away from the streak and back towards the midline (Yang, Dormann et al. 2002).

Recently, through a series of simulations, it was suggested that the formation of the PS employs chemotactic movement of a subpopulation of streak cells, as well as differential adhesion between the mesoderm cells and the other cells in the epiblast. Consequently, both chemo-attraction and chemo-repulsion between various combinations of cell types can create a streak (Vasiev, Balter et al. 2010).

So far, there is no experimental data to support this mechanism nor there have been identified any potential signalling molecules.

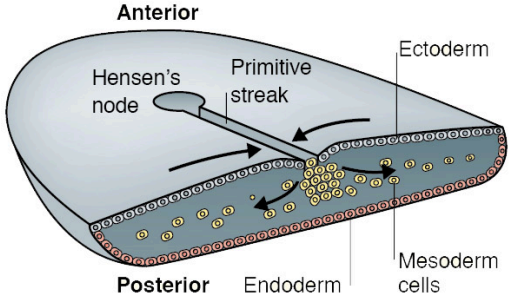

Figure 9| Schematic representation of a transversal section from the blastoderm of a chicken embryo at stage HH4. Arrows represent mesoderm cell migration through the Primitive Streak. From (Maroto, Bone et al. 2012)

I.4.1.2.2. HENSEN'S NODE

When the PS is fully extended at stage HH4, a small group of streak cells located at the anterior tip of the PS will form the Hensen's node (Bellairs 1986).

The Hensen's node is the amniote equivalent of the amphibian "Spemann's organizer" and analogous to the dorsal blastoporal lip of the amphibian embryo, it is usually considered as being the most important structure in the embryo during gastrulation. In addition to its ability to differentiate into several embryonic tissues (prechordal region, notochord, pre-somitic mesoderm, medial somites and gut) (Spratt 1958; Nicolet 1970; Selleck and Stern 1991; Schoenwolf, Garcia-Martinez et al. 1992), it has also the capacity to induce a secondary embryonic axis, when transplanted to a new host embryo (Tsung, Ning et al. 1965; Dias and Schoenwolf 1990) thereby giving it the condition of organizer (Grabowski 1957).

The cellular and molecular nature of organizer activity has long attracted the attention of developmental biologists. This special region of the vertebrate embryo self-differentiates into a number of embryonic tissues (Dias and Schoenwolf 1990; Selleck and Stern 1991).

To help in the understanding of how the embryo is built, researchers constructed “fate maps”, which show us the fate of early-embryonic cells in later embryonic stages. Fate maps, were generated using a variety of techniques to find out which structures in the body are eventually produced from particular cells or groups of cells in embryos. Extensive fate mapping studies have been performed in the Hensen's node by various tracing methods like, carbon particles (Spratt 1946), radiolabelled grafts (Rosenquist 1983) or vital dyes (Selleck and Stern 1991). Hence, it was possible to establish a precise knowledge of the avian organizer.

Selleck *et al* have mapped the Hensen's node more accurately using these lipophilic dyes and so traced the node cells contribution. They discovered that the Hensen's node could be divided into three regions: the more anterior midline that contains presumptive notochord cells and the two lateral regions containing notochord cells and presumptive medial somite cells (Fig. 10). The fate map study revealed that the node is not a homogeneous structure, but organized spatially. In addition, the fates of cells present in the node change with time (Selleck and Stern 1991).

Unlike what was initially thought, the node is not a fixed population of cells. Fate map and gene expression studies show that the cellular composition of the node changes constantly. Cells emigrate from the node and are replaced by cells from the surrounding epiblast, which then acquire node (organizer) properties according to their position. According to this, the node is not a committed cell population defined by its cellular

ancestry, but rather a cell state (Selleck and Stern 1991; Joubin and Stern 1999). This dynamic nature becomes also apparent, when the node is experimentally ablated and in just a few hours after being ablated the organizer markers reappear and reconstitute the node (Psychoyos and Stern 1996; Joubin and Stern 1999).

Despite the dynamic composition of the node at early stages, single cell lineage analysis has suggested that the node also contains a small population of resident cells with stem-cell characteristics (Selleck and Stern 1991). It was proposed that when these cells divide, one daughter remains in the node while the other leaves to contribute to notochord and/or medial somite (Selleck and Stern 1991; Stern, Hatada et al. 1992). Ever since this first description, the node has continued to fascinate generations of embryologists. It attracted much interest during the last decade with the discovery of molecular networks acting in and around it during patterning of the AP (cranio-caudal), the DV, and the transverse (left-right) body axes.

I.4.1.2.3 Primitive streak and Hensen's node regression

The final change that occurs in the PS is regression, a rostro-caudal shortening of the streak that continues until Hensen's node and a short persisting remnant of the PS is incorporated into the tail bud (Schoenwolf 1979; Bellairs 1986).

The PS starts to regress, while the mesodermal ingression continues and thus moving Hensen's node from near the center of the area pellucida to a more posterior position. Cells keep on moving out of the streak during the regression process. During regression the node gives rise to cells of the

notochord and the floor plate of the neural tube, while anterior streak cells will form somites, middle streak cells form lateral plate mesoderm and the posterior mesoderm cells form the vasculature and blood islands as well as other extra-embryonic structures (Fig. 10) (Psychoyos and Stern 1996; Yang, Dormann et al. 2002).

Regression of the node is likely also helped by the ingression of epiblast cells into the streak, which results in its shortening. However, convergent-extension also plays a major role in the process as mentioned earlier (Spratt, 1947; Bellairs, 1963; Lepori, 1966; Stern and Bellairs, 1984; Schoenwolf et al., 1992; Catala et al., 1996; Colas and Schoenwolf, 2001).

At the same time that the PS and the Hensen's node are regressing (meaning that they are moving posteriorly) the notochord is being left behind. So that the notochord can extend and so leading to node's regression, three cellular processes must occur: addition of cells to the posterior end of the notochord, which are supplied by cell division in the node (Sausedo and Schoenwolf 1993); cell division within the notochord, preferentially oriented parallel to the AP axis, which results to the contribution of the notochord length rather than its width and lastly, the cells must undergo medio-lateral intercalation as they move out of the node and into the notochord (Schoenwolf and Alvarez 1989).

While regression continues, the deposition of axial and paraxial mesoderm continue as the whole embryo narrows and elongates caudally to generate the tail bud (Sanders, Khare et al. 1986; Catala, Teillet et al. 1996; Knezevic, De Santo et al. 1998; Charrier, Lapointe et al. 2002). Eventually, the PS and node become condensed to form a mass of cells in the tail bud of the 3–4 day embryo (Schoenwolf 1979; Bellairs 1986).

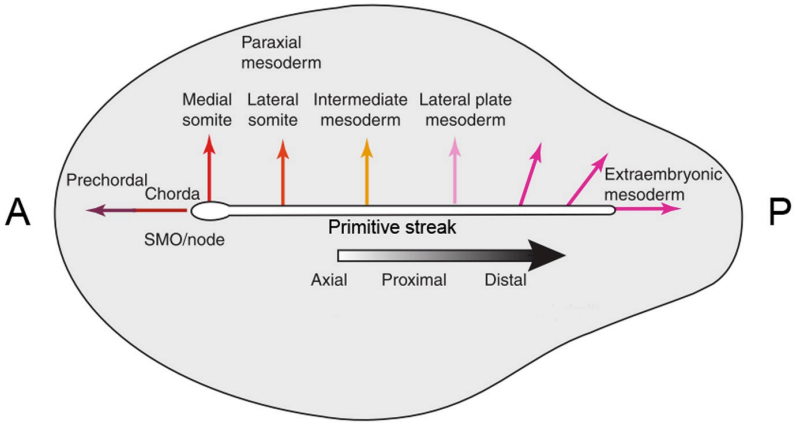

Figure 10| Mesodermal cell fates during vertebrate gastrulation. Schematic diagram of a chick embryo at stage HH4, when the PS is most elongated. The colored arrows point to the specific fate of the mesodermal cells that ingress at the corresponding axial level. A-anterior; P-posterior. Adapted from (Solnica-Krezel 2005).

I.4.2 Hensen's node - a Left-Right inducer

The chick node displays a number of striking asymmetries that appear well before any overt signs of asymmetry can be detected in any other part of the embryo. For instance, a transient morphological asymmetry is apparent at the chick node as early as stage HH4. Similarly, a number of genes are expressed asymmetrically at the chick node, immediately after it becomes asymmetric morphologically (Dathe, Gamel et al. 2002).

It is known that most vertebrates such as mouse (Sulik, Dehart et al. 1994), zebrafish and *Xenopus* (Essner, Vogan et al. 2002) have cilia in their nodes and it is also known that, the leftward fluid flow generated by cilia breaks the initial symmetry (reviewed in (Hirokawa, Tanaka et al. 2006)).

In the chicken, however, symmetry breaking does not appear to involve cilia-generated flow. Cilia are found in the Hensen's node long

after LR asymmetry has already been established, and in addition these cilia seem to be present only in the epiblast in a relatively small sub-population of cells at the node. This, together with the fact that the Hensen's node does not seem to be morphologically suited to create a fluid flow, suggests that there is no equivalent of the ventral mouse node in the chick embryo (Manner 2001).

In contrast, there are evidences showing that there are cilia in the node on the endodermal cells. The authors also observed that *lrdr* (*lrd*-related) was expressed during gastrulation within Hensen's node and PS (Essner, Vogan et al. 2002). Interestingly, chick mutant *talpid3* (encodes a centrosomal protein necessary for primary cilia formation) lacks primary cilia but does not exhibit LR asymmetry defects meaning that cilia in the chicken is not essential for LR asymmetry establishment (Yin, Bangs et al. 2009).

These findings make the chicken an exception to the fluid flow model. As a replacement for using cilia to generate a leftward fluid flow and thus establish the LR axis, the chicken seems to have adopted an alternative strategy to generate LR molecular asymmetries in the node.

Recently, it was discovered that cells from the epiblast in and around the node, migrate from the right to the left side at stage HH4 before *shh* and *fgf8* become asymmetrically expressed in the node. At stage HH5, and as a consequence of this transient leftward movements, *shh*-expressing cells that were initially located in the rostral part of Hensen's node are displaced to the left and *fgf8*-expressing cells initially detected in the PS/caudal part of Hensen's node are displaced to the node right side (Gros et al., 2009, Cui et al., 2009). Gros *et al*, (2009) also showed that these leftward cell movements that occur in the node region at stage HH4 are

promoted by the activity of the H^+/K^+ATPase exchanger. However, what directs these movements specifically to the left, it is not known (Fig. 11).

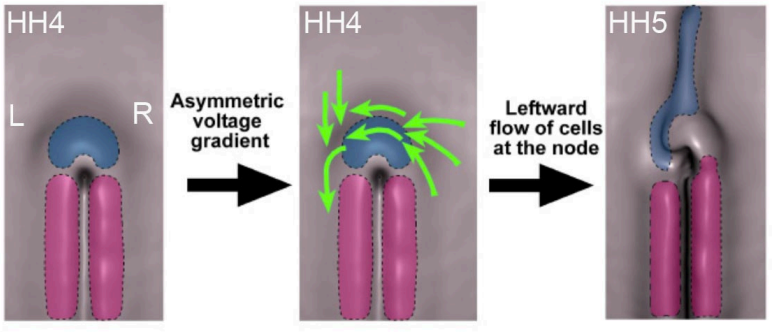

Figure 11| Leftward cell movements generates asymmetry in the chicken Hensen's node. By stage HH4 the node is morphologically symmetric as the expression of *shh* (blue) and *fgf8* (pink), then a differential transient membrane depolarization at stage HH4 drive the leftward movement of cells at the node, leading consequently to asymmetric expression of *shh* and *fgf8* in the node at stage HH5. Adapted from (Gros, Feistel et al. 2009).

There are several lines of evidence suggesting that LR pattern is not originated in the node but, rather, that it responds to signals from elsewhere in the blastoderm. Experiments where the node was ablated showed that it is able to regenerate with correct LR asymmetry, as assessed by the expression of the left-sided gene *shh* (Psychoyos and Stern 1996). In contrast, portions of the blastoderm, when cultured separately, also regenerate the node, but without proper patterning of the LR axis (Levin and Mercola 1998; Yuan and Schoenwolf 1998). One interpretation of these observations is that signals from potentially distant regions of the blastodisc may be required upstream of LR patterning of Hensen's node.

Several mechanisms have been proposed to act upstream of sided gene expression to orient LR asymmetry (H^+/K^+ATPase; Ca^{2+}; 5HT; H^+-V-ATPase) (Levin and Mercola 1998; Bunney, De Boer et al. 2003; Fukumoto, Kema et

al. 2005; Tanaka, Okada et al. 2005).

As it was already mentioned, a differential in H^+/K^+-ATPase activity across the Hensen's node creates a gradient in membrane potentials, which in turn may originate a differential ion flux across the LR axis (Levin, Thorlin et al. 2002). It has been proposed that small and charged molecules, which are, under physiological conditions, capable to cross through GJ, will accumulate on one side of the embryo's node. The previously mentioned 5HT may be one such molecule, and another likely candidate is Ca^{2+}.

In fact, H^+/K^+-ATPase activity does result in extracellular Ca^{2+} accumulation on the left side of Hensen's node. Raya *et al*. thought that the accumulation of Ca^{2+} on one side of the node could locally modulate the activity of the Notch signalling pathway. It has been known for some time that the EGF (epidermal growth factor) repeats found in the extracellular domains of both Notch and its ligands bind calcium ions (Rao, Handford et al. 1995; Rand, Lindblom et al. 1997). This means that Ca^{2+} accumulation will induce an asymmetric activation of Notch on the left side of the node that then translates this differential activity into asymmetric *nodal* expression (Raya, Kawakami et al. 2004).

The role of the Notch signalling pathway in providing polarity cues in various organisms, from nematodes to mammals, is well established (Raya, Kawakami et al. 2003).

I.4.2.1 LEFT SIDE GENE EXPRESSION IN THE NODE

The earliest observed asymmetry is at stage HH4, when the expression of *cAct-RIIa* (which encodes the Activin type IIa receptor,) was shown to be restricted to the right side of Hensen's node and the PS. This asymmetric

cActRIIa expression results in repression of the chicken *sonic hedgehog* (*shh*) gene on that side, so that *shh* becomes expressed only on the left side of the node at stage HH5 (Levin, Johnson et al. 1995).

These relationships were established by showing that implantation of Activin-coated beads in the left side downregulated the expression of *shh*. Likewise, applying beads coated with the Activin inhibitor (Follistatin) on the right side resulted in bilateral *shh* expression, suggesting that *shh* asymmetry results from Activin activity (Levin, Pagan et al. 1997).

Repression of *shh* by Activin signalling is far from being direct, and appears to be mediated by a regulatory gene network involving cMid1 (Granata and Quaderi, 2003), and Bmp4 (Monsoro-Burq and Le Douarin, 2000; Monsoro-Burq and Le Douarin, 2001). This last one is expressed in the posterior right side around Hensen's node and locally represses *shh* expression.

Left-sided expression of *shh*, in turn, would eventually result in left-sided expression of *nodal* (TGFβ-related gene) in a small domain just anterior to Hensen's node at HH5-HH7, and indeed, implanted cells expressing *shh* on the right side of Hensen's node was sufficient to induce an ectopic domain of *nodal* expression on the right side (Levin, Johnson et al. 1995). Similarly, to what happens with *shh*, the induction of Nodal by Hedgehog activity involves a complex regulation of BMP antagonism (Piedra and Ros 2002; Schlange, Arnold et al. 2002) that includes the secreted factor *caronte* (*cer1*) (secreted protein related to Cerberus/Dan family of Bone Morphogenetic Proteins (BMPs) antagonists) (Rodriguez Esteban, Capdevila et al. 1999; Yokouchi, Vogan et al. 1999; Zhu, Marvin et al. 1999).

More recently, another paper provided new evidences showing that a leftward cell movement around the node downstream of the proton pump is responsible to place asymmetrically *shh*-expressing cells in the node, as it was mentioned above (Darnell and Schoenwolf 2000; Cui, Little et al. 2009; Gros, Feistel et al. 2009). The authors do not contradict the epistatic relationships already found to be crucial to modulate asymmetries in the node. They argue that these cross-regulations might function secondarily to sharpen borders and provide robustness in those gene expression domains (Gros, Feistel et al. 2009).

I.4.2.2 RIGHT SIDE GENE EXPRESSION IN THE NODE

Furthermore, at the same time that the left sided genes are being activated, a right-sided regulatory cascade of gene expression is established around Hensen's node. This right-sided cascade is initiated by Activin signalling (as it was already mentioned above), that through activation of cMid1 (Granata and Quaderi 2005) and BMP4 (Monsoro-Burq and Le Douarin 2000; Monsoro-Burq and Le Douarin 2001), induces the expression of the *fgf8* at stage HH5 (member of the Fibroblast Growth Factor family) (Boettger, Wittler et al. 1999), probably mediated by Fgf18 (Ohuchi, Kimura et al. 2000).

The asymmetric expression of *fgf8* is responsible for the downregulation of *cer1* on the right side of the node (Rodriguez Esteban, Capdevila et al. 1999) (Fig 12). This was verified by applying beads soaked in Fgf8 on the left side of the node or beads soaked in Fgf receptor inhibitor on the right and confirmed that *cer1* expression was downregulated or induced, respectively (Rodriguez Esteban, Capdevila et al. 1999). *Fgf8* on the right side of the Hensen's node, starts at stage HH5

and is required to prevent the left-sided pathway from becoming inappropriately activated on the right side (Fig. 12) (Boettger, Wittler et al. 1999).

N-cadherin an adherent junction molecule was also found to be a crucial player in LR asymmetry, when a few years ago, it was discovered that this cell-cell adhesion molecule was asymmetrically expressed in the node and necessary to correct position the chicken heart (Garcia-Castro, Vielmetter et al. 2000). The authors observed that, the expression of N-cadherin starts to be symmetrically localized in the node and PS at stage HH4. However, at stage HH5 it becomes restricted to the right side of the node and on the left side of the PS (Garcia-Castro, Vielmetter et al. 2000). They also found that blocking N-cadherin activity does not affect the asymmetric gene expression in the node, but changed the expression of LPM genes, such as, *snail* (*snai1*) and *pitx2* that are important to dictate the laterality of the internal organs.

I.4.3 Left-Right asymmetry, downstream of the Node

The transient LR asymmetries that are established around the node during gastrulation are transferred to and stabilized in the LPM and subsequently coordinate the asymmetric development of the various organs primordia. Signals from the node lead to the conserved unilateral left-sided expression of *nodal* within the left LPM, and its downstream target genes: the feedback antagonist genes *lefty1* and *lefty2* and the effector transcription factor gene *pitx2* (Fig. 12).

Significantly, left-specific expression of *nodal* within the LPM has been observed in all vertebrates examined to date, and aberrant patterns of

nodal expression in the LPM are closely correlated with *situs* abnormalities (Levin, Johnson et al. 1995; Collignon, Varlet et al. 1996; Lowe, Supp et al. 1996; Lohr, Danos et al. 1997; Sampath, Cheng et al. 1997; Rebagliati, Toyama et al. 1998).

I.4.3.1 NODAL IN THE LEFT LATERAL PLATE MESODERM AND ASYMMETRIC GENE EXPRESSION

In the chicken embryo, *shh* in the node is necessary and sufficient for inducing *nodal* in the left LPM (Levin, Johnson et al. 1995; Pagan-Westphal and Tabin 1998) (Fig. 12). However, experiments involving explants of LPM have demonstrated that this induction of *nodal* in the LPM by *shh* is not direct, but rather it might be mediated by another secondary signal produced in the paraxial mesoderm (Pagan-Westphal and Tabin 1998).

Cer1 as a long-range signalling molecule fulfils the criteria to be such molecule. *Cer1* is necessary and sufficient to transmit the Shh signal from the node to the left LPM, leading *nodal* activation and subsequent establishment of LR-specific gene expression (Rodriguez Esteban, Capdevila et al. 1999). One of the models that support this hypothesis considers that, this induction of *nodal* by Cer1 is possible because this last one acts upstream of *nodal* in the LPM and also because *nodal* expression in the LPM results from the abolition of its repressor BMP by *cer1* (Rodriguez Esteban, Capdevila et al. 1999; Yokouchi, Vogan et al. 1999).

Another proposed model to induce *nodal* expression and its restriction on the left LPM, suggests that Nodal in the node directly induces *cer1* expression on the left LPM. The authors also propose that Nodal can activate its own transcription (reviewed in (Hamada, Meno et al. 2002)), leading to *nodal* amplification and *cer1* expression throughout the

left LPM (Tavares, Andrade et al. 2007).

The continuous expression of *nodal* can be regulated by a positive-feedback loop via the Nodal-responsive enhancer, which induces its own expression as well as its downstream targets *lefty1* in the notochord and *lefty2* in the left LPM. Both act as a feedback inhibitors of *nodal* activity, Lefty1 by restricting *nodal* expression to the left side, and Lefty2 by avoiding its spreading out (Fig. 12).

This combination of positive and negative feedback loops constitutes a Self-Enhancement and Lateral Inhibition (SELI) model, that can amplify a small expression into a robust one in the LPM (Nakamura, Mine et al. 2006). This SELI system seems to be conserved among vertebrate species (Nakamura, Mine et al. 2006; Marjoram and Wright 2011). Mathematical modelling indicates that the SELI system can establish correct LR patterning, only if the diffusion velocity of Lefty is higher than that of Nodal, this can be achieved by differences in travelling velocity. An early study suggested that in fact, Lefty travels faster than Nodal (Sakuma, Ohnishi Yi et al. 2002), and recent work has directly revealed such a difference in the diffusion velocities of Lefty and Nodal (Marjoram and Wright 2011).

Pitx2 is a transcription factor whose expression was shown to be downstream of Nodal activity and whose function is required for normal LR heart and gut morphogenesis in chick, mouse and frog embryos (Logan, Pagan-Westphal et al. 1998). Asymmetric expression of *pitx2* begins in the left LPM concomitantly with that of *nodal*, but it persists after *nodal* expression disappears (Ryan, Blumberg et al. 1998). *Pitx2* was the first gene identified to exhibit asymmetric expression in developing organs as they undergo left-side morphology. Thus, *pitx2* acts as a key transcription

factor conferring left-sided instructions to developing organ primordia in an evolutionary conserved signalling module initiated by *nodal* (Ryan, Blumberg et al. 1998).

Other transcription factors are likely to participate in the relay of left information mediated by Nodal, such as the homeobox gene *nkx3.2*, which is expressed in the left LPM of stage HH10-11 chick embryos in response to Nodal activity (Rodriguez Esteban, Capdevila et al. 1999; Schneider, Mijalski et al. 1999), although its exact role in this process has not been fully characterized.

I.4.3.2 RIGHT LATERAL PLATE MESODERM AND ASYMMETRIC GENE EXPRESSION

A right-sided regulatory cascade of gene expression is established around Hensen's node that ultimately leads to restriction in the expression pattern of *snail1* (*snai1*), a zinc finger transcription factor at the right LPM starting at stage HH8^{+} (Isaac, Sargent et al. 1997). *Fgf8* asymmetric expression on the right side of the node induces the transcriptional repressor *snai1* in the right LPM (Boettger, Wittler et al. 1999). Snai1 on the other hand, represses *nodal* expression in the chick embryo, which was also observed in mutant mice that conditionally lack *snai1* and exhibit bilateral *nodal* expression (Boettger, Wittler et al. 1999; Patel, Isaac et al. 1999; (Murray and Gridley 2006). More importantly, strong downregulation of Snai1 function results in ectopic *pitx2* expression in the right LPM (Patel, Isaac et al. 1999), which means that *snai1* functions to provide additional restriction of left-sided genes by expression of *pitx2* expression.

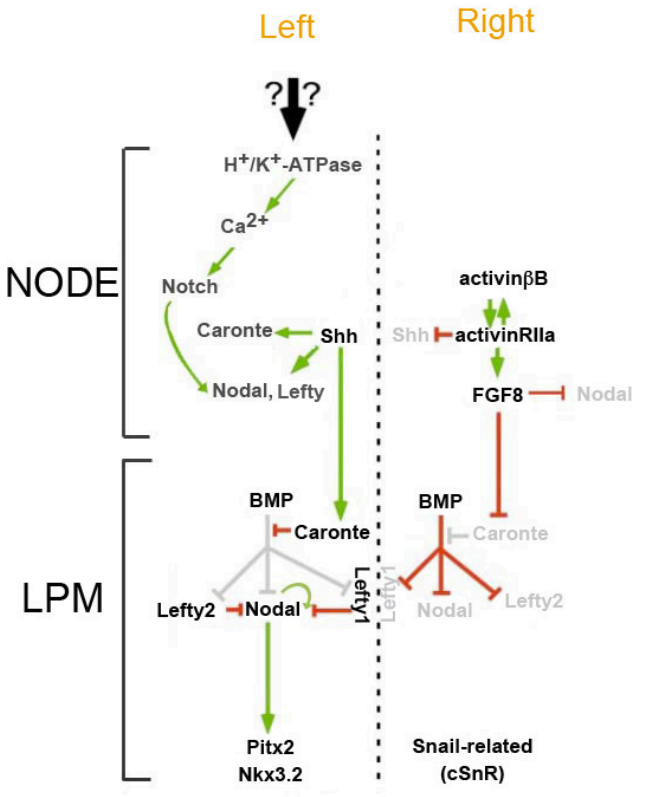

Figure 12| Schematic representation of the genes involved in chick left-right asymmetry pathway. On the right side, the earliest known gene to be asymmetrically expressed is *ActivinB,* which will inhibit *Shh* expression through BMP4 (not represented). In this way, *shh* pathway is inhibited on the right side. On the left side, *shh* is not inhibited therefore it induces *nodal* expression. Later in the LPM *caronte* inhibits *nodal* inhibitors, which will leads to Nodal expression and consequently the induction of other genes like *Lefty1* and *Pitx2*. Gray shading indicates that a pathway or expression of a particular gene is suppressed (e.g., *nodal* on the right side), whereas red and green denote suppression and induction, respectively. Dashed line corresponds to the midline. Adapted from (Mercola and Levin 2001)

I.4.4 Stabilization of side-specific gene expression – – Midline Barrier Model

As important as establishing wide domains of LR-sided gene expression in the LPM is the control of such gene products and/or functions to prevent their spread to the contralateral side. Several lines of evidence suggest

that the midline functions as a barrier to prevent this contralateral expansion of asymmetric signals (Levin, Roberts et al. 1996; Lohr, Danos et al. 1997). This is based on the fact that notochord removal caused LR alterations in *Xenopus* embryos (Danos and Yost 1995).

Similar conclusions were reached by analysis of cross-signalling between twin embryos (Levin et al., 1996) and it has been further confirmed by a number of mouse and zebrafish mutants analysis (reviewed in (Stemple 2005)). Molecularly, the role of the midline barrier is best exemplified by *lefty1*, a divergent TGFβ superfamily member expressed in the left side of the node and the left half of the prospective floor plate in the chick and mouse embryos (Meno, Saijoh et al. 1996). Lefty1 is a feedback inhibitor of Nodal that restricts the area of Nodal signalling and the duration of *nodal* expression.

Vertebrates possess two *lefty* genes, *lefty1* and *lefty2*, which are expressed in the midline and left LPM, respectively. Their expression is induced by Nodal signalling (Yamamoto, Mine et al. 2003). In the absence of *lefty1* or *lefty2*, asymmetric *nodal* expression in the LPM begins normally, but the Nodal signal subsequently leaks to the right side, resulting in bilateral *nodal* expression (Meno, Shimono et al. 1998; Meno, Takeuchi et al. 2001). Mutation in *lefty1* results in spread of left-specific genes to the right side of the mouse embryo, such as bilateral expression of *nodal*, *lefty2* and *pitx2* (left-side-specific genes), finally leading to pulmonary left isomerism (Meno, Shimono et al. 1998). These phenotypes indicate that *lefty1* induces/functions at the midline barrier, preventing an unknown left-side-specific signalling molecule from crossing the midline.

In order to function as such, the barrier would have to confine the passage of a signal (“X” factor) across the midline. One simple way of doing this is by physical interaction between Lefty1 protein and the signal

itself, so that it could prevent its diffusion. It has been suggested that Cer1 might be this “X” factor, as it is a long-range signal identified in chick that can induce *nodal* expression. It also inhibits BMP and relays LR information from the node to the left LPM (Rodriguez Esteban, Capdevila et al. 1999; Yokouchi, Vogan et al. 1999).

The supposed binding of these two molecules, Lefty1 and Cer1 would prevent this last one from interfering with the BMP mediated repression of *nodal* on the right side of the LPM. However, until now, there is no evidence for a direct interaction between the Cer1 and the Lefty1 proteins.

Another hypothesis could be that Nodal itself is the “X” factor, since Nodal is a long range-acting molecule (Chen and Schier, 2001; Meno et al., 2001). Lefty1 from the floor plate might bind to Nodal receptors in the adjacent area and prevent Nodal activity from being propagated across the midline.

Its known that *nodal* in the LPM diffuses over to the prospective floor plate and induces *lefty1,* which is consistent with the notion that *nodal* is able to act over a long distance (Chen and Schier 2001; Meno, Takeuchi et al. 2001). *Lefty1* expression in the left floor plate initiates slightly later than *nodal* in the left LPM, suggesting that the midline barrier might be required only when the left-side signals, such as *nodal* and *lefty2*, are already present.

In the absence of *lefty1* the ectopic expression of the left-side-specific genes occurs mainly in the anterior region of the right side of the LPM (Meno, Shimono et al. 1998), suggesting that the anterior and the posterior portions of the midline barrier are formed and/or maintained by distinct mechanisms. While *lefty1* might be a component of the anterior midline barrier, the posterior portion of the midline barrier might involve a different process.

Recently, in the zebrafish embryo, it was proposed that BMP signalling acts as a “posterior barrier” preventing Nodal propagation through the posterior LPM (Lenhart, Lin et al. 2011). In contrast to previous reports, the authors found that BMP represses Nodal signalling independently of *lefty1* expression and through the activity of a ligand other than BMP4. The “anterior barrier” that is mediated by *lefty2* expression in the left cardiac field prevents Nodal activation across the anterior limit of the notochord and its propagation down the right LPM (Lenhart, Lin et al. 2011).

Another evidence for a non-molecular midline barrier shows that there is a physical barrier composed by death cells in the streak midline of the chicken embryo that avoids the spread of signals from one side of the embryo to the other. Kelly et al, (2002) addressed if specific components of the midline could be at the base of LR expression maintenance.

They showed that, in the chick embryo, a distinct population of cells forms the midline of the PS. These cells in the dorsal midline of the PS express the gastrulation markers *fgf8* and *brachury* and undergo programmed cell death. These dead cells remain in the midline throughout gastrulation. If cell death is inhibited in the midline the early expression of left-sided genes, such as *shh* and *nodal*, is disrupted. The expression of *shh* is significantly down-regulated and expanded into the right side of the node. Although still expressed asymmetrically, *nodal* expression is also downregulated. These embryos exhibited randomized heart looping suggesting that cell death along the PS midline might be a novel mechanism involved in the regulation of LR asymmetry at the early stages of development (Kelly, Wei et al. 2002).

Table 1| Some of the asymmetrically expressed genes in the chicken embryo

GENE	ROLE	STAGE	EXPRESSION	REFERENCE
cAct-RIIa	TGFβ receptor	HH4-HH5	Right N	(Levin, Johnson et al. 1995)
Activin-βB	TGFβ signal	HH4	Right N	(Levin, Pagan et al. 1997)
Bmp4	TGFβ receptor (BMP)	HH5$^-$-HH7$^-$	Right N	(Monsoro-Burq and Le Douarin 2000)
Cer1	TGFβ antagonist	HH7	Left N	(Rodriguez Esteban, Capdevila et al. 1999; Yokouchi, Vogan et al. 1999)
		HH8-HH11	Left LPM	
Fgf8	FGF signal	HH5-HH8	Right N	(Boettger, Wittler et al. 1999)
Lefty1	TGFβ signal	HH5	Left N	(Rodriguez Esteban, Capdevila et al. 1999)
		HH7-HH11	Left midline	
		HH8-HH11	Left LPM	
Lfng	Notch modulator	HH6	Left N	(Raya, Kawakami et al. 2004)
cMid1	Cytoskeletal protein	HH5-HH7	Right N	(Granata and Quaderi 2003)
N-cadherin	Adhesion molecule	HH4$^+$-HH5	Right N	(Garcia-Castro, Vielmetter et al. 2000)
Nodal	TGFβ signal	HH5-HH7	Left N	(Levin, Johnson et al. 1995)
		HH7-HH11	Left LPM	
NKX3.2	Transcription factor	HH9-HH18	Left LPM	(Schneider, Mijalski et al. 1999)
Pitx2	Transcription factor	HH8-HH16	Left LPM	(Logan, Pagan-Westphal et al. 1998)
Shh	Hegdehog signal	HH5-HH7	Left N	(Levin, Johnson et al. 1995)
Snai1	Transcription factor	HH8-HH9	Left N Left LM	(Isaac, Sargent et al. 1997)

HH- Hamburger and Hamilton; LPM- lateral plate mesoderm; N- node

I.5 Late steps: Asymmetric organ morphogenesis

The final step of LR patterning is the translation of the asymmetric signals outlined above (see also Table 1) into the asymmetric morphology of the internal organs. Various visceral organs start to develop anatomic

asymmetries only after asymmetric *nodal* expression in the LPM has disappeared. The main player that regulates asymmetric organogenesis is the transcription factor Pitx2 (Logan, Pagan-Westphal et al. 1998; Yoshioka, Meno et al. 1998), whose asymmetric expression is induced by Nodal (Shiratori, Sakuma et al. 2001).

Like *nodal* and *lefty2*, *pitx2* is expressed asymmetrically in the left LPM, but asymmetric expression of *pitx2* persists until much later stages. Unlike other left-specific genes, *pitx2* is also expressed at subsequent stages on the left side of several organ primordia, including the heart, gut and stomach, which make it a good candidate to mediate the transfer of LR information from the LPM to the developing organs.

Transcriptional regulation analysis of *pitx2* in the mouse embryo showed that a left side-specific enhancer (ASE) contains three binding sites for FAST (*FoxH1*). The authors observed that the FAST binding sites functions as Nodal-responsive elements, which are sufficient for the initiation of *nodal* expression but not for its maintenance. For this, it is required an Nkx2.5 binding site also present within the ASE, which means that the left-sided expression of *pitx2* is initiated by Nodal signalling and is maintained by Nkx2.5 (Shiratori, Sakuma et al. 2001).

Recently it has been shown that *pitx2c* (mice *pitx2*), which encodes one of the isoforms of the *pitx2* gene (Essner, Branford et al. 2000), induces its own transcription, which could act as a maintenance mechanism after *nodal* expression fades in the left LPM (Schweickert, Campione et al. 2000). Ectopic expression of *pitx2* on the right side of the LPM can cause laterality defects in a variety of vertebrates (Logan, Pagan-Westphal et al. 1998; Ryan, Blumberg et al. 1998; Campione, Steinbeisser et al. 1999; Essner, Branford et al. 2000), and *pitx2*-deficient mice display laterality defects that include right pulmonary isomerism, which is

consistent with a role for *pitx2* as a left determinant (Gage, Suh et al. 1999; Kitamura, Miura et al. 1999). However, the direction of heart looping is normal in Pitx2-deficient mice, which clearly indicates that other factors, in addition to *pitx2*, contribute to the asymmetric development of the heart.

In zebrafish, the asymmetric migration of cardiac progenitor cells is responsible for this cardiac rotation. This asymmetric migration is regulated by BMP signalling, which is preferentially activated in the LPM on the left side and is controlled by early asymmetric Nodal signalling (de Campos-Baptista, Holtzman et al. 2008; Rohr, Otten et al. 2008). However, it remains unknown whether this migration depends on Pitx2 or not.

Another role of *pitx2* in asymmetry has been shown through its regulation on gonad morphogenesis. Although in most vertebrates the urogenital system is symmetrically bilateral in both genders, in birds the bilateral development of paired gonads is sex-dependent. Female chick embryos undergo asymmetrical gonad morphogenesis that results in only one functional ovary, the left one, while the right gonad degenerates at later stages of development. *Pitx2* is only expressed on the left gonad and it influences gonad shape and size by controlling somatic cell morphology, extra-cellular composition, spindle orientation and cell proliferation (Rodriguez-Leon, Rodriguez Esteban et al. 2008).
Looping of the chick gut is determined by LR asymmetries in the cellular architecture of the dorsal mesentery, the structure that connects the developing gut to the body wall (Davis, Kurpios et al. 2008; Kurpios, MacNeil et al. 2009; Plageman, Zacharias et al. 2011). In addition, the overlying epithelium shows LR asymmetries in cellular morphology that are under the control of Pitx2.

Snai1 (on the right side) and Nkx3.2 (on the left side) are two other transcription factors downstream of Nodal in the LPM that are likely to influence LR asymmetry development of organ primordia.

In the chick, *snai1* (Isaac, Sargent et al. 1997), like its mouse counterpart (Sefton, Sanchez et al. 1998) is initially expressed bilaterally in presumptive anterior cardiac mesoderm; however, as development proceeds, the expression of *snai1* in both species becomes stronger in the right LPM.

In the chicken *nodal* acts as a repressor of *snai1* and as an activator of *Nkx3.2*. The *snai1* gene appears to be negatively regulated by Nodal, given that misexpression of Nodal on the right side of chick embryos abolishes *snai1* expression. *snai1* seems to act independently on the right side to influence the direction of heart looping (Patel, Isaac et al. 1999).

Nkx3.2 encodes a homeodomain protein that is left-sided in the chick and right sided in the mouse (Rodriguez Esteban, Capdevila et al. 1999; Schneider and Mercola 1999). In chick it is repressed by *nodal*, but this situation is reversed in the mouse. Mutant mice lacking *Nkx3.2* do not have obvious *situs* defects (Lettice, Hecksher-Sorensen et al. 2001) but they lack a spleen and have morphological abnormalities of the gastroduodenal portion of the gut.

I.6 Evolutionary conservation

The symmetry-breaking step is the most variable step in the process of establishing asymmetry among vertebrates. Although the initial mechanisms that break symmetry remain mysterious, a detailed molecular

pathway involved in transferring positional information from the node to the periphery has been described in chick.

The genetic cascade for LR laterality in chick has been elegantly established, but several observations suggesting that certain aspects may not be conserved in other vertebrates. Studies of LR asymmetry establishment have exposed a number of components (Nodal signals, EGF-CFC factors, Pitx2, RA) and embryonic regions (midline and node) that probably have conserved roles among all vertebrates. However, it has also become clear that molecular processes such as the ones involving Activin, Fgf8 and Shh might not be strictly conserved. The patterning step regulated by Nodal and Lefty seems to be conserved among vertebrates such as the fish, frog, chick and mouse (Duboc, Rottinger et al. 2005; Imai, Levine et al. 2006). The morphogenesis step is also conserved, in the sense that it involves Pitx2 (Shiratori, Yashiro et al. 2006). However, an organ develops LR asymmetry in different ways among species.

Many questions persist without an answer in order to obtain a more detailed understanding of LR asymmetry:

- Are the first asymmetries generated in the node and/or are they transferred to the node?;
- how can a midline regulate laterality and thus restricts asymmetric gene expression to only one side of the embryo?;
- how many genes and pathways are conserved or divergent between the organisms?; and finally,
- what are the molecular interactions and additional components in the LR pathway?

Recent reports demonstrate that cell adhesion molecules (CAMs), namely N-cadherin (for review see section I.6 - Right Side regulatory cascade of gene expression) (Garcia-Castro, Vielmetter et al. 2000), Claudin (Brizuela, Wessely et al. 2001) and DE-cadherin (*Drosophila* E-cadherin) through physical interactions with β-catenin and unconventional type ID myosin (MyoID) (Petzoldt, Coutelis et al. 2012) also regulate LR asymmetry formation.

In *Xenopus* embryos it was shown that the Claudin protein (Xcla) presents a PDZ-binding site (helps to anchor transmembrane proteins to the cytoskeleton and hold together signalling complexes) that seems to be crucial for its correct localization on the cell membrane (Brizuela, Wessely et al. 2001). The authors observed that a truncated form of Claudin leads to delocalization of the tight-junction protein ZO-1. Interestingly, when the protein was overexpressed it caused alterations in cell adhesion properties of the blastomeres leading to changes in regulation of cell-cell interactions and consequently a randomization of the internal organs (Brizuela, Wessely et al. 2001).

Another adhesion molecule DE-cadherin was recently correlated to LR asymmetry establishment when it was discovered that DE-cadherin co-immunoprecipitates with MyoID and is required for MyoID LR activity (Petzoldt, Coutelis et al. 2012). It was also demonstrated that MyoIC, a closely related unconventional type I myosin, can antagonize MyoID LR activity by preventing its binding to adherens junction components. Interestingly, DE-cadherin inhibits MyoIC an anti-dextral promoter, providing a protective mechanism to MyoID function. Taken together, these data indicated that DE-cadherin controls both the LR determinants

MyoID and its repressor MyoIC activity and protein levels in *Drosophila* (Petzoldt, Coutelis et al. 2012).

These discoveries highlight the importance of correct cell-cell interactions for LR axis determination during vertebrate development and introduce a novel type of molecules (CAMs) involved in this process.

I.7 Cadherins

Cadherins constitute a large superfamily of calcium-dependent cell adhesion proteins, which play a major role in development and tissue morphogenesis (Takeichi 1995). They are often concentrated in the adherens junction (AJ), and appear to modulate adhesion through dynamic interactions with the actin cytoskeleton.

During development, cadherins direct cell segregation and the formation of distinct tissue interfaces such as the formation of tissue boundaries (Kim, Jen et al. 2000; Tepass, Godt et al. 2002), changes in the shapes of tissues owing to cell rearrangements (Zhong, Brieher et al. 1999; Keller 2002) and the long-range migration of cells and neuronal processes (Matsunaga, Hatta et al. 1988; Geisbrecht and Montell 2002).

In adults, interactions between cadherins on adjacent cells maintain the structural integrity of solid tissues and regulate the turnover and reorganization of tissue structures such as the lining of the gut and the epidermis (Hermiston, Wong et al. 1996), the plasticity and regulation of neuronal synapses and the maintenance of stable tissue organization to prevent the dissociation and spread of tumour cells (Berx, Nollet et al. 1998; Cano, Perez-Moreno et al. 2000).

The cadherin superfamily comprises the 1) classical cadherins that are the major component of cell-cell adhesive junctions, 2) protocadherins, 3) desmosomal cadherins and 4) cadherin-like proteins that do not fall into the other subfamilies (e.g., the *fat* protein of *Drosophila*). The classical cadherins are the most extensively studied to date.

Classical cadherins are named according to the tissues where they are most prominently expressed, but it has become clear that these expression patterns are not exclusive, and most cadherins can be expressed in many different tissues. For example, E-, N-, and R-cadherins were derived from epithelial, neural, and retinal tissues, respectively.

E-cadherin (epithelial cadherin) is expressed primarily in epithelial cells and is associated with the zonula adherens of the epithelial junctional complex. E-cadherin and the zonula adherens help the cells form a tight, polarized cell layer that can perform barrier and transport functions (Gumbiner, Stevenson et al. 1988).

N-cadherin and R-cadherin (neural and retinal cadherins, respectively) are widely expressed in the nervous system, and are associated with small adherens-type junctions at synapses, as well as at growth cones and other parts of the neuron (Matsunaga, Hatta et al. 1988; Uchida, Honjo et al. 1996). VE-cadherin (vascular-endothelial cadherin) is expressed in endothelial cells that line the vasculature and, similar to E-cadherin, it is associated with the adherens junctions that help these cells to form transport barriers (Carmeliet, Lampugnani et al. 1999; Venkiteswaran, Xiao et al. 2002). Due to their diverse patterns of expression, other classic cadherins, such as cadherin-11, are often numbered.

Classical cadherins are composed of an extracellular region that mediates calcium-dependent homophilic interactions between cadherin

molecules; a transmembrane and a cytoplasmic domain. The later interacts with a number of different cytoplasmic proteins, which allows them to carry out their functions, including cell-cell adhesion, cytoskeletal anchoring and signalling (Figure 13) (Takeichi 1995; Gumbiner 2000; Yagi and Takeichi 2000).

Cadherins have multiple functions, as they were already mentioned above, one of them includes signalling. Signalling is localized to the cytoplasmic domain, whereas adhesion and selectivity are mapped to the extracellular region (Yap, Brieher et al. 1997). Although selectivity and adhesion are assumed to involve the same site, given the modular architecture of the cadherin ectodomain, this is not necessarily the case.

Cadherin-mediated cell-cell adhesion is initiated by the *trans* dimerization of cadherin monomers located on opposing cell surfaces (reviewed in (Troyanovsky 2005). The interplay between *trans* binding and lateral (*cis*) (Fig. 13) interactions among proteins on the same membrane appears to play a crucial role in the clustering of cadherins into junctions.

Desmosomal cadherins are exclusively expressed in the desmosomes (adhesive junctions that associate with the intermediate filaments of the cytoskeleton) of epithelial cells and cardiac muscle cells (Garrod, Merritt et al. 2002; He, Cowin et al. 2003).

Protocadherins are the less well-characterized subfamily of cadherins and they are only expressed in vertebrates (Nollet, Kools et al. 2000; Yagi and Takeichi 2000). Most attention has focused on their expression throughout the nervous system but protocadherins are also expressed elsewhere.

Since their discovery, it has become clear that the role of cadherins is not

limited to mechanical adhesion between cells. Rather, cadherin function extends to multiple aspects of tissue morphogenesis, including cell recognition and sorting, boundary formation and maintenance, coordinated cell movements, and the induction and maintenance of structural and functional cell and tissue polarity (reviewed in (Yagi and Takeichi 2000; Qin, Capaldo et al. 2005)). Given the breadth of their functions, it is not surprising that defective cadherin expression has also been linked directly to a wide variety of diseases including the disruption of normal tissue architecture, such as metastatic cancer (reviewed in (Berx and Van Roy 2001)).

I.7.1 Cadherins are involved in multiple Biological Processes

Organized cell division and cell rearrangements during development are usually associated with spatio-temporal changes in cadherin expression (Takeichi 1991; Takeichi 1995; Gumbiner 1996).

Major morphological defects and loss of tissue structure result from ectopic or altered expression of cadherins (Detrick, Dickey et al. 1990; Fujimori, Miyatani et al. 1990; Radice, Rayburn et al. 1997) or from cadherin inhibition by antibodies (Matsunaga, Hatta et al. 1988; Bronner-Fraser, Wolf et al. 1992).

Cadherins play a major role in maintaining tissue integrity, they are important in regulating apoptosis, maintaining tissue morphology and cell differentiation, and in establishing tissue polarity (Ong, Kim et al. 1998; Makrigiannakis, Coukos et al. 1999). The establishment of distinct tissue interfaces during development is attributed to specific recognition

between cadherins on adjacent cells (Thomas, Edelman et al. 1981; Nose, Nagafuchi et al. 1988; Miyatani, Shimamura et al. 1989). The common view is that the formation of these junctions is due to specific matchmaking in which cadherins on one cell only adhere to an identical protein on an adjacent cell.

Cadherins can also be signalling molecules and influence cell differentiation, cell movement, and tissue organization (Qin, Capaldo et al. 2005). Ultimately, determining how cadherins form cell-cell junctions is crucial to understanding their role in biology. As such, a fundamental challenge is to determine the mechanism of intercellular adhesive bond formation.

The principal, bidirectional, force transducer is the ectodomain at the junctions, which transmits mechanical stimuli to the cytoplasm and possibly alters its properties in response to changes in the cell. Nevertheless, the identities of the functional regions of the protein remain controversial. In addition to forming mechanical linkages, the ectodomain also determines cadherin specificity. Although other factors such as inside-out signalling may affect cadherin adhesion (Gumbiner 1996; Gumbiner 2005), a large body of work focuses on the ectodomain properties and the mechanism of adhesion.

I.7.2 Structural and functional organization of the cytoplasmic domain

The cytoplasmic domains are highly conserved among the classic cadherin members, collectively called catenins. The cytoplasmic part of classic

cadherins contains binding sites for two armadillo-domain-containing catenins, β-catenin and p120-catenin (p120ctn), γ-catenin; but it also binds to the cytoplasmic partner α-catenin (Fig. 13).

β-CATENIN is an armadillo-repeat protein, named after its homologue in *Drosophila melanogaster*, Armadillo. The armadillo repeats form a central rod-like domain that serves as a binding site for most of its numerous binding partners. The N and C termini are regulatory domains that control its degradation, binding and signalling activities. β-catenin is also an intracellular signal transduction molecule that mediates signalling in the Wnt growth factor pathway (Moon, Bowerman et al. 2002).

Normally, in the absence of an extracellular Wnt ligand, the cytosolic (non-cadherin bound) levels of β-catenin are low because it is targeted for degradation by a complex of proteins. Wnt signalling through its receptor (Frizzled-LRP) inhibits the targeting of β-catenin for degradation, which allows it to accumulate in the cytosol. It enters the nucleus, interacts with the nucleus, where it activates the transcriptional factor T-cell factor (Tcf)/lymphoid enhancer factor (Lef), and thereby stimulates the expression of target genes (reviewed in (Kikuchi, Kishida et al. 2006)).

P120-CATENIN is another armadillo-repeat-containing protein that was initially discovered as a substrate for the Src protein tyrosine kinase (are proto-oncogenes that play key roles in cell morphology, motility, proliferation, and survival). It binds to a different region of the cadherin cytoplasmic domain from β-catenin, and both proteins can bind cadherin simultaneously. The role of p120ctn in cadherin function is probably regulatory rather than structural. The p120ctn-cadherin interaction is crucial for cell-surface stability by regulating endocytosis (Xiao, Oas et al.

2007). Furthermore, p120ctn has emerged as a major regulator and integrator of signalling by the Rho family of small GTPases (Anastasiadis 2007) and this is at least partially dependent on its interaction with the cadherin (Wildenberg, Dohn et al. 2006).

Y-CATENIN, also known as Plakoglobin, is an armadillo-repeat protein that is similar to β-catenin and that can bind to the β-catenin-binding region of cadherins. It is a homolog of β-catenin that can substitute for it under some circumstances. It is highly enriched in desmosomes, where it helps to mediate a link to the intermediate filament cytoskeleton, but can also be found at adherens junctions. It does not seem to have the same Wnt-pathway signalling function as β-catenin, but could be involved in other signalling pathways (reviewed in (Gumbiner 2005)).

α-CATENIN is a cytoskeletal protein that generates extensive flattening between neighbouring cell surfaces (reviewed in (Kobielak and Fuchs 2004). It binds to actin and several other actin-binding proteins, as well as to the N-terminal region of β-catenin (it does not interact directly with cadherins). It binds to signalling proteins, such as formin-1, which regulate the actin cytoskeleton. It also seems to have a signalling role that regulates cell proliferation.

These catenins in turn associate with a variety of other molecules, including cytoskeletal proteins and their regulators. These cytoplasmic components of AJ affect the adhesive action of the extracellular domain of cadherins in various ways, leading to alterations in the strength and stability of cell-cell contacts.

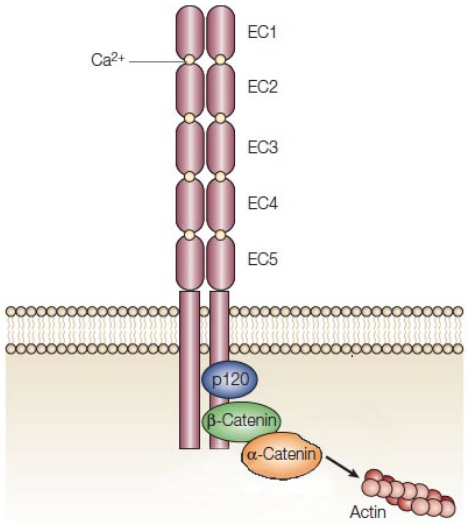

Fig. 13| The classic cadherin–catenin protein complex. The cadherin is a parallel or *cis* homodimer. The extracellular region of classic cadherins consists of five cadherin-type repeats (EC domains; extracellular cadherin domains) that are bound together by Ca^{2+} ions (yellow circles). The core universal-catenin complex consists of p120ctn, bound to the juxtamembrane region, and β-catenin, bound to the distal region, which in turn binds α-catenin. In a less well-understood way, α-catenin binds to actin. Adapted from (Gumbiner 2000).

I.7.3 Interactions with the Actin Cytoskeleton

The AJ is morphologically associated with actin filaments raising the question of how this association is established and what role the actin plays in AJ organization and function. A key player is thought to be α-catenin that binds to β-catenin, linking cadherins to actin, resulting in the formation of the cadherin-β-catenin complex (Nagafuchi and Takeichi 1989).

Biochemical studies have showed that α-catenin can interact with actin filaments (Rimm, Koslov et al. 1995) giving rise to the general belief that α-catenin acts as a linker between the cadherin-β-catenin complex and F-actin (Filamentous actin; regulates cellular shape changes and force generation in cell migration and division). However, it was recently shown, using a combination of direct binding studies with purified proteins and measurement of protein dynamics in live cells that α-catenin does not interact with β-catenin and F-actin simultaneously (Drees, Pokutta et al. 2005; Yamada, Pokutta et al. 2005).

I.8 Cadherin expression and function in development

I.8.1 Cadherins and morphogenetic movements

Many of the changes in cell shape or movement observed during development occur while cells are in direct contact and require, therefore, dynamic changes in adhesive interactions. These changes may play a permissive role, as the release of adhesion is important for the relative movement of cells that are in contact. However, adhesive interactions also directly promote movement, as traction must be generated between cells for cell rearrangements to occur in solid tissues. Classical cadherins also contribute to morphogenetic movements that involve cell-cell rearrangements within tissues (Gumbiner 1992). Although less well appreciated than EMT as a mode of cell locomotion, these movements are commonly found during early embryogenesis and take many forms.

I.8.1.1 Convergent and Extension movements

The regulation of C-cadherin-mediated adhesion in response to growth factors and fibronectin in gastrulating *Xenopus* embryos is required for the convergence and extension tissue movements that underlie the elongation of the body axis (Zhong, Brieher et al. 1999; Marsden and DeSimone 2003).

Convergence and extension movements are driven by local rearrangements of cells with respect to neighbouring cells (Keller 2002), and require the continuous breaking and reforming of C-cadherin adhesive bonds (Fig. 14a). Therefore, dynamic regulation of adhesion is required so that moving or migrating cells can continually break and remake adhesive bonds to change cell neighbours. The dynamic regulation of cadherin adhesions might also drive cell movements in a process, called intercellular

motility.

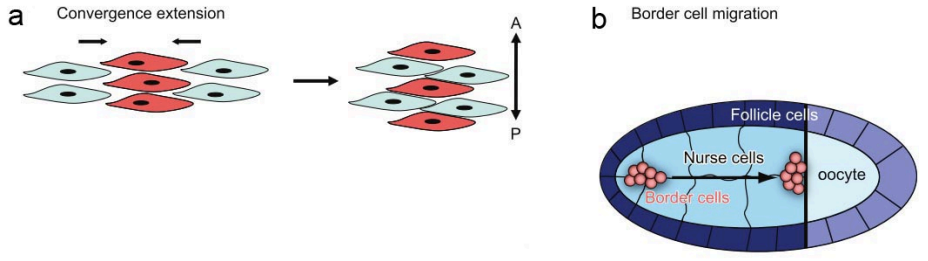

Figure 14| Cadherin in morphogenetic movements. Cadherin function is essential for morphogenetic movements, such as cell-on-cell motility and convergent extension movements. (**a**) Convergence extension movements in which cells align in the plane of the tissue and intercalate to drive anterior-posterior extension of tissues and/or embryos. (**b**) *Drosophila* border cells that through a complex signalling pathway switch on E-cadherin to migrate on E-cadherin expressing nurse cells. Adapted from (Niessen, Leckband et al. 2011).

I.8.1.2 BORDER CELL MIGRATION

Another well-characterized form of cadherin-dependent morphogenetic movement is the border cell migration that undertake a highly coordinated, directional migration and also occurs in the *Drosophila* egg chamber (Montell 2003).

In this case a small group of follicle cells emerges from the epithelium that covers the egg chamber and migrates through the nurse cells within the egg chamber to the anterior border of the oocyte. This type of invasive cell migration leads to the movement of border cells upon the nurse cells being subject to several regulatory signals. DE-cadherin is one key target of regulation, which is induced in the border cells at the time of migration (Montell, Rorth et al. 1992). DE-cadherin is also necessary, in both the border cells and in their surrounding nurse cells, for the border cell cluster to migrate, indicating that it is a form of cadherin-dependent cell-upon-cell locomotion (Fig. 14b).

These examples of morphogenetic movements in the early embryo are likely to require the cells to use cadherins and other cell-cell adhesion receptors as the traction apparatus for intercalation and cell-upon-cell locomotion. An important challenge, then, is for cells to remodel their adhesive interactions with one another without disrupting the overall integrity of the tissue.

I.8.2 Classical cadherins in cell sorting

A fundamental developmental process is the ability of cells with different cell fates to physically segregate from one another (Fig. 15). This phenomenon was discovered as early as in the 1950s. In classical experiments of Townes and Holtfreter (Townes and Holtfreter 1955) who showed that when cells from dissociated gastrula stage embryos were allowed to re-aggregate, the cells would rearrange to re-associate with those from the same germ layer.

In addition, the relative position of these cell populations within the reformed aggregate mirrored what happens in the embryo (Townes and Holtfreter 1955). They proposed that this sorting behaviour was based on differential adhesion between different cell populations. Similarly, when cells of differing adhesive properties are mixed, strong, more stable interactions will supplant weaker ones such that cells with the highest strength interactions will form the centre of the aggregate, and weaker interacting cells will form the surface of the aggregate.

Cells expressing different kinds of cadherins will sort themselves into separate populations. Notably, when cells expressing different levels of the same type of cadherin are mixed, those expressing higher levels of cadherins moved to the inside of the aggregate and those expressing

lower levels sorted to the external layers (Fig. 15a).

All this clearly shows that affinity differences can account for the reaggregation behaviours of cells and tissues that have been dissociated and reassociated in culture. There are a few examples, mostly in *Drosophila,* where genetic analyses have shown the importance of cell sorting *in vivo* (Godt and Tepass 1998; Gonzalez-Reyes and St Johnston 1998). Perhaps the clearest example of cell sorting *in vivo* is the movement of the oocyte to the posterior of the ovary (Fig. 15c).

During oogenesis DE-cadherin is found at all the cell-cell contacts in the egg chamber and when either DE-cadherin (Godt and Tepass 1998) or armadillo (*Drosophila* β-catenin) is disrupted, oocytes become mispositioned in the egg chamber and lose polarity. Importantly, correct positioning of the oocyte required DE-cadherin to be expressed both in the germline cells as well as in the follicle cells (Godt and Tepass 1998; Gonzalez-Reyes and St Johnston 1998), implicating adhesive interactions between these two cell types in controlling oocyte patterning.

Another critical factor that plays a role in the correct positioning of the oocyte is the level of cadherin expression. The posterior follicle cells, with which oocytes normally interact, have the highest level of cadherin expression of the somatic cells. Moreover, when posterior cells were genetically ablated, oocytes then preferentially interacted with the anterior follicle cells, the next most abundant sites of DE-cadherin expression. Positioning thus appeared to reflect a sorting process, where the oocyte preferentially interacted with follicle cells expressing the highest level of cadherin, independent of other morphogen or paracrine signalling events that might occur (Fig. 15c). Overall, this example illustrates the capacity for quantitative differences in cadherin expression,

and by implication differences in adhesion, to have profound, long-lasting effects on developmental patterning.

Another classic example of cell sorting is displayed by neural crest cells, which form over a long development time period from gastrulation through early organogenesis (Fig. 15b) (Sauka-Spengler and Bronner-Fraser 2008). The presumptive neural crest population is first induced at what becomes the border between the neural and non-neural ectoderm. During neurulation, these precursors become incorporated into the neural folds and the neural tube itself before eventually delaminating from the neuroepithelium and becoming migratory.

A series of cadherin switches occur during this process (Hatta, Takagi et al. 1987): neural crest precursors downregulate E-cadherin during their initial induction, express N-cadherin and cadherin-6b when they reside in the neuroepithelium, and then downregulate the latter when they delaminate (Fig. 15b). The downregulation of E-cadherin by transcriptional repression appears to be an essential early stage in the epithelial-to-mesenchymal transition (EMT) that this cell population undergoes, while N-cadherin and cadherin-6b are necessary at later stages (Sauka-Spengler and Bronner-Fraser 2008). Such cadherin switching (typically from E-cadherin to N-cadherin) is commonly seen in many other forms of EMT (Thiery 2002).

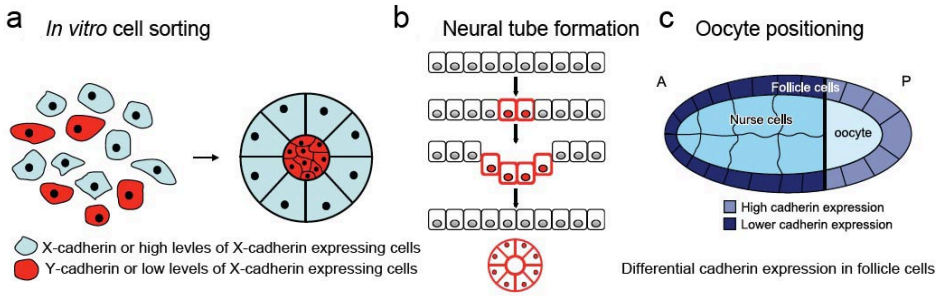

Figure 15| The role of cadherin in cell sorting and positioning. (**a**) Differential type or levels of cadherin expression on cells drive cell sorting in vitro in cell (re)aggregation assays. (**b)** Formation of the neural tube, E-cadherin is switched off in a subset of ectodermal cells, whereas N-cadherin expression is turned on in these cells (red cell membranes) driving segregation of these cell populations. (**c**) *Drosophila* oocyte positioning where differential cadherin expression in the follicle cells is crucial to properly position the oocyte at the posterior end of the embryo. Adapted from (Niessen, Leckband et al. 2011).

I.9 N-cadherin

N-cadherin is a classic cadherin, also known as cadherin 2. It is one of the transmembrane adhesion proteins that engage in homophilic binding in a calcium-dependent manner, and play an important role in the formation of adherens junctions. N-cadherin was first identified in 1982 (Grunwald, 1982) as a 130 kD molecule in the chick neural retina that was protected by calcium from proteolysis, and in 1984 A-CAM was identified (now called N-cadherin) as a molecule that was localized at the adherens junctions (Volk and Geiger, 1984). The protein has been referred to also as CDHN (Neural calcium-dependent adhesion protein).

As for all classic cadherins, the extracellular region of N-cadherin is folded into five repeats EC domains, containing Ca^{2+}-binding sites (Takeichi, 1988.). N-cadherin is a cell adhesion molecule that typically interacts with other N-cadherin molecules in a homotypic homophilic manner. N-cadherin can engage also in heterotypic homophilic and heterophilic

interactions with other cadherins (Shan et al, 2000). The short cytoplasmic domain interacts with catenins and other proteins that connect N-cadherin to the cytoskeleton and link it to signalling pathways regulating the formation and remodelling of cell-cell adhesions, and promoting cell survival and migration (Qin, Capaldo et al. 2005).

I.9.1 N-cadherin in development

N-cadherin is expressed early during embryonic development in different tissues and is associated with a lot of molecules that regulate its function. N-cadherin is involved in a set of processes like cell-cell adhesion, differentiation, embryogenesis, migration, LR asymmetry, invasion, and signal transduction (reviewed in (Derycke and Bracke 2004)).
In embryogenesis, during gastrulation, cells undergo an EMT leading to the expression of N-cadherin and the downregulation of E-cadherin in the PS to form mesoderm (Hatta, Takagi et al. 1987; Takeichi 1988). During neurulation, a similar change in expression occurs in the developing neuroepithelium.

N-cadherin is the primary cadherin that is expressed in the neural tube, but it is only temporarily expressed in the neural crest before the onset of migration.

Migrating neural crest cells do not express either E- nor N-cadherin and this may contribute to segregate them from the overlying ectoderm that expresses E-cadherin, and from the neural tube that expresses N-cadherin (Takeichi 1988). N-cadherin is again detectable in some neural crest cells after they have reached their destinations and begin differentiating. During nervous system development, N-cadherin also

contributes to the regionalization of the neural tube, characterized by the segregation and rearrangement of cell populations into different regions, to axon growth and to synapse establishment (Tanaka, Shan et al. 2000).

The transcription factor Snai2/Slug is involved in both the formation of the neural crest precursors and in neural crest migration. Snai2 downregulates cadherins, leading to a loss of cell-cell contacts and allowing cell migration, meaning that when neural crest cells are still associated with the neural tube, they express N-cadherin but once they start migrating, N-cadherin is downregulated (Fig. 15b). At the end of the dorso-ventral migration N-cadherin is re-expressed in aggregating cells, just before the formation of the dorsal root and sympathic ganglia. After the dorso-lateral migration only the dermal melanocytes express N-cadherin and establish contacts with the fibroblasts in the dermis (Nieto 2001; Pla, Moore et al. 2001).

Recently, N-cadherin mutations have been identified in the zebrafish at the *parachute* (*pac*) locus (Birely, Schneider et al. 2005). Although N-cadherin expression is reported as ubiquitous throughout early development of the zebrafish embryo (Bitzur, Kam et al. 1994); (Lele, Folchert et al. 2002), the phenotypes observed in *pac* alleles suggest that N-cadherin is only essential for neural development, where it is necessary for the convergence of the ectoderm during neurulation, and later, the cellular organization of the brain and retina (Lele, Folchert et al. 2002; Malicki, Jo et al. 2003).

A recent publication shows that N-cadherin is an early and crucial mechanism in neuronal polarity (Gartner, Fornasiero et al. 2012). Local stimulation with extrinsic N-cadherin was sufficient for the specification of the site from which the first neurite would grow and where Golgi and

centrosome are recruited.

In two different experiments, *in vivo* and *in vitro*, the authors have demonstrated that neurons with a defective N-cadherin are not able to properly establish their radial alignment of the cell axis, which later on leads to migration defects. In this paper the authors have shown the instructive role of N-cadherin on the very first steps of neuronal polarity and its role in the orientation of the neuronal cell axis, which means that N-cadherin plays an essential role in an earlier event in cortical development: neuronal first polarization (Gartner, Fornasiero et al. 2012).
Outside the nervous system, N-cadherin seems to be only required during late somitogenesis for the radial migration of a select population of slow muscle fibers to the surface of the myotome (Cortes, Daggett et al. 2003).

N-cadherin is also implicated in several aspects of organ normal development, starting for cardiac development (Nakagawa and Takeichi 1997; Radice, Rayburn et al. 1997; Piven, Kostetskii et al. 2011), gut looping (Kurpios, Ibanes et al. 2008), sorting out of the precardiac mesoderm (Linask and Lash 1993) and trabeculation of the myocardial wall (Ong, Kim et al. 1998).

N-cadherin plays an important role in cardiac development, being involved in several steps of heart formation (Linask 1992; Linask, Knudsen et al. 1997; Nakagawa and Takeichi 1997). The importance of N-cadherin in the cardiovascular system has been highlighted by studies in N-cadherin-knockout mice. The homozygous mutant embryos die during mid-gestation (E10) with several developmental defects, including malformed somites, undulated neural tube, lack of vascularization of the yolk sac and severe abnormalities in the heart (Radice, Rayburn et al. 1997).

Cartilage formation in the developing vertebrate embryonic limb consists of highly coordinated and orchestrated series of events involving the commitment, condensation and chondrogenic differentiation of mesenchymal cells and the production of cartilaginous matrix. Here, N-cadherin has a role in the cellular condensation (Delise and Tuan 2002), being a direct target of SOX9, a transcription factor that is essential for chondrocyte differentiation and cartilage formation (Panda, Miao et al. 2001).

N-cadherin, also plays an important role in skeletal muscle differentiation. Cells with the potential to undergo skeletal myogenesis are present in the epiblast layer. All cells express the skeletal muscle-specific transcription factor MyoD but only the epiblast cells that express N-cadherin but not E-cadherin will differentiate into skeletal muscle (George-Weinstein, Gerhart et al. 1997). N-cadherin is involved in myoblast migration as well in muscle differentiation (Brand-Saberi, Gamel et al. 1996).

I.9.1.1 N-CADHERIN AND LEFT-RIGHT ASYMMETRIES

It was also uncovered that N-cadherin is one of the earliest proteins to be asymmetrically expressed in the chicken embryo and its activity is required during gastrulation for a proper establishment of the left-right axis (Garcia-Castro, Vielmetter et al. 2000).

So far, the chicken embryo is the only example where it was shown the asymmetric expression of N-cadherin in or around the node and its importance for the correct positioning of the heart. Yet, in other structures, N-cadherin has also been implicated in asymmetric phenotypes, like for instance leftward tilt of the primitive gut tube. N-cadherin asymmetrically localized in the left side of the mesentery of the gut in chicken is necessary

for the asymmetric packing of the mesenchymal cells and thus for the future leftward tilt of the primitive gut tube (Kurpios, Ibanes et al. 2008).

Recently, it was demonstrated that also in the mouse N-cadherin played a role in gut tube morphogenesis. Analysis of mouse embryos lacking one allele of both Shroom3 (cytoskeletal protein that induces epithelial cell shape change) and N-cadherin revealed that they possess shorter and wider left epithelial dorsal mesentery cells when compared with Shroom3 or N-cadherin heterozygous embryos. The authors showed that N-cadherin interacts with Shroom3 downstream of Pitx2 to directly regulate cell shape changes necessary for early gut tube morphogenesis (Plageman, Zacharias et al. 2011).

I.9.1.2 N-CADHERIN AND COLLECTIVE CELL MIGRATION

All multicellular organisms depend on cell movement as a driving force for embryogenesis, tissue remodelling and repair. Migrating cells maintain contact with neighbouring cells, which is thought to provide a spatial cue for collective cell migration.

During embryogenesis a variety of different cell movements are observed. Whereas some cells migrate as individuals, others migrate collectively in groups or cohesive cell sheets, which are defined as tissue movements. During recent years a growing number of reports underlined the importance of such tissue movements in early embryogenesis, organ formation and tumour progression, which are based on different types of cell behaviour. Interestingly, all of these tissue movements have one thing in common: they change their cell and tissue polarity and show a modulated and dynamic cell-cell adhesion (reviewed in (Becker, Langhe et al. 2012)).

N-cadherin is one of the cadherins examples that promote cell migration during embryogenesis. In zebrafish, N-cadherin mutants like *biber* (dominant gain-of-function) show significant morphogenesis defects on mesoderm during gastrulation, such as a strange enlargement of the paraxial mesoderm (Warga and Kane 2007). Time-lapse analysis allowed the visualization of the cause for this altered phenotype. Interestingly, in *biber* mutants the movements of the lateral mesoderm cells were compromised, meaning that they were slower and less straightforward (Warga and Kane 2007).

In vertebrates the invagination of an epithelium is a crucial step in the formation of neural tube, ear (otic) vesicle and eye (optic) cup. The evagination and formation of the optic vesicle is based on massive cell migration of the progenitor cells, first directed to the dorsal midline and then turning outwards (Rembold, Loosli et al. 2006). These cells express N-cadherin due to their neuroectodermal origin. How N-cadherin adhesion is modulated in this process remains to be investigated.

Additionally, N-cadherin is also required for ear development. In chicken, N-cadherin and N-CAM are expressed in the otic placode under the control of the transcription factor Pax2. Both adhesion proteins are required for the elongation of the placodal cells to form a columnar epithelium and for its proper invagination (Christophorou, Mende et al. 2010).
In general, studies of tissue movements in embryogenesis help to understand the tangled regulatory network driving cell migration and the involvement of cadherins. The implication of cadherins in cell and tissue movements is obvious by the diseases correlated to their dysfunctions (reviewed in (Friedl and Gilmour 2009)).

Cell migration is a critical step of normal development processes and disease progression. Often, migrating cells interact and maintain contact with neighbouring cells. However, the precise roles of cell-cell adhesion in cell migration have thus far been poorly defined. Often in aggressive cancers, N-cadherin is prominently upregulated (reviewed in (Stemmler, Beelmann et al. 2007)).

I.9.2 N-cadherin and cancer

Recent studies have revealed that the physiologic function of N-cadherin in adult tissues is not only important in maintaining the proper architecture of certain tissues (structural–adhesive function), but it also plays a role in cell communication (signalling function), being involved in the establishment of functional synapses in neurons and in the formation of a vascular wall that is essential for vascular stabilization (Halbleib and Nelson 2006)).

The signalling function of N-cadherin is complex and is differentially regulated depending on the cell context. The capacity of N-cadherin to affect the cytoskeleton, to cross-talk with other membrane receptors and to mediate cell adhesion between cells of the same or of different types suggest that the deregulation of its function may significantly contribute to the development of pathologic situations, including cancer (reviewed in (Stemmler, Beelmann et al. 2007)).

During tumour progression, cancer cells undergo dramatic changes in the expression profile of adhesion molecules resulting in detachment from original tissue and acquisition of a highly motile and invasive phenotype.

A hallmark of this change, also referred as EMT, (for review see

section I.12.2), is a degenerated process also observed in physiological events throughout normal development. In cancer, the switch from E-cadherin to N-cadherin expression is a property of cancer progression and is often observed in metastatic tumours (reviewed in (Derycke and Bracke 2004; Wheelock, Shintani et al. 2008)). Therefore, upregulated N-cadherin become known as a potential regulator of collective cancer cell migration.

During gastrulation, the downregulation of E-cadherin is a property of EMT, and therefore E-cadherin is regarded as a tumour or invasion suppressor (Vleminckx, Vakaet et al. 1991; Birchmeier 1995). The expression of E-cadherin is negatively regulated by a number of zinc-finger-family transcription factors, including Snai1, Slug and Twist (among others), each of which has been reported to bind to the E-cadherin promoter and repress its transcription (Bolos, Peinado et al. 2003; Castro Alves, Rosivatz et al. 2007), (Hajra, Chen et al. 2002) (Hajra, Chen et al. 2002; Huber, Kraut et al. 2005).

This repression effect promoted by Snai1 on E-cadherin is evident from the fact that carcinoma cells can be reverted to a normal epithelial phenotype by overexpressing E-cadherin (Vleminckx, Vakaet et al. 1991). In many tumours, E-cadherin downregulation is correlated with de novo expression of N-cadherin or cadherin-11 (Li and Herlyn 2000; Tomita, van Bokhoven et al. 2000).

It is also known that growth factor receptors regulate many aspects of cell behaviour, including cell motility and invasion (McKay and Morrison 2007). A number of studies have implicated cadherins as modulators of receptor tyrosine kinase signalling. It was suggested that N-cadherin might facilitate dimerization of the FGF receptor (FGFR1) to initiate a growth-factor

independent signal (Skaper, Moore et al. 2001). The authors argue that *cis* dimerization of N-cadherin activates an FGFR-dependent signal and demonstrated that N-cadherin mediated signalling is distinct from its adhesive activity (Utton, Eickholt et al. 2001; Williams, Williams et al. 2002).

Earlier studies also suggested that N-cadherin influences tumour cell behaviour via interactions with the FGFR and that downstream inhibitors of FGFR signalling reduce N-cadherin-mediated invasion (Nieman, Prudoff et al. 1999). The extracellular domain 4 of N-cadherin is necessary and sufficient for this activity and might therefore interact directly with the FGFR. Similarly, this domain of N-cadherin is required for FGFR-dependent neurite extension (Kim, Islam et al. 2000; Williams, Williams et al. 2001).
N-cadherin stimulates migration and invasion of cells, which promotes tumour cell survival, migration and invasion, and a high level of its expression is often associated with poor prognosis.

Cadherin switch has been observed in biopsies of various types of cancers, including melanoma, breast and prostate cancers, bladder carcinoma, some types of ovarian and gastric carcinomas, and adrenal tumours (reviewed in (Friedl and Gilmour 2009)). However, there are invasive tumours where N-cadherin does not stimulate cell migration, on the contrary, N-cadherin inhibits cell migration and the formation of metastasis, like for instance in osteosarcoma (Kashima, Kawaguchi et al. 1999; Kashima, Nakamura et al. 2003), gliobastoma (Asano, Kubo et al. 2000), ovarian carcinoma (Patel, Madan et al. 2003).

Until now the mechanism by which increased/decreased expression of N-cadherin promotes or not malignancy is not completely understood.

I.10 Aims and scopes of this thesis

The aim of this work is to study the role of N-cadherin, a cell-cell adhesion molecule, in the molecular and morphological asymmetries of the Hensen's node of the chicken embryo.

One of the symmetry breaking mechanisms in vertebrates is the leftward fluid flow generated by cilia in the embryonic node (Nonaka, Tanaka et al. 1998). Since cilia in the chicken embryo seems to be unnecessary and unsatisfactory to create a fluid flow (Manner 2001), this always brought up the puzzling question of how is asymmetry generated in the chick. Recently, a leftward cell migration in the chicken's node was described to be the driving force to asymmetrically displace the cells in the node, and so generate the asymmetric *gene* expression in that region (Gros, Feistel et al. 2009). Much attention has been given to the processes/signals that initiate LR asymmetry in the vertebrate embryo, however less is known about what terminates them.

N-cadherin is asymmetrically localized on the right side of the Hensen's node at the moment in which the leftward cell movements have stopped. Also, it was described as being a crucial molecule in the correct establishment of the chicken's heart (Garcia-Castro, Vielmetter et al. 2000). Taking these findings into account, we investigate whether N-cadherin could be the adhesion key necessary to lock LR asymmetry in the chicken Hensen's node.

This Thesis is organized into six Chapters:

In Chapter I, I present a general introduction on LR asymmetry establishment. I describe its components and its regulators in different model systems, in particular, in the chicken embryo. I briefly summarize the initial steps of chicken embryo development and describe how its LR asymmetry is initiated, stabilized, propagated and lastly, translated into the asymmetric positioning of the heart.
In the end, I succinctly review the function of cadherins in development and in particular the role of N-cadherin during embryonic development, LR asymmetries and its relation to abnormal cell migration.

In Chapter II, I describe the experimental procedures used in this work.

In Chapter III, I describe for the first time the Kaede photo-convertible fluorescent protein tool, combined with *in vivo* confocal microscopy to track single cell movements in the chicken node. I show the importance of N-cadherin in regulating these movements and how this is necessary to maintain the previously established LR asymmetries in the Hensen's node. In addition to this chapter, I will also provide Supplementary Data that will complement and reinforce the results presented in Chapter III.

In Chapter IV, I describe further studies of N-cadherin's effect on asymmetry, in particularly at the level of Hensen's node morphology. To understand how N-cadherin influences the node asymmetric shape, I compare node's cell morphology, cell density and cell number between the left and the right sides. I describe the work done to determine if different levels of N-cadherin in the node are important to sort-out the

cells from the left and from the right sides. To achieve this, cell labelling on the left and on the right sides of the node with two different colour dyes was used.

In Chapter V, I describe my studies on the new asymmetric c*Hes6-1* Notch target (Vilas-Boas and Henrique 2010) in LR asymmetry of the chicken embryo.

I investigate whether or not c*Hes6-1* gene is under the H^+/K^+-ATPase, the first mechanism known to break symmetry in the chicken embryo. I also investigated if Nodal signalling can regulate the expression of c*Hes6-1* in the mesoderm lateral to the primitive streak. And last, I analyse and compare c*Hes6-1* expression in quail and m*HEs6-1* mouse in order to understand if *Hes6* asymmetric expression is conserved between chick, quail and mouse embryos.

Finally, in Chapter VI, I present the conclusions achieved along this thesis and present various future experiments that should be considered for the purpose of increasing our knowledge in LR asymmetry establishment/maintenance.

Chapter II

MATERIAL and METHODS

MATERIAL and METHODS

II.1 Preparation and transformation of competent *E. coli* bacteria

Preparation of chemically competent bacteria was based on (Hanahan 1983). The bacterial strains of *Escherichia coli* used were DH5α. Cultures of these bacterial strains were made competent for transformation with plasmid DNA by treatment with calcium chloride ($CaCl_2$). Single colony was placed in 10 ml of LB medium and shaken at 37ºC overnight (o.n). The o.n culture was inoculated in 400ml of LB and shaken at 37ºC until an OD_{600nm} of 0.6/0.8. After cooling to 4ºC, the culture was centrifuged for 15 minutes (min) at 4000 rpm. The pellet was re-suspended in 100 ml of a cold solution consisting of 30 mM KCH_3COO : 50 mM $MnCl_2$: 10 mM $CaCl_2$: 100 mM KCl : 15 % glycerol and the centrifuged at 4000 rpm for 8 min. The bacteria were again re-suspended in 20 ml of a second cold solution consisting of 20 mM NaMops (pH 7) : 75 mM $CaCl_2$: 10 mM KCl : 15 % glycerol and then frozen as 0.5 ml aliquots nitrogen and stored at -80ºC.

II.1.1 PLASMID TRANSFORMATION OF COMPETENT BACTERIA

Frozen aliquots of competent cells were thawed on ice. Plasmid DNA (0.01-0.8µg) was incubated with 150 µl of cells on ice for 30 min. The cells/DNA mix was heat-shocked for 30 seconds (sec) at 42ºC and then incubated on ice for 2 min. 600µl of SOB solution was added to the mix, which was then incubated with shaking at 37ºC for 1 hour. The mix was centrifuged for 30 sec and 600 µl of solution were removed. The cells were re-suspended in the remaining volume and plated on appropriate selective LB agar media and incubated at 37ºC o.n.

II.1.2 PLASMID DNA PURIFICATION

For small scale preparation of plasmid DNA, 2ml of a 3ml o.n bacterial culture of transformed competent cells, in the appropriate selective LB medium, was processed using the *Wizard® Plus Minipreps DNA purification System* (Promega) according to the manufacturer's instructions.

For large sale preparation of plasmid DNA, 200 ml of the appropriate selective LB medium was inoculated with 0.5 ml of plasmid bacterial culture and shaken at 37ºC o.n and processed using the *Nucleobond® AX* (Macherey-Nagel) according to the instructions of the manufacturer.

II.1.3 DNA QUANTIFICATION

The concentration of DNA was determined by spectrophotometry using Nanodrop spectrophotometer. One A_{260} units corresponds to 50 µg/ml of double stranded DNA. The purity of the nucleic acid preparation was estimated by the ratio between the readings obtained at 260 nm and 280 nm.

II.1.4 RESTRICTION DIGESTIONS AND LIGATION REACTION

Enzymatic restriction of DNA was performed for approximately 1 hour using 5-10U of commercially available restriction enzymes and respective buffers (Promega, Roche, Fermentas, New England Biolabs). The volume of enzyme used in each reaction never exceeded 10% of the total reaction volume. Ligation reactions were carried out in a final volume of 10µl, for a total DNA amount of 0.5 µg. The ligation reactions were performed o.n at 15ºC using a 1 U of T4 DNA ligase (Promega) and a suitable ligation buffer.

II.1.5 ANALYSIS AND ISOLATION OF DNA BY AGAROSE GEL ELECTROPHORESIS

To separate and estimate the size of DNA fragments, agarose gel electrophoresis was carried out. Gels were prepared by heating agarose (SeaKem® LE Agarose; Lonza) until complete dissolution of 1X TAE buffer. The final agarose concentration depended on the size of the DNA fragments to be resolved: 1.2% (w/v) for < 1 kb and 1.0% (w/v) for 1-10kb. DNA was visualized by the addition of Gel Red (Biotium) to the gel to a final volume of 0.08 µl/ml. DNA samples were mixed 1X DNA loading buffer (60% Glycerol (v/v): 10mM EDTA with traces of OrangeG – Sigma) and electrophoresis was carried in 1X TAE buffer.

II.2 Anti-sense RNA probe synthesis

During the course of this work several Digoxigenin RNA anti-sense probes were used for *in situ* hybridization on whole-mount chick embryos.
Digoxigenin RNA anti-sense probes were synthesized by T3, T7 or Sp6 polymerase, from plasmid templates containing the cDNAs of several genes (Table 1).

II.2.1 DNA TEMPLATE PREPARATION

DNA template preparation was performed as follows: 10µg of plasmid DNA was linearized in a final volume of 100µl, using 50 U of the restriction enzyme, for 2 hours at 37ºC. After confirmation of complete digestion, the DNA template was subjected to a phenol-chloroform extraction (5' centrifugation). And finally the DNA template was precipitated using

ethanol (2.5X volume) + NaCl (3M-1:2) at -20ºC o.n or 30' at -80ºC and re-suspended in 50µl of RNAse-free water.

II.2.2 PROBE SYNTHESIS

Anti-sense transcripts were produced using 1µg of linearized plasmid DNA and 20 U of the appropriate RNA polymerase in the presence of 30 mM DTT, 1x DIG-NTP mix, 40 U RNAsin (Promega) and 1x Transcription Buffer (Stratagene), in a final volume of 25µl. After incubating at 37ºC for 3 hours, the sample was precipitated by adding 20.5 µl of RNAse-free water, 2µl of 0.5 M EDTA (pH 0.8), 2.5 µl of 4 M LiCl and 75 µl of ethanol and incubated o.n at -20ºC. After centrifugation, the RNA precipitate was washed with 70% ethanol, re-suspended in 50 µl of 10 mM EDTA and, checked by agarose gel electrophoresis.

The templates used in this thesis for *in vitro* transcription reactions are listed in Table 1.

Table 1. Appropriate restriction enzyme and RNA polymerase for each probe

Probe	Linearization site	RNA polymerase	References
Cer1	*ApaI*	Sp6	(Yokouchi, Vogan et al. 1999)
Fgf8	*NotI*	T3	(Crossley, Minowada et al. 1996)
Hes6-1	*EcoRI*	T7	(Vilas-Boas and Henrique 2010)
Cdh2	PCR product *(see II.4)*	T7	(Garcia-Castro, Vielmetter et al. 2000)
Nodal	*XhoI*	T7	(Levin, Johnson et al. 1995)
Shh	*XhoI*	T3	(Riddle, Johnson et al. 1993)
Snai1	*SalI*	T7	(Marin and Nieto 2004)

II.3 Oligonucleotides

The Oligonucleotides used for PCR during the course of this work are listed in Table 2. The oligonucleotides (primers) were synthesized by Sigma.

II.4 Polymerase Chain Reaction (PCR)

II.4.1 PCR

To produce inserts for cloning the DNA vectors, PCR primers were designed for the specific target sequence on the insert DNA.

Reactions were prepared in a final volume of 50 µl (100ng template plasmid DNA, 10x PCR buffer with 50 mM $MgCl_2$, 2 mM dNTPs, 2.5 U PFU DNA polymerase – Stratagene – and 3.2 pmol of each primer).

Table 2. Oligonucleotides

Oligonucleotide	Oligonucleotide sequence
N-cad Fw1	5'-CCACCACCTGTGAAACACTG
N-cad T7 Rev1	5'-TAATACGACTCACTATAGGGGGATTGGCCTTTCATCAAGA

II.4.2 CYCLE SEQUENCING

The DNA samples to be sequenced were processed according to a protocol provided by the Genomics Unit at Instituto Gulbenkian de Ciência (IGC). 2µl of Terminator Ready Reaction Mix, 2 µl of buffer (both supplied by the Genomics Unit), 500 ng of double stranded DNA and 3.2 pmol of forward or reverse primer were mixed in a final volume of 10 µl and submitted to a PCR reaction. Cycle sequencing was performed with the following conditions: a denaturation step at 96ºC for 1 min, followed by 25 cycles at 96ºC for 10 sec, 50ºC for 5 sec, 60ºC for 4 min and a final step at 4ºC until ready to precipitate. The samples were ethanol/NaAc precipitated and the dry pellets sent to Genomics Unit (IGC) for analysis with ABI 3130XL DNA Sequencer Applied Biosystem. Alternatively, samples were sequenced by STABVIDA.

II.5 DNA constructs

II.5.1 MOLECULAR CLONING TECHNIQUES

Two different plasmid constructs were generated, one was a smaller insert of N-cadherin (461bp) in the pBluescript SK II and the other was the pCAGGS-NLS_Kaede. The first was generated for RNA visualization by *in*

situ hybridization, the second one was used to electroporate and follow single cell migration.

N-cadherin in the pBluescript SK

The full-length chicken N-cadherin (kindly provided by M. Takeichi) was digested with PstI, and a 461-base-pair fragment corresponding to the extracellular domain was cloned into pBS II SK (+) and used to detect N-cadherin expression.

NLS_Kaede in the pCAGGS

NLS_Kaede in pCS2^{+} vector (Fior, R. *et al*, 2012) was first cloned at EcoRI/BamHI site of the pSK. Then, it was inserted in a pCAGGS-MCS vector (this vector was modified by E. Bekman to contain the MCS of pSK) at the ClaI/SacI sites.

DNA CONSTRUCTS ALREADY AVAILABLE

pCAGGS-GFP

Was kindly provided by Dr. D. Henrique.

pCAGGS-N-cadherinYFP

Was kindly provided by Dr. C. Kalcheim (Cinnamon, Ben-Yair et al. 2006).

II.6 Embryological methods

II.6.1 EGGS AND EMBRYOS

Fertilized chicken (*Gallus gallus*) eggs were obtained from commercial sources (Quinta da Freiria, S.A., Roliça, Portugal), fertilized Japanese quail (*Coturnix coturnix japonica*) eggs were obtained from (Interaves Portugal) and incubated at 37ºC in a 17% humidified incubator. Embryos were staged according to the Hamburger and Hamilton development table (Hamburger and Hamilton 1992) in the chick and to corresponding HH-stages in the quail.

Mouse embryos (*Mus musculus*) WT C57BL/6 were collected at specific stages (8.0-8.5 dpc).

II.6.2 EX VIVO NEW CULTURE

Chicken embryos at stage HH3^{+} were explanted from the egg. Carefully the embryo was transferred to a Petri dish containing 1X Phosphate Buffer Saline (1x PBS: 136 mM NaCl; 2.7 mM KCl; 8.0 mM $Na_2HPO_4.H_2O$; 1.5 mM KH_2PO_4 pH 7.4-7.6).

The vitelline membrane was then stretched around a glass ring, making sure that the embryo stays in the centre of the ring. The ring with the vitelline membrane and embryo attached was then lifted and transferred into a small plastic Petri dish, filled with egg albumin and incubated in a humidified incubator during several hours depending on the required developmental stage.

II.7 Drug treatment

Embryos were collected at stage $HH3^+$ (as described above) and cultured with the specific inhibitors: 5 µl of Y27632 (100µM, Sigma). 3 µl of monoclonal rat antibody raised against mouse N-cadherin (39 µg/ml; MNCD2 - Hybridoma bank), 3 µl of polyclonal rabbit antibody raised against chicken N-cadherin (135 µg/ml; Anti-N-cad - a kind gift from M. Takeichi) and 3 µl of Rat IgG2a (100 µg/ml; Invitrogen) served as a control. All compounds were applied on the ventral surface of embryos at stage $HH3^+$, after which they were incubated until specific stages of development for further *in situ* hybridization analysis.

II.8 Bead implantation

For the administration of Omeprazole (28µM; Sigma), recombinant Nodal protein (0.5 mg/ml; R&D Systems) or SU5402 (96µM; Calbiochem) in the embryos, AG1-X2 anion-exchange beads (Bio-Rad) were soaked during at least 1 hour at 4ºC in one of these two drugs. For the Omeprazole delivery, two beads were placed, one on each side of the anterior region of the Primitive streak at stage $HH3^+$ in the New culture embryos (with ventral side up). For the SU5402, only one bead was placed on the right side and below the Hensen's node at stage HH5. Using a tungsten needle a small hole was made in which the bead was inserted between the epiblast and the hypoblast.

Both experiments had as a control, beads embedded in DMSO (0.2%).

Embryos were then placed at 37ºC during the time necessary to grow to the desired stage of development.

II.9 *In vitro* chick embryo electroporation in New culture

pCAGGS-NLS_Kaede and full length chicken pCAGGS_N-cadherin-YFP (kindly provided by C. Kalcheim) were injected in the perspective cells of the future node region at stage $HH3^{+}$ at a concentration of 4µg/µl in exception of the pCAGGS-CherryNLS (kindly provided by D. Henrique), pCAGGS-GFP and Venus-NLS-PEST (VNP), which were used at 1µg/µl.

Embryos processed for New culture (New, 1955) at HH3 - $HH3^{+}$ were transferred into a silicon pool containing a 2mm-square cathode (CUY701P2E electrode; Nepa Gene). The New's culture was covered with HBSS (Gibco) and the embryo injected with the DNA solution (1µl DNA; 0,1% Fast Green).

Platinum electrode with a 2mm-square anode (CUY701P2L electrode, Nepa Gene) was placed over the embryo and five pulses of 5V for 50ms at 500ms intervals were applied, using an Electro Square Porator^{TM} ECM830 (BTX). Embryos were incubated for 4h, until the plasmids started to be expressed.

II.10 Cell labelling in the Hensen's node with the lipophilic dyes DiI and DiO

DiI (1,1'-dioctadecyl-3,3,3'-tetramethylindocarbocyamine perchlorate) (red) and DiO (3,3'-dioctadecyloxacarbocyanine perchlorate) (green) (Molecular Probes) two different colour lipophilic dyes were used to label the cells in the node. The lipophilic dyes were injected in the node cells using borosilicate capillaries (Harvard Apparatus) with an outer diameter of 1.0mm and inner diameter of 0.58mm. The node cells were carefully injected with 3mg/ml of DiI and 7mg/ml of DiO diluted in dimethylformamide (DMF) on the left or on the right sides of the node at a

HH5 stage embryo. After this, the embryos were photographed (LEICA DFC320) for the first time to register the injection site (time 0 hours) and then after 3 and 6 hours of incubation to follow cell movement.

II.11 Whole-mount *in situ* hybridization

Chicken embryos were collected and fixed in 4% paraformaldehyde/PBS at 4ºC o.n. Whole-mount *in situ* hybridizations were performed as described in (Henrique, Adam et al. 1995) with modifications, using the digoxigenin (DIG) labelled antisense RNA probes.

Staining reaction was performed using BMP-Purple (Roche).

Embryos were photographed with a LEICA Z6 PRO stereoscope coupled to a LEICA DFC490 camera.

II.12 Tissue embedding and preparation of cryostat sections

After fixation, the embryos were washed in 1x PBS, passed first through a solution of 15% sucrose in PBS, followed by 30% sucrose in PBS for cryoprotection. The embryo was then embedded in solution containing 7.5% gelatin and 15% sucrose in PBS and frozen in cold isopenthane at -70ºC. Frozen embedded embryos were stored at -80ºC until sectioned in a cryostat (Leica CM 3050). Embryonic tissue was sectioned at 16µm and 20µm and collected on superfrost slides. Finally the slices were de-gelatinized and photographed (Leica DM 2500).

II.13 Imunofluorescence

The embryos in New culture were fixed for 2h at room temperature and processed for immunohistochemistry as described:

1- Embryos were permeabilized with 1% Triton-X100; 0.5% PBS and 2% bovine serum albumin (BSA) during 2h at room temperature.
2- Overnight incubation at 4ºC with Anti N-cadherin (clone 32, 1:100, BD Biosciences); ZO-1 antibody diluted in 1% BSA in PBS.
3- Secondary antibody used was Alexa 488-conjugated anti-mouse (Molecular Probes). Nuclei were visualized using ToPro3 (1:1000, Molecular Probes).
4- Embryos were treated with ribonuclease A (10 mg/ml, Sigma), slowly dehydrated in methanol and cleared with methylsalicylate (Sigma).

II.14 Fluorescence imaging

Immunofluorescence was analysed using the laser confocal microscope Zeiss LSM 510 Meta or the Zeiss LSM 710. Several Z stacks with optical sections spanning the thickness of the Hensen's node were acquired using a 40 x /1.3 NA oil-immersion objective.
Images were processed and analysed using the ImageJ software.

II.15 Live imaging

II.15.1 EMBRYO PREPARATION

All embryos electroporated with the constructs, except the ones with the full length N-cadherin_GFP, were incubated with 1µl of rat IgG2a (Invitrogen) or anti-N-cadherin antibody for 4h before screened under a fluorescent dissecting stereomicroscope (Leica MZ10F).

The ones that showed fluorescence in and around the node were selected and mounted for time-lapse imaging.

Stage $HH3^{+}$ - $HH4^{-}$ embryos were mounted ventral-side up in a glass-bottom Petri dishes with 35 mm diameter and 0.17 mm thickness (World Precision Instruments), with 1 ml albumin in the bottom and sealed with parafilm.

II.15.2 TIME-LAPSE IMAGING

For live imaging, electroporated embryos were transferred to glass-bottom Petri dishes containing a minimum amount of albumen to minimize image aberrations. 4D time-lapse Z-stacks of the node region where acquired on either a Zeiss LSM 510 Meta or a Zeiss LSM 710 inverted confocal microscopes using dry 20x 0.8NA objectives, every 10 minutes for a period of 7–12 hours. In Kaede-expressing embryos, before imaging, a 405nm laser was used to photo-convert cells in the anterior-right quadrant of the node region spanning a 50 µm width and 40 µm height by slow scanning with 100 interactions and maximum laser power.

II.15.3 IMAGE PROCESSING

For cell movement analysis, we first obtained maximum intensity projections of the 4D series using the ImageJ software (http://rsb.info.nih.gov/ij). To correct for embryo drift, we used the stack alignment function of the Amira v5.3 (Visage Imaging, Inc.) software in order to maintain “stationary” the center of the primitive pit during the whole imaging period; this involved both manual and automatic corrections. Brightness and contrast were adjusted for the optimal

identification of individual cells, after which the movies were analyzed and cell movements tracked by using “MTrackJ” plugin in ImageJ.

II.16 Statistical analysis

Fisher's exact t-test was used to evaluate the statistical significance for the rescue *in situ* hybridization experiments.

ANOVA followed by Tukey t-test comparisons were used to establish significance among different time points and treatments.

Student's t-test was used to compare a single treated group with controls.

Chapter III

N-cadherin locks left-right asymmetry by ending the leftward movement of Hensen's node cells

Raquel V. Mendes, Gabriel G. Martins, Ana M. Cristóvão and Leonor Saúde. "N-cadherin locks left-right asymmetry by ending the leftward movements of Hensen's node cells". Developmental Cell, *in press*

ABSTRACT

The stereotypic left-right (LR) asymmetric distribution of internal organs is due to an asymmetric molecular cascade in the lateral plate mesoderm (LPM) that has its origin at the embryonic node. In chicken embryos, molecular asymmetries at Hensen's node are created by leftward cell movements that occur transiently. What terminates these movements, and moreover what is the impact of prolonging them on the LR asymmetry cascade, was entirely unknown. Here, we show that leftward movements last longer when N-cadherin function is blocked and cease prematurely when N-cadherin is overexpressed on the right side of the node. The prolonged leftward movements lead to loss of asymmetric expression of *wnt3a*, *fgf8* and *nodal* at the node region. This originates an abnormal expression of the asymmetric genes *cer1* and *snai1* in the LPM, resulting in a mispositioned heart. We conclude that N-cadherin stops the leftward cell movements, and that this termination is an essential step in the establishment of LR asymmetry.

INTRODUCTION

In spite of the external bilateral symmetry of the vertebrate body, the internal organs display left-right (LR) asymmetric orientations essential for their function. The asymmetric positioning of internal organs is controlled by the conserved Nodal cascade initiated in the node at the onset of gastrulation (Lourenço and Saúde 2010). How is the initial LR molecular asymmetry generated in the node remained unanswered for a number of years. Seminal experiments showed that the Nodal cascade on the left side of the embryo is induced by a leftward fluid flow created by motile cilia found on the mouse node, zebrafish Kupffer's vesicle and *Xenopus* gastrocoel roof plate (Lourenço and Saúde 2010).

An alternative strategy to generate LR molecular asymmetries was recently found in chicken embryos. At stage HH4, and downstream of H^+/K^+-ATPase pump activity, there is a transient leftward movement of cells around Hensen's node that by stage HH5 is stopped. As a consequence of these transient leftward movements, the initial bilateral expression of *shh* on the rostral part of the node becomes restricted to the left side, while the early bilateral *fgf8* expression in the primitive streak (PS) turns into an asymmetric expression on the right side of the node (Cui, Little et al. 2009; Gros, Feistel et al. 2009). On the left side of the node, Shh induces *nodal* expression in the perinodal region (Levin 2005), while on the right side Fgf8 inhibits *nodal* expression (Boettger, Wittler et al. 1999), thus placing the Nodal cascade on the left side. An excess of Nodal activity on the left perinodal region is transferred to the left lateral plate mesoderm (LPM). The expression of *nodal* is amplified in the left LPM through a positive feedback on its own transcription (Nakamura, Mine et al. 2006). At the same time, Nodal activates its negative regulators, the

lefty genes and *cerberus-like 1* (*cer1*), restricting the range of Nodal signalling to the left side. The induction of *pitx2* by Nodal on the left LPM and of *snail1* (*snai1*) by Fgf8 on the right LPM will promote asymmetric morphogenesis of internal organs (Lourenço and Saúde 2010).

How are the transient leftward movements of Hensen's node cells terminated once the asymmetric signals are established, and moreover what is the outcome if these movements continued for an extended period of time, are fundamental questions to understand LR asymmetry establishment. The adhesion molecule N-cadherin is a good candidate to stop the leftward movements. N-cadherin protein and its mRNA (*cdh2*) are initially expressed in a symmetric fashion in the PS, but become asymmetrically expressed on the right side of the node at stage HH5 (Garcia-Castro, Vielmetter et al. 2000), which corresponds to the time point when the leftward movements stop. Moreover, it was shown that N-cadherin inhibition leads to heart mispositioning in chicken embryos (Garcia-Castro, Vielmetter et al. 2000).

In this study, we used for the first time the Kaede photo-convertible fluorescent protein tool combined with in vivo confocal microscopy to track single cell movements in the chicken node. We show that a cell-cell adhesion mechanism mediated by N-cadherin terminates the leftward movements of node cells, thus locking LR asymmetries established earlier. Furthermore, we show that locking LR asymmetries in the node is essential to transfer the correct molecular information to the LPM, allowing the proper asymmetric looping of the heart.

III.1 RESULTS

III.1.1 N-cadherin asymmetric expression in Hensen's node is generated by the leftward cell movements downstream of the H^+/K^+-ATPase pump

We investigated if the leftward cell movements downstream of the H^+/K^+-ATPase activity are responsible for generating an asymmetric displacement of *cdh2*-expressing cells in the node, similarly to what was shown to underlie the dynamics of *shh* and *fgf8* expression.

We treated chicken embryos at stage $HH3^+$ with the H^+/K^+-ATPase inhibitor omeprazole. From a total number of 46 treated embryos, 27 (58%) showed symmetric expression of *cdh2* in the node at stage HH5 (Figs. 1G, I). This is in contrast to control DMSO-treated embryos, which showed an asymmetric *cdh2* expression in 83% (n=19) of the cases (Figs. 1B, E). Accordingly, N-cadherin protein distribution was also found in equal levels on both sides of the node in 50% (n=16) of omeprazole-treated embryos (Figs. 1H, J), in contrast to control DMSO-treated embryos, which showed asymmetric distribution in 80% (n=5) of the cases (Figs. 1C, F).

We then blocked cell movements by applying the Rho Kinase inhibitor Y27632 (Uehata, Ishizaki et al. 1997; Itoh, Yoshioka et al. 1999) over stage $HH3^+$ embryos. By stage HH5, *cdh2* expression was no longer asymmetric but equal on both sides of the node in 59% (n=57) of Y27632-treated embryos (Figs. 1O, P) in contrast to controls where 75% (n=44) displayed an asymmetric expression (Figs. 1L, N).

Altogether these results show that *cdh2* expression becomes asymmetric with more expression on the right side of the node by stage HH5 due to

the leftward cell movements that occur at stage HH4 downstream of the H^+/K^+-ATPase pump.

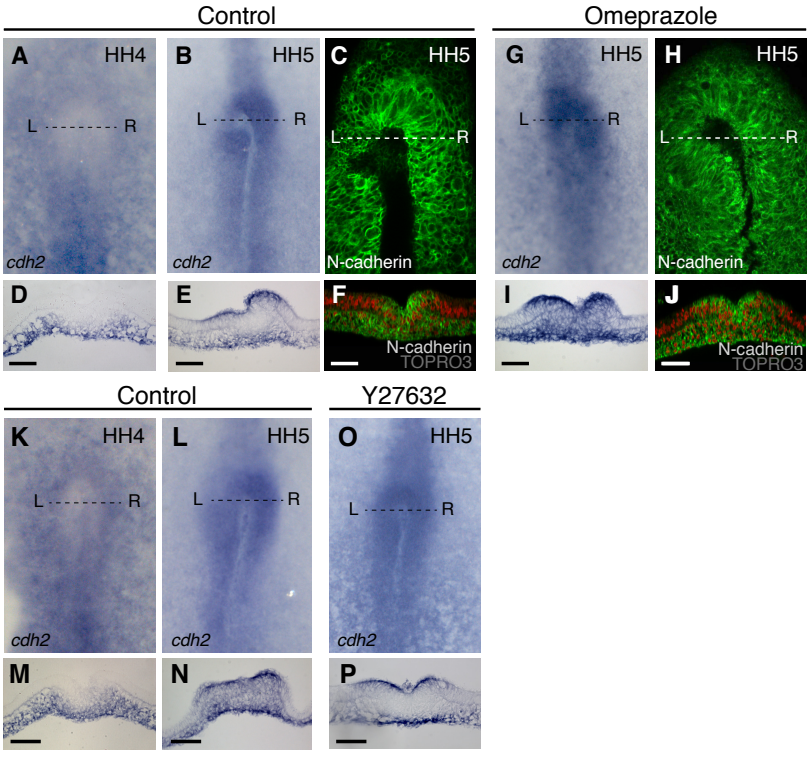

Figure 1| *cdh2* asymmetric expression in Hensen's node is promoted by leftward cell movements downstream of the H^+/K^+-ATPase pump. Embryos treated with vehicles DMSO (**A-F**) or water (**K-N**) show normal expression of *cdh2* mRNA in the PS at stage HH4 (**A, D, K, M**) and normal increased levels of *cdh2* mRNA (**B, E, L, N**) and N-cadherin protein (**C, F**) on the right side of the node at stage HH5. (**G, I**) *cdh2* mRNA expression is bilateral and (**H, J**) N-cadherin protein is symmetrically localized in the node in embryos treated with the H^+/K^+-ATPase pump inhibitor omeprazole. (**O, P**) In an embryo treated with Rho Kinase inhibitor drug Y27632, *cdh2* expression in the node is symmetric. (**D, E, I, M, N, P**) Cryostat sections at the dashed line level in A, B, G, K, L, O. (**F, J**) Confocal axial sections at the dashed line level in C and H. N-cadherin protein in green; DNA in red. Scale bars, 50 μm.

III.1.2 N-cadherin asymmetric activity halts the leftward cell movements in Hensen's node

Since N-cadherin activity can modulate cell migration during embryogenesis (Becker, Langhe et al. 2012) we decided to investigate

migratory behaviours in the Hensen's node region in response to N-cadherin perturbations.

For this purpose, stage HH3$^+$ chicken embryos were electroporated with a Kaede-NLS photo-convertible fluorescent protein (Sato, Takahoko et al. 2006) that allowed us to specifically label a group of cells on the right side of the node at stage HH4 (Fig. 2A) and then again at stage HH5 in the same embryo (Fig. 2H). The movement of photo-converted fluorescent labelled cells at each time point was imaged using time-lapse confocal microscopy.

In agreement with previous reports (Cui, Little et al. 2009; Gros, Feistel et al. 2009) we observed that in control embryos, cells marked on the right side of the node moved leftward and crossed the midline during stage HH4 (Figs. 2B-D; Table 1; Movie 1; n=6 embryos). However, cells labelled on the right side of the node at stage HH5 did not display such a movement (Figs. 2I-K; Table 1; Movie 1; n=6 embryos) demonstrating that the movement at stage HH4 is transient. When we blocked N-cadherin activity, by placing the Anti-N-cad antibody (Hatta, Nose et al. 1988) over the embryo at stage HH3$^+$, we found that cells were displaced from right to left at stage HH4 (Figs. 2E-G, Table 1; Movie 2; n=5 embryos), but, rather than ceasing, this leftward cell movements continued during stage HH5 and HH6 (Figs. 2L-N, Table 1; Movie 2; n=5 embryos). Similar results were obtained when we used the N-cadherin antibody MNCD2 (Matsunami & Takeichi 1995) (Supplementary Data; Figs. S1E-G, S1L-N; Movie S2; n=5 embryos).

In the converse experiment, we electroporated a fluorescent version of full-length N-cadherin (Fujimori and Takeichi 1993) on the right side of the node at stage HH3$^+$ and imaged the cell movements during stages HH4 and HH5. We found that by prematurely inducing an asymmetric

expression of N-cadherin, the leftward movements during stage HH4 did not occur (Figs. 2O-Q; Movie 3; n=6 embryos). Instead, the cells aggregated and started to adopt a cell displacement pattern typical of stage HH5 (compare Fig. 2Q with Fig. 2K), with cells moving rostrally as a consequence of the rostral-caudal body axis extension.

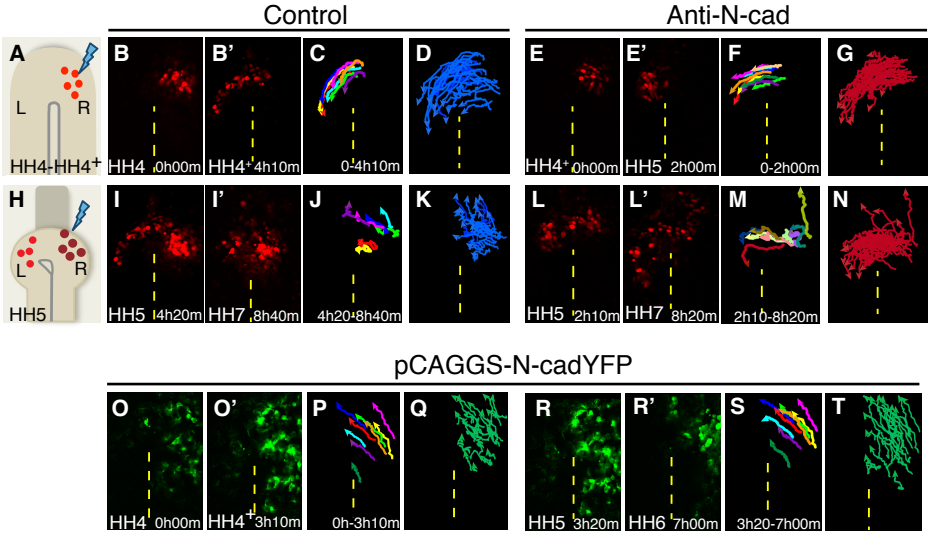

Figure 2| Transient leftward cell movements in Hensen's node are promoted by asymmetric N-cadherin activity. (**A**) A stage HH4/HH4^{+} diagram showing photoconverted cells (red dots) on the right side of the node. Position of photoconverted cells at two time-points and their tracks in a control (**B-C**) and an Anti-N-cad treated embryo (**E-F**). Overlay tracks of all cells analyzed from six controls (**D**) and five Anti-N-cad treated embryos (**G**) photoconverted at stage HH4/HH4^{+} and tracked until stage HH5. (**H**) A stage HH5 diagram where photoconverted cells at stage HH4/HH4^{+} (light-red dots) moved to the left and new cells were photoconverted (dark-red dots) on the right side of the node. Position of photoconverted cells at two time-points and their tracks in a control (**I-J**) and an Anti-N-cad treated embryo (**L-M**). Overlay tracks of all cells analyzed from six controls (**K**) and five Anti-N-cad treated embryos (**N**) photoconverted at stage HH5 and tracked until stage HH7. Position of full-length N-cadherin-YFP expressing cells at two time-points and their tracks imaged during stage HH4 (**O-P**) and from stage HH5 onwards (**R-S**). Overlay tracks of all cells analyzed from six embryos imaged during stage HH4 (**Q**) and from stage HH5 onwards (**T**).

Table 1. Number of cells that crossed the midline at different stages of development in control versus Anti-N-cad treated embryos

Beginning of cell tracks			Nº of tracked cells	Nº of cells that cross the midline during stages				Nº of cells that do NOT cross the midline #
				HH4	HH4^{+}	HH5	HH6	
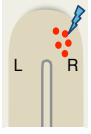	HH4	Control	27	16*	6	**0**	**0**	5
		Anti-N-cad	22	2*	4	**12**	**0**	4
	HH4^{+}	Anti-N-cad	13	n/a	7	**4**	**0**	0
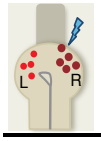	HH5	Control	28	n/a	n/a	**0**	**0**	28
		Anti-N-cad	24	n/a	n/a	**9**	**4**	11

***** The higher number of cells that cross the midline at stage HH4 in control embryos when compared to Anti-N-cad embryos is most probably due to a technical issue. In controls we managed to start the tracks at an earlier time point (spanning on average 3 hours before reaching stage HH4^{+}), while in Anti-N-cad embryos we only managed to start the tracks at a later time point (spanning on average 2 hours before reaching stage HH4^{+}).
# The cells that did not cross the midline, either stayed on the right side of the node and were displaced anteriorly or died or divided or aggregated. n/a, not applicable.

We propose that asymmetric N-cadherin expression on the right side of Hensen's node at stage HH5 is required to halt the leftward cell movements at this stage, thus ensuring that the LR displacement of cells initiated at stage HH4 is only a transient phenomenon.

III.1.3 Blocking N-cadherin activity perturbs Left-Right asymmetry establishment

We evaluated the impact of the prolonged leftward cell movements, revealed in the absence of N-cadherin activity, on asymmetric gene expression in the node and LPM.

In embryos where N-cadherin was blocked, using the Anti-N-cad antibody, *shh* was expressed on the left side of the node (96%, n=23; Fig. 3B) as observed for control embryos (96%, n=28; Fig. 3A), similarly to what has been described by Garcia-Castro *et al*. (2000). However, there was an impact on the expression of *fgf8,* which in this experimental situation became bilaterally symmetric in 62% (n=21) of the embryos (Fig. 3D) in contrast to controls where asymmetric expression was found in 73% (n=22) of the embryos (Fig. 3C). We must point out that Garcia-Castro *et al*. (2000) did not describe changes in *fgf8* expression after blocking N-cadherin activity, probably be due to the use of a different antibody.

Our interpretation of these results is that, as shown above, without N-cadherin function, the leftward cell movements at stage HH4 proceed normally and therefore *shh*-expressing cells move leftward and its expression becomes asymmetric as normal. However, as these movements continue towards the left side for longer when N-cadherin activity is inhibited, a symmetric expression of *fgf8* is obtained. These results seem to indicate that at stage HH5, N-cadherin function is required to lock the asymmetries established by the leftward cell movements, which occurred earlier in the node.

To test this further, we used anti-N-cad antibody to block N-cadherin function, pass stage HH4 and then by adding the Y27642 compound at stage HH4^{+} and let it act for 1h-1h30m we wanted to stop these prolonged movements and see if in this situation the expression of *fgf8* would be

rescued. We found that in embryos treated with Anti-N-cad/Y27632 the normal *fgf8* expression was poorly increased from 53.8% (n=13) (Fig. 3E) to 58.3% (n=24) (Fig. 3F), this was not statistically significant, p= 1.0 (Fisher's exact test). This particular experiment is very challenging because we are adding in the same embryo two different molecules: one that should prolong cell movement and the other that should stop cell movement. By adding Anti-N-cad at stage $HH3^{+}$ we were allowing the movements to occurs pass stage HH4 and then by adding the Y27642 compound at stage $HH4^{+}$ and let it act for 1h-1h30m we wanted to stop these prolonged movements and see if in this situation the expression of *fgf8* would be rescued. We think that defining in a precise manner the amount and timing of the addition of these molecules might be too critical for the outcome.

In addition, we found that without N-cadherin function the expression of *nodal* in the perinodal region was downregulated in 76% (n=34) of the embryos (Fig. 3H) in contrast to its asymmetric expression in controls 80% (n=15) (Fig. 3G). Since Shh induces *nodal* (Pagan-Westphal and Tabin 1998) and Fgf8 inhibits it (Boettger, Wittler et al. 1999), we can consider that the abnormal translocation of *fgf8*-expressing cells to the left side of the node creates an abnormally Fgf8-rich environment on that side. In spite of the normal Shh levels on the left side of the node, we hypothesize that the increased levels of Fgf8 push the signalling equilibrium towards a configuration where *nodal* expression is downregulated on the left side.

Given that *nodal* expression in the perinodal region was downregulated without N-cadherin function (Fig. 3H), we expected that *nodal* expression in the LPM would be downregulated. However, when we examined the expression of *nodal* in the LPM, it was unaffected (94%, n=17; Fig. 3J) compared with controls (100%, n=16; Fig. 3I) similarly to

what has been described by (Garcia-Castro, Vielmetter et al. 2000). According to the self-enhancement and lateral-inhibition model (Nakamura, Mine et al. 2006) it is possible to envision a scenario where a small amount of Nodal could induce a normal expression of *nodal* in the LPM through its positive feedback loop, given that its inhibitors are down-regulated. We found that *cer1* expression on the left side was indeed downregulated in embryos where N-cadherin was blocked (46%, n=24; Fig. 3L) compared with the normal levels in controls (84%, n=32; Fig. 3K). Furthermore, we found that *snai1* expression was bilateral in the LPM when N-cadherin was blocked (38%, n=16; Fig. 3N), a phenotype that contrasts to the right-sided expression observed in controls (100%, n=10; Fig. 3M), as previously described by (Garcia-Castro, Vielmetter et al. 2000). Again, we must emphasize that similar results were obtained when we used the N-cadherin antibody MNCD2 (Matsunami and Takeichi 1995) (Supplementary data; Figs. S1P, S1R, S1T, S1V, S1X, S1Z).

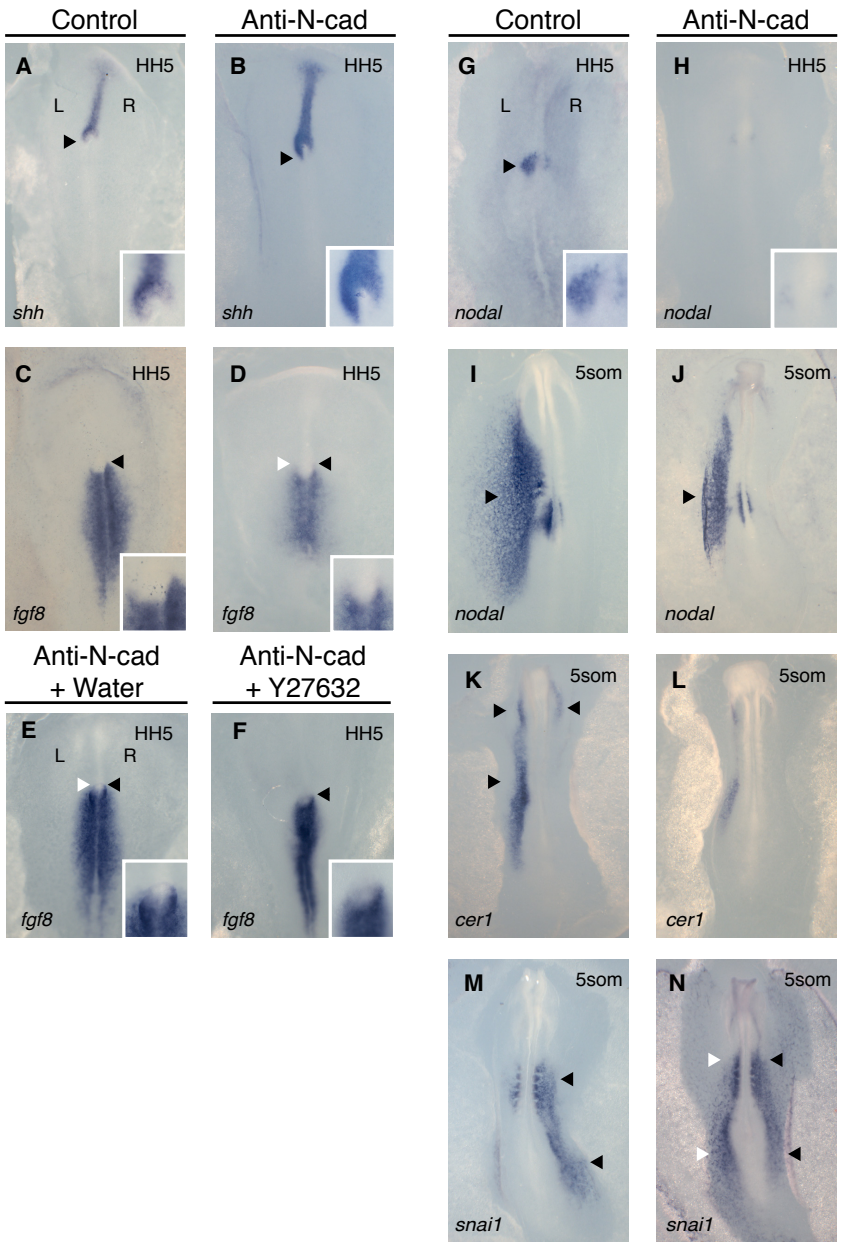

Figure 3| Loss of N-cadherin activity affects asymmetric gene expression in Hensen's node and Lateral Plate Mesoderm. *shh*, *fgf8* and *nodal* expression at stage HH5 in control (**A, C, H**) and Anti-N-cad treated embryos (**B, D, H**). *fgf8* expression at stage HH5 in an embryo exposed to the Anti-N-cad at stage HH3^{+}, followed by treatment with water vehicle (**E**) or Rho inhibitor drug Y27632 (**F**) at stage HH4^{+}. Asymmetric expression of *nodal* and *cer1* at 3-5 somite stage and *snai1* at 5-7 somite stage in the LPM in control (**I, K, M**) and Anti-N-cad treated embryos (**J, L, N**). Insets are magnifications of the node region. Black and white arrowheads indicate normal and abnormal expression, respectively. Dorsal views with rostral up. L, left; R, right

We propose that these results are a consequence of the abnormal expression of *fgf8* on the left side, since it was shown that Fgf8 represses expression of *cer1* (Rodriguez Esteban, Capdevila et al. 1999) and induces *snai1* (Boettger, Wittler et al. 1999).

III.1.4 Inhibition of Fgf signalling on the left side of the node, rescues normal gene expression in the left Lateral Plate Mesoderm

Accordingly to the previous results, the abnormal expression of *cer1* and *snai1* on the left LPM seemed to be caused by the misexpression of *fg8* on the left side of the node. To test this hypothesis, we analyzed if in those cases where N-cadherin was blocked using the MNCD2 blocking antibody (please see Supplementary data, for) and therefore the expression of *cer1* and *snai1* became abnormal, we could rescue these phenotypes by placing a bead soaked in Fgf signalling inhibitor SU5402 (Mohammadi, McMahon et al. 1997) on the left side of the node at stage $HH5^{+}$. Indeed, we could recover the percentage of normal *cer1* expression from 31.2% (n=16) in MNCD2 + DMSO control embryos (Fig. 4B) to 71.4% (n=14) in MNCD2 + SU5402 treated embryos (Fig. 4C); and of asymmetric *snai1* expression from 15.4% (n=13) in MNCD2 + DMSO control embryos (Fig. 4E) to 53% (n=17) in MNCD2 + SU5402 treated embryos (Fig. 4F); p= 0.0656 and 0.0575 for *cer1* and *snai1*, respectively (Fisher's exact test). In this rescue experiment, the percentage of normal heart looping increased from 20% (n=10) in MNCD2 + DMSO control embryos (Fig. 4H) to 83.3% (n=6) in MNCD2 + SU5402 treated embryos (Fig. 4I), p= 0.035 (Fisher's exact test).

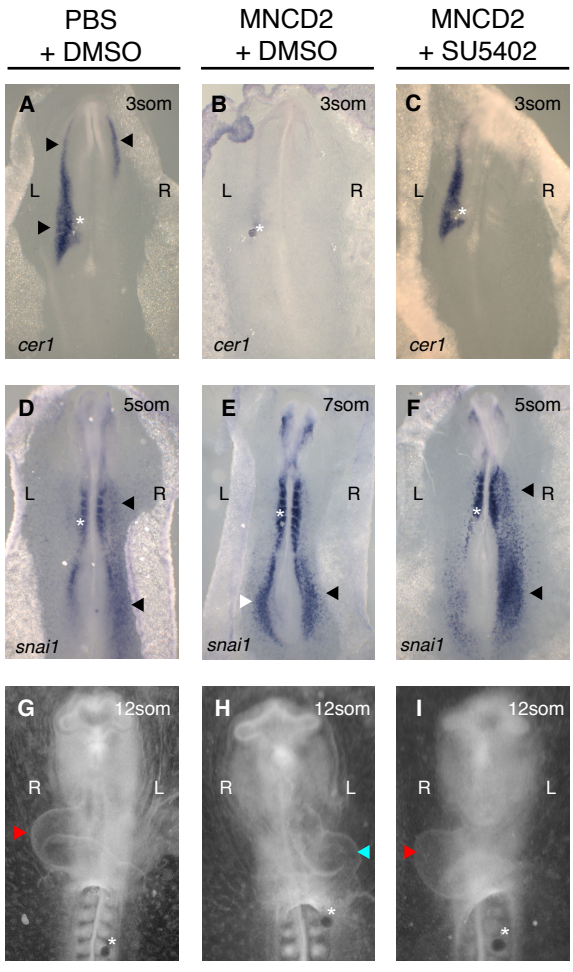

Figure 4| N-cadherin controls *cer1* and *snai1* expression in the Lateral Plate Mesoderm by controlling Fgf signalling. LPM expression of *cer1* at 3-somite stage and *snai1* at 5-somite stage in embryos treated with PBS at stage HH3^{+} followed by the implantation of a DMSO-soaked bead (**A**, **D**) and in MNCD2-treated embryos at stage HH3^{+} followed by the implantation of a DMSO-soaked bead (**B**, **E**) or a Fgf signalling inhibitor drug SU5402-soaked bead on the left side of the node at stage HH5^{+} (**C**, **F**). (**G**) In embryos treated with PBS followed by the implantation of a DMSO-soaked bead (n=6), 5 showed the heart on the right and 1 in the middle. (**H**) In MNCD2-treated embryos followed by the implantation of a DMSO-soaked bead (n=10), 2 showed the heart on the right, 4 in the middle and 4 on the left. (**I**) In MNCD2-treated embryos followed by the implantation of a Fgf signalling inhibitor drug SU5402-soaked bead (n=6) 5 showed the heart on the right and 1 in the middle. Black and white arrowheads indicate normal and abnormal gene expression, respectively. Red and blue arrowheads indicate normal and abnormal heart looping, respectively. Asterisks mark the final position of implanted beads. L, left; R, right.

These results show that the downregulation of *cer1* and induction of *snai1* in the left LPM observed in the absence of N-cadherin function is due to an abnormally *fgf8*-rich environment on the left side of the node.

III.1.5 Overexpression of N-cadherin on the right side of the node does not affect Left-Right gene expression in the node and Lateral Plate Mesoderm

Next, we wanted to understand what could be the impact on *shh*, *fgf8* and *nodal* in the node and *cer1* in the LPM (Fig. 5A-X), when N-cadherin was prematurely expressed on the right side of the node at stage HH4. According to Fig. 2O-T and Movie S3, cells on the right side of the node when overexpressing full-length N-cadherin (pCAGGAS-N-cadYFP) migrate rostrally at stage HH4, instead of crossing to the left side of the node. These rostral movements displaced *shh*-expressing cells located on the right side of the node into an anterior position leading to an increase in the notochord width (106.9 ± 7.546 µm in full-length N-cadherin versus 80.60 ± 8.176 µm in controls; Figs. 5C, F insets) but still created an asymmetric node expression (81%, n= 16; Fig. 5F compare with control 100%, n=11; Fig. 5C). At the same time, these movements displaced *fgf8*-expressing cells located on the right side of the PS into an anterior position also leading to an asymmetric node expression (63%, n= 16; Fig. 5L compare with control 69%, n= 13, Fig. 5I). As expected, the expression of downstream targets of *shh* and *fgf8*, namely *nodal* (100%, n=13; Fig. 5R compare with control 79%, n=14; Fig. 5O) and *cer1* (62%, n= 13; Fig. 5X compare with control 70%, n= 10; Fig. 5U), were not affected.

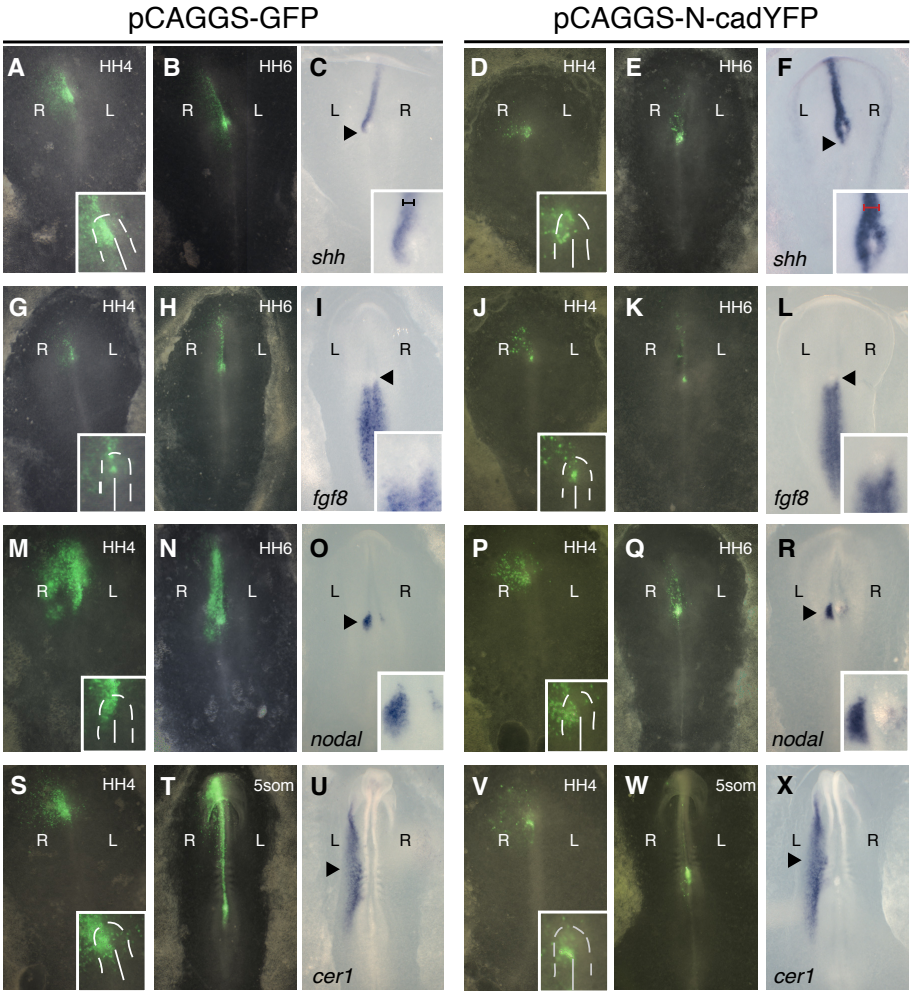

Figure 5| N-cadherin overexpression on the right side of the node does not affect asymmetric gene expression. Chicken embryos electroporated with pCAGGS-GFP or pCAGGS-N-cadYFP on the right side of the node at stage HH3^{+} and photographed at stage HH4 (**A, G, M, S, D, J, P, V**). The same embryos photographed at stage HH6 (**B, H, N, E, K, Q**) or at 5-somite stage (**T, W**) and *in situ* hybridized with *shh* (**C, F**), *fgf8* (**I, L**) *nodal* (**O, R**) and *cer1* (**U, X**). Insets are magnifications of the node region. Arrowheads indicate normal gene expression. Black bracket, notochord width in pCAGGS-GFP electroporated embryo; red bracket, notochord width in a pCAGGS-N-cadYFP embryo. Black arrowheads indicate the asymmetric expression. White arrowheads show the abnormal expression. Dotted circle represents the node. L, left; R, right.

The expression of *shh*, *fgf8, nodal* and *cer1* obtained when N-cadherin was overexpressed on the right side of the node at stage HH4, were not affected, which leads us to assume that N-cadherin does not regulate

these genes expression. However, it was able to create in advance, a naturally HH5 type of cell movement on the right side of the node.

III.2 DISCUSSION

We provide evidence for a mechanical basis for LR asymmetry establishment by showing that N-cadherin on the right side of Hensen's node at stage HH5 is required to halt the leftward cell movements initiated at stage HH4. This is crucial to stabilize the molecular asymmetries generated in the node, so that the correct asymmetric information is conveyed to the LPM and the proper looping of the heart is achieved (Fig. 6).

The *cdh2* gene encodes N-cadherin, a cell surface receptor that mediates cell-cell adhesion (Takeichi, 1995). The fact that *cdh2* becomes asymmetrically expressed on the right side of the node, at the same time that the leftward cell movements are stopped, raised the possibility that an asymmetric cell-cell adhesion mechanism could be involved in stopping these movements. Indeed we found that without N-cadherin function, the leftward movements continued during stage HH5, strongly suggesting that N-cadherin on the right side of the node is necessary to terminate these movements. This interpretation is consistent with the results obtained when we forced a premature asymmetric expression of N-cadherin on the right side of the node and showed that these cells were never displaced to the left side at stage HH4 or HH5.

Our results can be explained by the adhesive properties of N-cadherin that were shown to be sufficient to completely block the migration of neural crest cells (Monier-Gavelle et al., 1995; Nakagawa & Takeichi, 1998;

Shoval et al., 2007), muscle progenitors (Brand-Saberi et al., 1996; Nuessle et al., 2011), osteosarcoma and breast carcinoma tumour cells (Kashima et al., 2003; Potthoff et al., 2007). We should not discard the possibility that a cell sorting mechanism might also be in place. We could envision a scenario where cells with different levels of N-cadherin between the right and the left side of the node would be unable to mix. In fact, differences in the levels of N-cadherin were shown to be enough to mediate cell sorting not only in cell culture (Friedlander et al., 1989; Steinberg & Takeichi, 1994) but also in an intact embryonic tissue (Godt et al., 1998; González-Reyes et al., 1998).

The prolonged leftward cell movements that occur in the absence of N-cadherin function strongly impact on the establishment of LR asymmetries in the node. Specifically, we show that the expression of genes initially located in the PS, like *fgf8* does not become asymmetric on the right side of the node and in turn is detected on both sides. As a consequence of *fgf8* misexpression on the left side of the node, without N-cadherin function, *nodal* expression becomes downregulated around the node while in the left LPM *cer1* is repressed and *snail1* is ectopically activated.

Most developmental events occur within a specific time window, whether they are activation of gene expression in a particular cell type or alterations in the behaviour of a certain population of cells. If a particular event fails to occur within its proper time window, development is compromised. Therefore, to fully understand a particular developmental process, it is essential to understand what initiates it, but to uncover what terminates it is also of great importance.

Much attention has been given to the processes/signals that initiate LR asymmetry in the vertebrate embryo, but a clear gap of information

exist when we think about the processes/signals that terminate them. In this study, we show that N-cadherin is a key molecule responsible for finishing the leftward cell movements at the node and that stopping these movements at the right time is a crucial step in LR patterning.

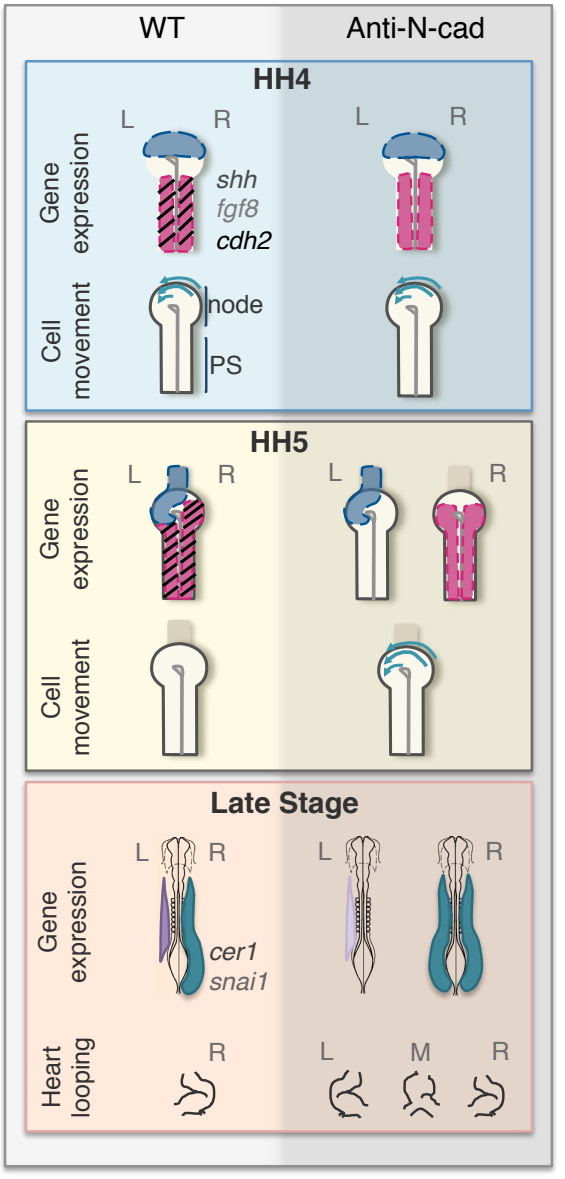

Figure 6| Proposed model for N-cadherin function in the establishment of Left-Right asymmetry in the chick embryo. At stage HH4, *shh* is symmetrically expressed on the rostral part of the node, while *fgf8* and *cdh2* are bilaterally expressed in the primitive streak/caudal part of node. Leftward movements of cells occur transiently during this specific stage and as a result an asymmetric displacement of cells is generated in the node at stage HH5 leading to an asymmetric expression of *shh* on the left and *fgf8* and *cdh2* on the right side of the node. Asymmetric expression of *cdh2* on the right side of the node at stage HH5 is crucial to halt the leftward cell movements at this stage and in this way stabilize the asymmetries generated in the node. These asymmetries are then transferred to the LPM allowing the proper asymmetric looping of the heart at later stages. When N-cadherin function is blocked early in development, the leftward movements that should have stopped after stage HH4 continue during stage HH5. Consequently, an abnormal gene expression in and around the node impacts the normal LR gene cascade of information to the LPM and as a consequence compromises the normal looping of the heart.

Movie 1. Time-lapse movie of a chicken embryo electroporated on the right side with Kaede-NLS photoconvertible fluorescent protein and treated with IgG2a control antibody.

Cells on the right side of the node were photoconverted from green to red at stage HH4 and followed for a period of 4 hours and 10 minutes after which some cells were found on the left side of the node. When the embryo reached stage HH5, new cells on the right side of the node were photoconverted from green to red and followed over a period of 4 hours and 20 minutes, after which, no cells were found to cross to the left side of the node. Cell tracks of the photoconverted cells are shown in the end. The yellow dashed line in the first frame marks the position of the primitive pit and primitive groove, and the pink circle highlights the photoconverted region.

Movie 2. Time-lapse movie of a chicken embryo electroporated on the right side with Kaede-NLS photoconvertible fluorescent protein and treated with anti-N-cad antibody.

Cells on the right side of the node were photoconverted from green to red at stage HH4 and followed for a period of 2 hours after which some cells were found on the left side of the node. When the embryo reached stage HH5, new cells on the right side of the node were photoconverted from green to red and followed over a period of 6 hours and 10 minutes, after which some cells were found to cross to the left side of the node. Cell tracks of photoconverted cells are shown in the end. The yellow dashed line in the first frame marks the position of the primitive pit and primitive groove, and the pink circle highlights the photoconverted region.

Movie 3. Time-lapse movie of a chicken embryo electroporated on the right side with full-length N-cadherinYFP.

The time-lapse starts at stage HH4 and finishes at stage HH6, spanning a 7-hour period. Fluorescent cells overexpressing N-cadherin found on the right side of the node never crossed to the left side. Cell tracks of fluorescent cells are shown in the end. The yellow line in the first frame marks the position of the primitive pit and primitive groove.

Supplemantary Data for Chapter III

There are several reports showing that the polyclonal rabbit antibody raised against chicken N-cadherin (Anti-N-cad), and the monoclonal rat antibody raised against chicken N-cadherin (NCD2) have a blocking activity both, *in vitro* and *in vivo* (Matsunaga, Hatta et al. 1988; Linask, Knudsen et al. 1997; Nakagawa and Takeichi 1997; Ganzler-Odenthal and Redies 1998). However, there was no evidence that the monoclonal rat antibody raised against mouse N-cadherin (MNCD2) was capable of recognizing chicken N-cadherin, and moreover, that it would exert a blocking activity in this protein in a different organism.

In collaboration with the laboratory of Prof. Takeichi (RIKEN, Japan) that developed both antibodies (Anti-N-cad and MNCD2), several experiments were performed in order to find out whether MNCD2 can affect chicken N-cadherin mediated cell-cell adhesion.

SI.1 MNCD2 recognizes chicken N-cadherin and weakly blocks cell-cell adhesion

Chicken N-cadherin-transfected L cells (cNLm-1) where analysed in the presence of NCD2 (monoclonal rat antibody raised against chicken N-cadherin) (Hatta and Takeichi 1986); or MNCD2 (monoclonal rat antibody raised against mouse N-cadherin) (Matsunami and Takeichi 1995) or Anti-N-cad (polyclonal rabbit antibody raised against chicken N-cadherin) (Hatta, Nose et al. 1988). We found that cNLm-1 cells treated with NCD2, MNCD2 and Anti-N-cad showed cell-cell adhesion defects when compared to control non-treated cells. These defects were more pronounced upon Anti-N-cad treatment but were also seen upon NCD2 and MNCD2 treatments (Fig. S1A).

We also looked for beta-catenin distribution in these cells after the antibody treatments (Fig. S1C). In the Anti-N-cad-treated cells, the junctional distribution of beta-catenin, as well as N-cadherin (Fig. S1B) was almost abolished, suggesting that this antibody strongly blocks N-cadherin function inducing the internalization of the N-cadherin-catenin complex. Although beta-catenin remained at cell-cell contact sites in both NCD2 and MNCD2-treated cells, beta-catenin distribution was disturbed when compared to control non-treated cells (Fig. S1C).

We found that both, NCD2 and Anti-N-cad immunostained these cells, while MNCD2 did not (Fig. S1B). Nevertheless, this result does not exclude the possibility that MNCD2 has an activity to affect chicken N-cadherin function for the following reason: early studies from Takeichi's lab found that an antibody designated as NCD1, did inhibit Cadherin activity by binding to the cell surface. This binding was detected by an indirect method but not by immunofluorescence staining (Hatta et al., 1985). Thus, the negative results in immunofluorescence staining of live cells do not mean that the antibodies do not recognize the antigens on them. And indeed, we could show that in Western Blot, MNCD2 recognizes not only mouse N-cadherin expressed in mouse N-cadherin transfectants (mNL), but also chicken N-cadherin, expressed in chicken N-cadherin transfectants (cNLm-1) (Fig. S1D). As expected, NCD2 recognizes chicken N-cadherin, expressed in chicken N-cadherin transfectants (cNLm-1) but does not recognize mouse N-cadherin (mNL) (Fig. S1D).

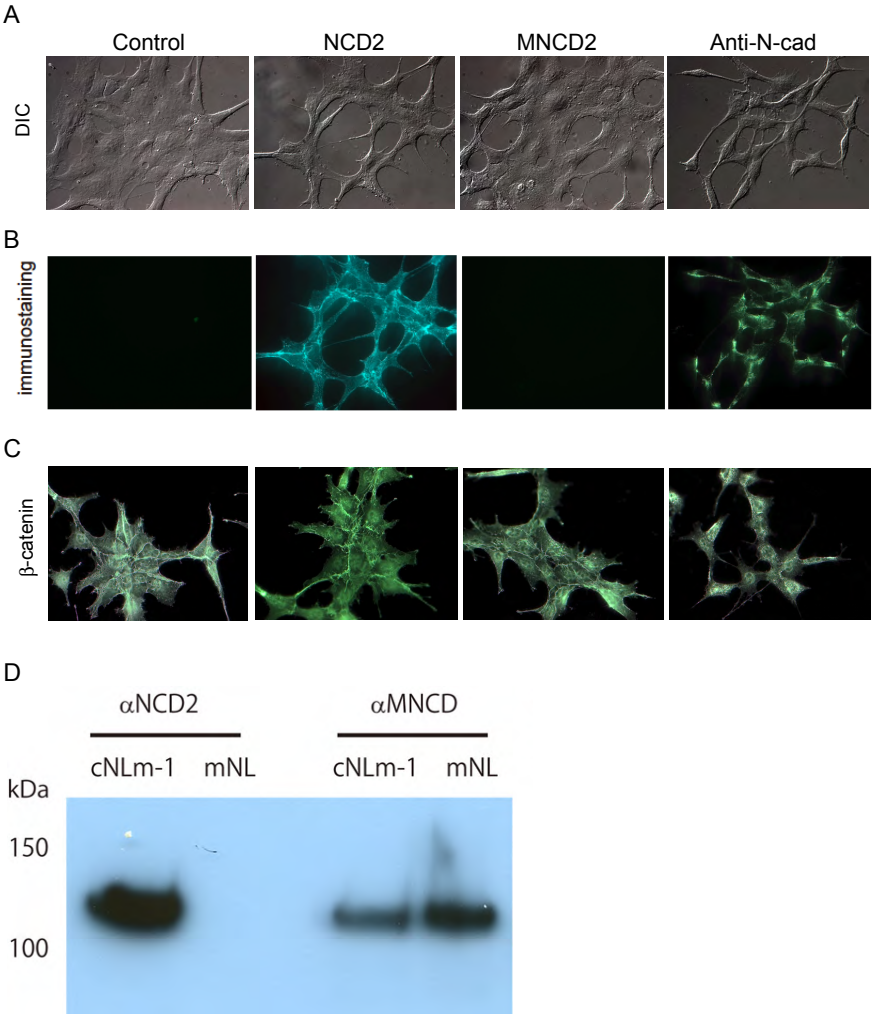

Figure S1| MNCD2 recognizes chicken N-cadherin and weakly blocks cell-cell adhesion. (**A**) DIC images of chicken N-cadherin-transfected L cells (cNLm-1) treated with NCD2, MNCD2 and Anti-N-cad showing cell-cell adhesion defects when compared to control non-treated cells. These defects were more pronounced upon Anti-N-cad treatment but were also seen upon NCD2 and MNCD2 treatments. (**B**) The same cells shown in (**A**) showing that in live cells NCD2 and Anti-N-cad immunostained cNLm-1 cells, while MNCD2 did not. (**C**) β-catenin immunostaining in cNLm-1 cells treated with NCD2, MNCD2 and anti-N-cad showing perturbations in β-catenin distribution. (**D**) Western blot analysis showing that MNCD2 recognizes mouse N-cadherin, expressed in mouse N-cadherin transfectants (mNL), but also chicken N-cadherin, expressed in chicken N-cadherin transfectants (cNLm-1). NCD2 recognizes chicken N-cadherin, expressed in chicken N-cadherin transfectants (cNLm-1) but does not recognize mouse N-cadherin (mNL).

Although NCD2 was characterized as an inhibitory antibody, we have now confirmed that its blocking action is subtle, and MNCD2 stands similar when compared with Anti-N-cad antibody.

Using NCD2 antibody to block N-cadherin function has been shown to lead to left-right defects (Garcia-Castro, Vielmetter et al. 2000) like, *snai1* and *pitx2* altered expression and chicken's heart randomization. In this supplementary chapter, we show that the ability of MNCD2 to block N-cadherin activity leads to left-right patterning defects similar to the ones we have shown in Chapter III using the Anti-N-cadherin blocking antibody.

SI.2 N-cadherin asymmetric activity halts the leftward cell movements in Hensen's node

Given that, N-cadherin activity can modulate cell migration during embryogenesis (Becker, Langhe et al. 2012) we decided to investigate migratory behaviors in the Hensen's node region in response to N-cadherin perturbations.

For this purpose, stage $HH3^{+}$ chicken embryos were electroporated with a Kaede-NLS photo-convertible fluorescent protein (Sato, Takahoko et al. 2006) that allowed us to specifically label a group of cells on the right side of the node at stage HH4 (Fig. S2A) and then again at stage HH5 in the same embryo (Fig. S2H). The movement of photo-converted fluorescent labeled cells at each time point was imaged using time-lapse confocal microscopy.

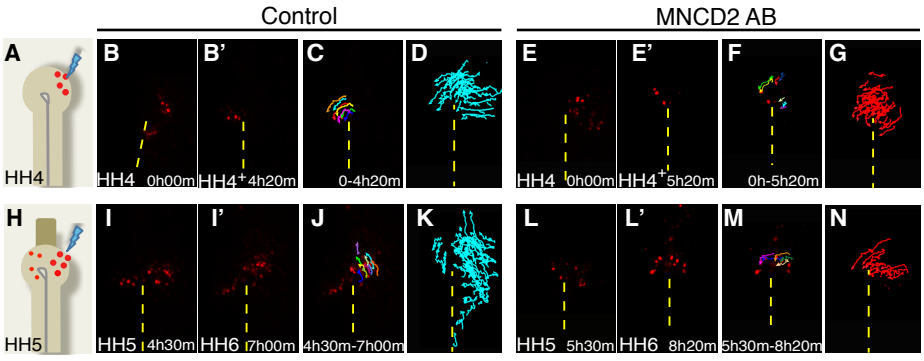

Figure S2| Transient leftward cell movements in Hensen's node are promoted by asymmetric N-cadherin activity.
(**A**) A stage HH4 diagram showing photoconverted cells (red dots) on the right side of the node. Position of photoconverted cells at two time-points and their tracks in a control (**B-C**) and in a MNCD2 antibody-treated embryo (**E-F**). Overlay tracks of all cells analyzed from six controls (**D**) and five MNCD2 antibody-treated embryos (**G**) photoconverted at the beginning of stage HH4 and tracked until stage HH5. (**H**) A stage HH5 diagram where photoconverted cells at stage HH4 **(**light-red dots) moved to the left and new cells were photoconverted (dark-red dots) on the right side of the node. Position of photoconverted cells at two timepoints and their tracks in a control (**I-J**) and in a MNCD2 antibody-treated embryo (**L-M**). Overlay tracks of all cells analyzed from six controls (**K**) and five MNCD2 antibody-treated embryos (**N**) photoconverted at the beginning of stage HH5 and tracked until stage HH6. In control embryos, 11 out of 20 labeled cells at stage HH4 crossed the midline and 0 out of 34 labeled cells at stage HH5 crossed the midline; in MNCD2 antibody-treated embryos, 7 out of 24 labeled cells at stage HH4 crossed the midline and 10 out of 16 labeled cells at stage HH5 crossed the midline.

SI.3 Blocking N-cadherin activity perturbs Left-Right asymmetry establishment

We evaluated the impact of the prolonged leftward cell movements, uncovered in the absence of N-cadherin activity, on asymmetric gene expression in the node and lateral plate mesoderm (LPM).

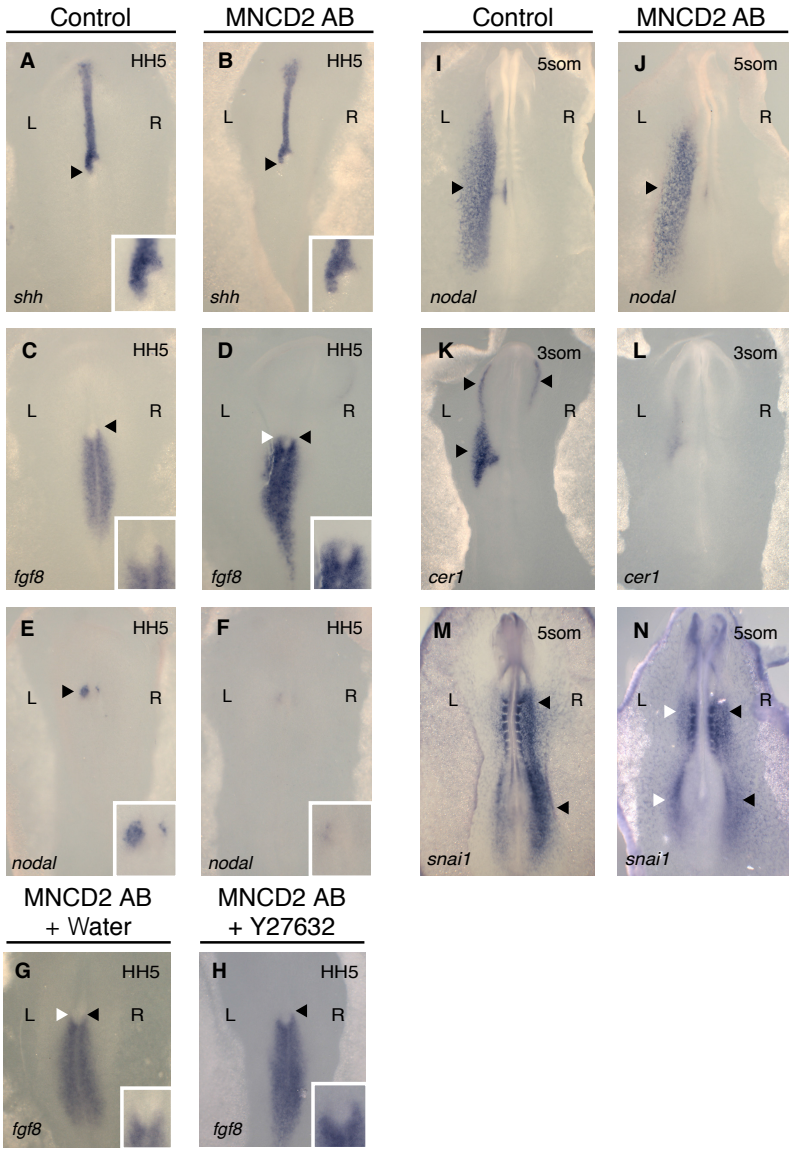

Figure S3| Loss of N-cadherin activity affects asymmetric gene expression in Hensen's node and Lateral Plate Mesoderm. *shh*, *fgf8* and *nodal* expression at stage HH5 in control (**A, C, E**) and MNCD2 treated embryos (**B, D, F**). *fgf8* expression at stage HH5 in an embryo exposed to the MNCD2 at stage HH3^{+}, followed by treatment with water vehicle (**G**) or Rho inhibitor drug Y27632 (**H**) at stage HH4. Accordingly to Fisher's exact test this is not statistically significant (the two-tailed P value equals 0.4401). The expression of *shh* was asymmetric on the left side of the node in 93% (n=16) of controls (**A**) and in 100% (n=19) of MNCD2-treated embryos (**B**). The expression of *fgf8* was asymmetric on the right side of the node in 80% (n=30) of controls (**C**) and became bilaterally symmetric in 43% (n=37) of MNCD2-treated embryos (**D**). In MNCD2-treated embryos the expression of *nodal* in the perinodal region was downregulated in 63% (n=30) of the embryos (**F**) in contrast to controls where asymmetric expression on the left perinodal region was found in 75% (n=12) (**E**). The expression of *nodal* was found to be restricted to the left LPM in 100%

(n=5) of controls (**I**) and in 100% (n=5) in MNCD2-treated embryos (**J**). The expression of *cer1* was asymmetric on the left side of the LPM in 87% (n=15) of controls (**K**) and downregulated in 53% (n=15) of MNCD2-treated embryos (**L**). The expression of *snai1* was asymmetric on the right side of the LPM in 97% (n=31) of controls (**M**) and became bilateral in 32% (n=38) of MNCD2-treated embryos (**N**). Insets in all panels show a magnification of the node region. Black and white arrowheads indicate normal and abnormal expression, respectively. L, left; R, right; AB, antibody.

Movie S1. Time-lapse movie of a chicken embryo electroporated with Kaede-NLS photo-convertible fluorescent protein on the right side.

Cells on the right side of the node were photo-converted from green to red at stage HH4 and followed for a period of 4 hours and 20 minutes after which some cells were found on the left side of the node.

When the embryo reached stage HH5, new cells on the right side of the node were photo-converted from green to red and followed over a period of 2 hours and 30 minutes, after which no cells were found to cross to the left side of the node. Cell tracks of the photoconverted cells at stage HH4 and later at stage HH5 are shown in the end. The yellow dashed line in the first frame marks the position of the primitive streak, and the pink circle highlights the region of photoconverted cells.

Movie S2. Time-lapse movie of a chicken embryo electroporated with Kaede-NLS photo-convertible fluorescent protein on the right side and treated with the N-cadherin blocking MNCD2 antibody.

Cells on the right side of the node were photo-converted from green to red at stage HH4 and followed for a period of 5 hours and 20 minutes after which some cells were found on the left side of the node. When the embryo reached stage HH5, new cells on the right side of the node were photo-converted from green to red and followed over a period of 2 hours and 50 minutes, after which some cells were found to cross to the left side of the node. Cell tracks of the photoconverted cells at stage HH4 and later at stage HH5 are shown in the end. The yellow dashed line in the first frame marks the position of the primitive streak, and the pink circle highlights the region of photoconverted cells.

Chapter IV

N-cadherin preserves the asymmetric morphology of the node and its left-right cell identity

ABSTRACT

The Hensen's node is a globular and epithelial structure that is formed in the rostral primitive streak when this gets full extension at stage HH4. It undergoes asymmetrical morphogenesis a few hours after its appearance, becoming an asymmetric structure around stage HH4^{+} with the right lip more prominent then the left lip. What determines this morphological difference between the two sides is a question that has not been completely answered yet.

Tissue morphogenesis describes the processes by which a tissue takes shape, which typically involves changes in cell number, size, shape, and position. Changes in cell position are caused by either cell migration or cellular rearrangements, such as cell intercalations and/or neighbour exchanges. What is necessary for these cellular processes to take place is some sort of force transmitted between individual cells that will generate tissue shape changes, usually mediated by cell-cell adhesion. An excellent candidate for promoting Hensen's node asymmetry is the cell adhesion molecule N-cadherin.

In this chapter, I show that the asymmetric localization of N-cadherin on the right side of the node at stage HH5 may contribute to shape the asymmetric morphology of the node. Blocking N-cadherin's function with MNCD2 compromised the asymmetric architecture of the node, not through cell shape changes but instead, by equalizing the number of cells between the right and the left sides of the node. Furthermore, it was also observed that N-cadherin function prevents mixing of left and right node cells beyond stage HH5. All together, these results suggest that different levels of N-cadherin in the Hensen's node preserve LR morphological and molecular identity of this embryonic region.

INTRODUCTION

The Hensen's node is a regional cellular thickening localized in the anterior end of the primitive streak, when this last one has reached its maximal length at stage HH4 of chicken development (Bellairs 1986). The Hensen's node is the amniote equivalent of the amphibian “Spemann's organizer”, and for that reason, can be considered as the most important region of the gastrulating embryo. It contains progenitors of the prechordal plate mesoderm, notochord and median regions of the presomitic mesoderm and somites (Spratt 1958; Selleck and Stern 1991; Psychoyos and Stern 1996), but it is also responsible for inducing and patterning the entire central nervous system (Tsung, Ning et al. 1965; Dias and Schoenwolf 1990).

Fate map and gene expression studies show that the cellular composition of the node changes constantly. Cells emigrate from the node and are replaced by cells from the surround epiblast, which then acquire node properties. For this reason, the node is constituted by a transient population of cells and not by a fixed one (Selleck and Stern 1991; Joubin and Stern 1999).

When we look closely to the Hensen's node with scanning electron microscopy (SEM) we can see that the node is an asymmetric structure between stages HH4^{+}-HH7, being the right side of the node thicker than the left one (Dathe, Gamel et al. 2002; Tsikolia, Schroder et al. 2012).

In this chapter, I extended our study of N-cadherin's role in the Hensen's node by analysing its effect on node's morphology. For this end, I compared cell shape and cell number between the left and the right sides in the presence and in the absence of functional N-cadherin. I show that N-cadherin maintains the asymmetric node morphology not by modifying its

cell shape but rather, by keeping the number of cells on the right side higher than the one on the left side.

Cell migration and cell mixing were also analysed in the node in the absence of functional N-cadherin. The results point to a scenario where different levels of N-cadherin expression in the node seem to prevent cell mixing.

IV.1 RESULTS

IV.1.1 N-cadherin preserves the asymmetric morphology of the Hensen's node

The asymmetry in N-cadherin on the right side of the node arises slightly after the Hensen's node becomes asymmetric, as seen by *in situ* hybridization and immunohistochemistry (Chapter III, Figs. 1B, C, E, F). Taking this into account, we wondered whether N-cadherin function could assist in the asymmetric morphology of this embryonic structure.

We analyzed the contour of the node region in transverse sections of embryos at stages HH5 and HH6, immunostained with the tight junction protein ZO-1, known to be expressed in epiblast node cells (Nakaya, Sukowati et al. 2008), and with the adherent junction protein N-cadherin, known to be localised in the epiblast and hypoblast at the node region between stages HH5-HH6 (Garcia-Castro, Vielmetter et al. 2000). In control embryos immunostained with ZO-1 (n=6; Fig. 1B) and N-cadherin (n=7; Fig. 1C), we found, as expected, that the right lip of the node was more prominent that the one on the left in 100% of the cases. In contrast, when N-cadherin function was blocked by placing the MNCD2 antibody (Matsunami and Takeichi 1995) over the embryos at stage $HH3^{+}$, we found that in 50% (n=4) of the embryos immunostained with ZO-1 (Fig. 1E) and 40% (n=5) of the embryos immunostained with N-cadherin (Fig. 1H) the asymmetries between the two sides of the node were no longer observed.

These results suggest that the cell-adhesion protein N-cadherin might play a role in maintaining the asymmetric structure of the node.

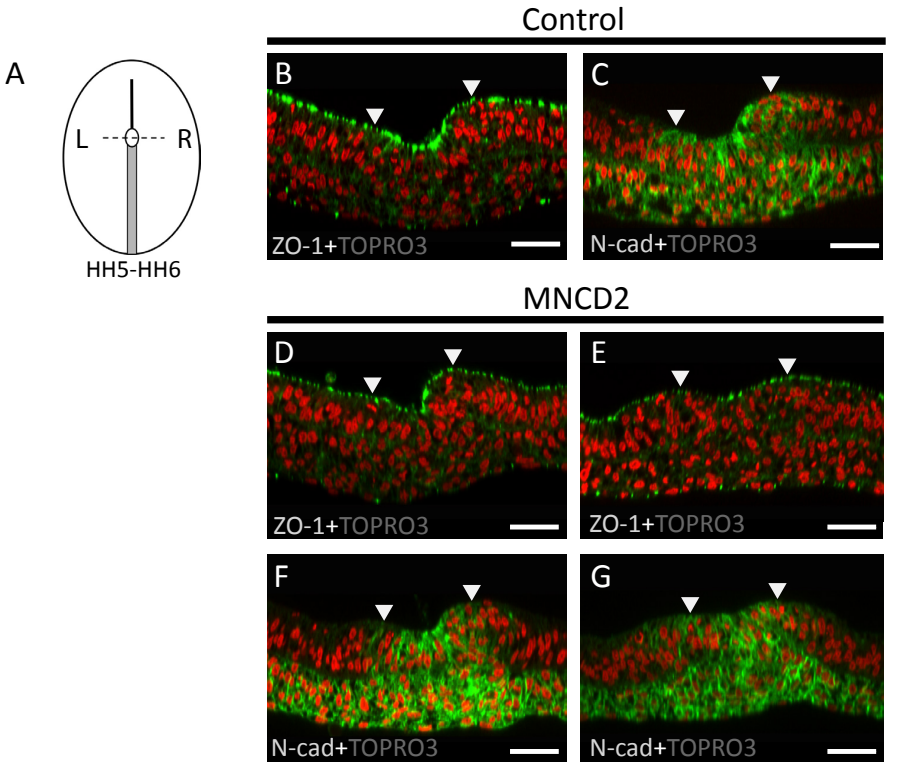

Figure 1| Blocking N-cadherin activity impacts on Hensen's node asymmetric morphology. (**A**) Schematic representation of a stage HH5-HH6 embryo showing the level (dotted line) at which the sections were obtained. (**B-H**) Transverse sections of the node region. Control embryos immunostained with ZO-1; n=6 (**B**) and N-cadherin; n=7 (**C**). MNCD2-treated embryos immunostained with ZO-1; n= 3 (**D-E**) and N-cadherin; n=8 (**F, G**). (**B, C**) Control embryos with an asymmetric node. In MNCD2-treated embryos, asymmetric nodes (**D, F**). Slightly asymmetric nodes (**E, G**). Arrowheads mark the left and the right lips of the node. L, left; R, right. Scale bars 25µm.

IV.1.2 Asymmetric number of cells between both sides of Hensen's node underlies its morphological asymmetry.

The acquisition of morphological asymmetries between the cells located on the left and right sides of an organ have been demonstrated to be able to shape it (Davis, Kurpios et al. 2008; Plageman, Zacharias et al. 2011). Having those examples in mind, we wondered if the changes in the node

morphology caused by the absence of N-cadherin function could be due to an alteration in the cell morphology *per se*.

To better understand the morphology of node's cells, we used the TOPRO3 nuclear staining to infer cell size and shape. The embryos analyzed were co-immunostained with ZO-1 or N-cadherin. The ZO-1 immunostaining makes it easier to delineate the node morphology, because it labels the tight junctions of the epiblast and N-cadherin helps to restrict the cells that should be considered, because it localizes specifically to the node region. For these reasons, both immunostainings were used to examine node cell morphology. To quantify the left-right differences in the shape of epiblast node cells, a mid section of the node was chosen from either control embryos (n=13) or MNCD2-treated embryos (n=11). The left cells were contoured in blue and the right side cells contoured in orange. The height and width of the nuclei traces were quantified (Figs. 2A-E). In control embryos the nuclei on the left side of the node are taller (height=9.879 ± 0.3012; n=30 cells; Fig. 2C) than the nuclei on the right side (height=7.512 ± 0.2595; n=30 cells; Fig. 2C) and the same trend stands true in embryos treated with MNCD2 (height of nuclei on the left=9.565 ± 0.2672; n=25 cells; height of nuclei on the right=7.481 ± 0.3540; n=25 cells; Fig. 2C).

In relation to the width of the nuclei in controls (Fig. 2D), we found that nuclei on the left side of the node (width=3.823 ± 0.1246; n= 30 cells) are equivalent to the nuclei on the right (width= 4.235 ± 0.1744; n=30 cells) and the same trend was found in embryos treated with MNCD2 (width of nuclei on the left= 4.181 ± 0.1146; width of nuclei on the left= 4.253 ± 0.1421; Fig. 2D).

These results, led us to conclude that the cells are different in height between the left and the right sides of the node, however, blocking N-

cadherin function did not alter this difference. On the other hand, the width of the cells with or without N-cadherin function was equal between the left and the right sides of the node (Figs. 2C, D).

Together these results show that there is a small difference in the shape of the cells that constitute the left and the right side of the node. Nonetheless, the symmetric morphology of the node resultant from blocking N-cadherin function with MNCD2 antibody does not seem to be due to an alteration in cell size or shape. The implication would be that the asymmetric morphology of the node is not cell size or shape dependent.

An alternative possibility for the asymmetric morphology of the node could be a difference in cell density between the two sides. To analyze cell density, a small square of 20 μm^2 was drawn on both sides of epiblast of the node (Fig. 2A, B). The nuclei labelled with TOPRO3 within this square were counted on both sides, with and without N-cadherin function.

In control embryos, the left epiblast of the node shows a cell density (n=10.77 cells/20 μ m^2) that is similar to the right epiblast (n=13.23 cells/20 μ m^2) (Fig. 2E). Interestingly, when we treated the embryos with the MNCD2 antibody against N-cadherin there was a decrease in cell density on both sides of the epiblast of the node (left side n=8.4 cells/20 μ m^2; right side n=9.88 cells/20 μ m^2; Fig. 2E). A statistically significant difference in cell density was found between the right sides of the controls (13.23 cells per 20 μ m^2) and MNCD2-treated embryos (9.88 cells per 20 μ m^2) (Fig. 2E). Overall these results indicate that the asymmetric morphology of the node does not seem to be dependent on cell density.

Finally, we tested if the asymmetric morphology of the node could simply be due to an increase in cell number on the right side of the node. Cell number was determined from manual counts of TOPRO3-stained nuclei on the left and right sides of transversal sections of the node in control or MNCD2-treated embryos (Figs. 2A, A', B, B', F).

In control embryos, the left epiblast of the node seemed to have less cells (n=21.27 ± 1.382 cells) than the right epiblast (n=30.20 ± 1.682 cells) (Fig. 2F). Interestingly, when we treated the embryos with the MNCD2 antibody against N-cadherin there was an increase in the number of cells on the left side (n=28.91 ± 2.113 cells; Fig. 2F). However, the number of cells on the right side was kept more or less unchanged (n=28.27 ±1.308 cells; Fig. 2F).

These results support the conclusion that the observable left-right difference in node's morphology is cell density independent and stems from changes in the packing of different numbers of cells on the left side versus the right side.

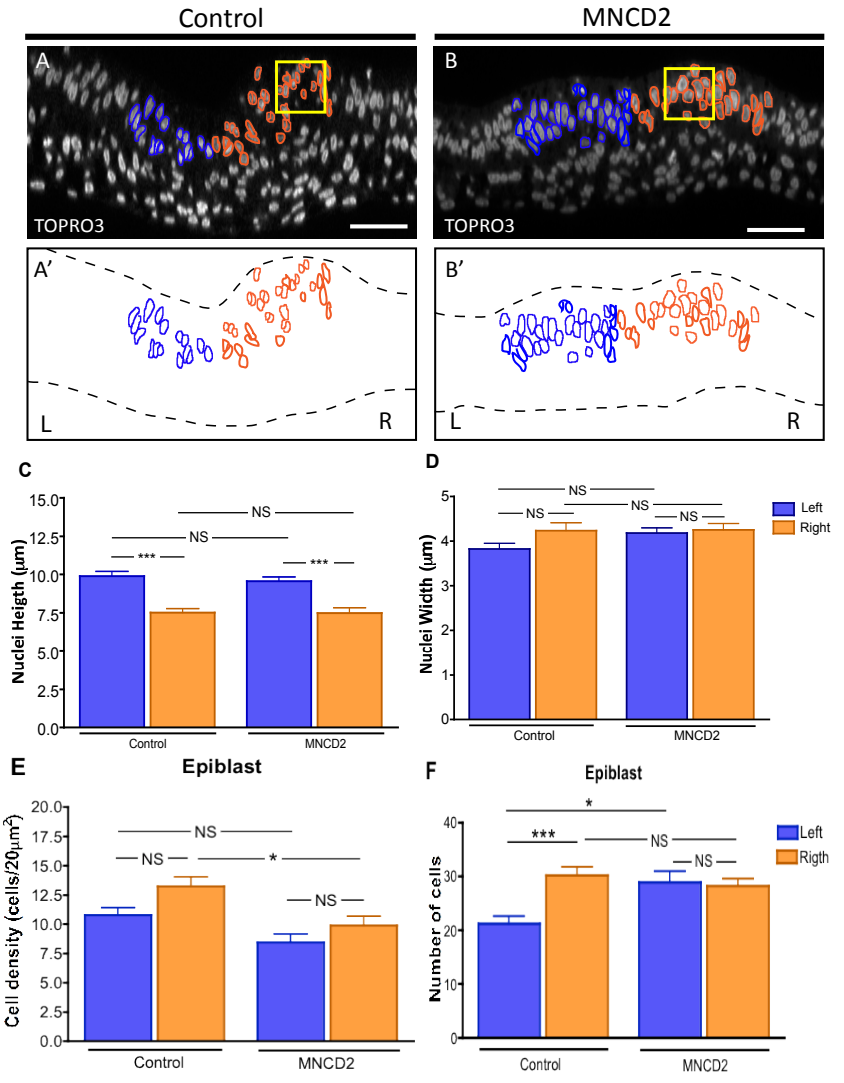

Figure 2| Blocking N-cadherin activity does not affect cell shape in the Hensen's node. Transverse sections at the node region in embryos between stage HH5-HH6. (**A**) Control embryo immunostained with TOPRO3 with nuclei of cells on the left side of the node outlined in blue and nuclei of cells on the right side of the node outlined in orange. (**A'**) Representation of the outlined nuclei that were quantified in the embryo shown in A. (**B**) MNCD2-treated embryo immunostained with TOPRO3 with nuclei of cells on the left side of the node outlined in blue and nuclei of cells on the right side of the node outlined in orange. (**B'**) Representation of the outlined nuclei that were quantified in the embryo shown in B. (**C, D**) Individual nuclei of left and right epiblast node cells were outlined and their average height and width were quantified. (**E**) Cell density measured in a 20µm^2 square placed in epiblast region on the right side of the node. (**F**) Number of cells counted in the epiblast region. Results are shown as means ± SEM (* p value < 0.05; *** p value < 0.001; one-way ANOVA with the Tukey's test). NS-not significant. Dotted lines – node morphology; L, left; R, right. Scale bars = 25µm

IV.1.3 N-cadherin prevents cell mixing in the Hensen's node

Accordingly to our previews results, node's morphological asymmetry was compromised in the absence of N-cadherin function, due to a disturbance in the difference of cell number between the two sides of the node. We asked whether cell retention on the right side could be due to a sorting mechanism promoted by different levels of N-cadherin.

To test this possibility, first, the embryos were treated at stage $HH3^{+}$ either with PBS or MNCD2 blocking antibody, and then when the embryos reached stage HH5-HH6, a small group of cells on the right and on the left side of the node were meticulously labelled with two different lipophilic colour dyes - DiI (red) and DiO (green). The two different dyes were used in order to distinguish the left from the right side labelled cells. Only the embryos that were labelled at the same anterior-posterior (AP) and left-right (LR) levels within the node were chosen for further analysis. We then looked at the fate of the labelled cells at different time points, namely: at three, six and fourteen hours after dies injection.

At 3 hours after dyes injection, we could see that some of the descendants of the labelled cells have already started to be left behind while the Hensen's node is regressing caudally as a consequence of the rostral-caudal body axis extension. Still, some of the cells remained in the node, and this is evident by the superimposed yellow area (Figs. 3A', D'). The same type of cell displacement was observed in the MNCD2-treated embryos, however the cell mixed area was bigger than in controls (yellow area, Figs. 3G', J'). Again, 3 hours later (which means 6 hours after dyes injection), the same embryos were photographed. In control embryos, we observed that the first cells that left the node contributed to the medial part of the somites, as expected (Figs. 3B, E), while, some cells still continued in the node with some mix (yellow area; Figs. 3B, E). Once again,

the MNCD2-treated embryos showed a similar type of cell displacement as the controls, but a larger mixed area in the node was observed (yellow area; Figs. 3H', K'). To guarantee that these results were independent of the dies being used, we decided to alternate the injection of the dye in the node (compare Figs. A with D and G with J) and we could conclude that the difference in the cell mixed area present in the node is independent of the dye used to label the cells.

In order to quantify the mixed area of the node in the two groups of embryos (controls versus MNCD2-treated), we used the ImageJ program to outline the merged areas (Figs. 3A', B', D', E', G', H', J' and K'). The results demonstrate that in the controls the percentage of merged area increased from a mean of 13% ± 1.67 SEM at 3 hours after injection to 16% ± 1.691 SEM at 6 hours (N=23 embryos; Fig. 3E). In the MNCD2-treated embryos, there was also a slight increased from 21% ± 1.25 SEM at 3 hours to approximately 23% ± 1.397 (N=37 embryos; Fig. 3E) at 6 hours. Although there wasn't a significant increase in the merged area from 3 to 6 hours in the MNCD2-treated embryos in relation to the controls, yet the merged area at 3 hours in the MNCD2-treated embryos was already considerably bigger (Figs. 3H', M) than the controls (Figs. 3E', M).

It was also observed that the cells from the right side crossed to the left side of the node in embryos where N-cadherin was blocked (Figs. 3H, H') (as we have already seen in chapter III), however, it was also interesting to notice that cells from the left side of the node were able to cross to the right side (Figs. 3H, H'). These results indicate that cells in the node are allowed to mix in the absence of N-cadherin function.

Despite the increased cell mixing in the node in embryos without N-cadherin function, this was not due to holding back the cells in the node,

neither to a slow cell migration, since it was not observed any difference in cells contribution at the AP level.

On the basis of our results, we put forward the hypothesis that different levels of N-cadherin might prevent cell mixing between the two sides of the node enabling them to maintain a left and a right distinct identity.

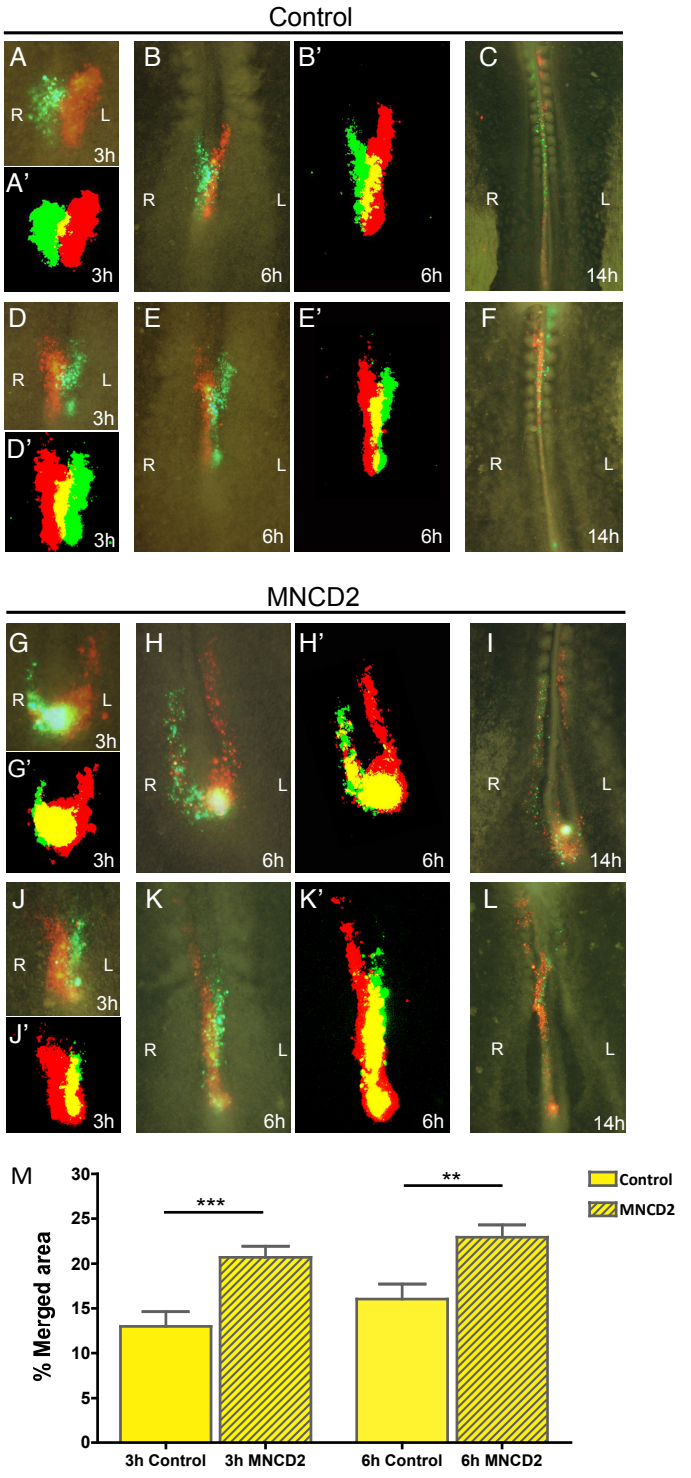
Control
A
R
L
3h
A'
3h
B
R
L
6h
B'
6h
C
R
L
14h
D
R
L
3h
D'
3h
E
R
L
6h
E'
6h
F
R
L
14h
MNCD2
G
R
L
3h
G'
3h
H
R
L
6h
H'
6h
I
R
L
14h
J
R
L
3h
J'
3h
K
R
L
6h
K'
6h
L
R
L
14h
M
% Merged area
30
25
20
15
10
5
0
***
**
Control
MNCD2
3h Control
3h MNCD2
6h Control
6h MNCD2

Figure 3| Cell mixing in the Hensen's node at different stages of development. (**A-C**) Control embryo where the node cells on the right were labelled with DiO (green) and the cells on the left were labelled with DiI (red) at stage HH5 and photographed 3, 6 and 14 hours-post-labelling. **(A', B'**) ImageJ-treated images of the embryos shown in A and B, respectively. (**D-F**) Control embryo where the node cells on the right were labelled with DiI (red) and the cells on the left were labelled with DiO (green) at stage HH5 and photographed 3, 6 and 14 hours-post-labelling. **(D', E'**) ImageJ-treated images of the embryos shown in D and E, respectively. (**G-L**) Embryos treated at stage HH3 with MNCD2 antibody, incubated until stage HH5. (**G-I**) MNCD2-treated embryo where the node cells on the right were labelled with DiO (green) and the cells on the left were labelled with DiI (red) at stage HH5 and photographed 3, 6 and 14 hours-post-labelling. **(G', H'**) ImageJ-treated images of the embryos shown in G and H, respectively. (**J-L**) MNCD2-treated embryo where the node cells on the right were labelled with DiI (red) and the cells on the left were labelled with DiO (green) at stage HH5 and photographed 3, 6 and 14 hours-post-labelling. **(J', L'**) ImageJ-treated images of the embryos shown in J and L, respectively. (**M**) Percentage of overlapping cells in the node in the presence versus absence of N-cadherin activity. The percentage of overlapping cells was calculated at 3 and 6 hours after the embryos were labelled using the formula: $\% = A_{mix} X\ 100 / A_L + A_R$, where A_{mix}= mixed area, A_L= area populated by the cells that were labelled on the left side of the node, A_R= area populated by the cells that were labelled on the right side of the node. Results are shown as means ± SEM (***p=0.004; **p=0.03; T-test). The number of control analysed embryos was n=23 and MNCD2-treated embryos was n=37. L, left; R, right.

IV. 2 DISCUSSION

In this chapter, I studied the impact of N-cadherin in the morphological LR asymmetry of the Hensen's node. The results show that N-cadherin can modulate the node asymmetric architecture by influencing its cellular number between the left and the right side. I also show that different levels of N-cadherin in the node play a role in cell sorting in that region, suggesting that differential N-cadherin expression might have the potential to promote cell segregation.

IV.2.1 Asymmetric morphology of the Hensen's node is attributed to differences in cell numbers

The asymmetric morphology of the Hensen's node is the first morphological asymmetry observed in the chicken embryo in the very first hours of its development (Dathe, Gamel et al. 2002). It becomes asymmetric soon after N-cadherin expression appears more abundantly on the right side of the node (Garcia-Castro, Vielmetter et al. 2000). This correlation prompted us to investigate the role of asymmetric N-cadherin expression in the morphology of the node.

Analysis of transverse sections of the node with and without N-cadherin function revealed that N-cadherin impacts on node's asymmetric morphology, since in the absence of N-cadherin function the node become symmetric (Fig. 1). Nevertheless, we show that this symmetric node produced in the absence of N-cadherin function is not due to alterations in cell shape or size. These findings contrast with what was found to underlie asymmetric morphogenesis of the gut (Kurpios, Ibanes et al. 2008; Plageman, Zacharias et al. 2011) and the heart (Manasek, Burnside et al. 1972) in the chicken embryo, where cell shape changes where found to be a relevant driving force. There is some evidence that the cell shape changes in the gut are driven by N-cadherin, as for the heart it is not known.

Dathe et al. (2002) proposed that the asymmetric morphology of Hensen's node was due to differences in cell density between the left and the right sides. According to our results, cell density does not seem to be the cause for the asymmetric morphology of the node, and instead our data clearly show that it is due to differences in cell numbers between the left and the right sides. We believe that this difference in cell number between the left and the right sides is due to N-cadherin's adhesion

properties that retain the cells on the right side and not due to cell proliferation. Supporting this, Sanders *et al* (1993) have already shown that proliferation in the node itself is noticeably low (Sanders, Varedi et al. 1993)

IV.2.2 N-cadherin prevents cell mixing in the Hensen's node during gastrulation

During development, progenitor cells which are initially specified in overlapping domains, eventually will need to segregate into separate compartments, such as germ layers and organ primordia so that they can give rise to different tissues and organs. Differences in adhesive, mechanical, and motile cell properties are thought to drive the initial sorting out of different progenitor cell populations (reviewed in (Tepass, Godt et al. 2002; Krens and Heisenberg 2011)).

The results presented here, show that in embryos where N-cadherin function was blocked, the node cells from the left and from the right side tend to mix more with each other, in relation to what happens in the control embryos. On the basis of our results, we put forward the hypothesis that different levels of N-cadherin present in the node seem to be important to segregate the cells from the two sides of the node and so, enabling them to maintain a left and a right distinct identity.

This ability of cells to sort out depending on the levels of cell adhesion molecules has been documented in *in vitro* culture assays (Friedlander, Mege et al. 1989; Jaffe, Friedlander et al. 1990; Steinberg and Takeichi 1994) (Yajima, Yoneitamura et al. 1999; Ninomiya, David et al. 2012) and *in vivo* (Godt and Tepass 1998). Indeed, cells expressing high levels of

cadherin sort out from cells expressing low levels of the same cadherin (Friedlander, Mege et al. 1989; Duguay, Foty et al. 2003).

It is known that to avoid cells from losing their early-acquired identity, cell movements must be highly regulated, so the cells that are in the node, preserve their early LR specification. Taking this into account, it should be expected that cell mixing in the node must be avoided; otherwise the future cells contribution would be severely compromised.

Chapter V

Notch target gene – c*Hes6-1*, a novel player in left-right asymmetry?

ABSTRACT

Notch is a local signalling mechanism that is evolutionarily conserved throughout the animal kingdom. It participates in a variety of cellular processes, like: cell fate specification, differentiation, proliferation, apoptosis, adhesion, epithelial-mesenchymal transition, migration, angiogenesis and left-right asymmetry establishment. The best characterized Notch targets belong to the Hairy-Enhancer of Split family. Recently, two subgroups of Hes6 genes that seem to be conserved in most vertebrate species were identified. One of them, chicken c*Hes6-1* is asymmetrically expressed on the left side of the mesoderm lateral to the primitive streak, suggesting that it might have a role in left-right patterning.

Here, I show that c*Hes6-1* asymmetric expression is controlled by the left-right cascade initiated by the H^+/K^+-ATPase pump and the Nodal signalling pathway. Additionally, by the analysis and comparison of the expression of *Hes6* genes in chicken, quail and mouse embryos, I could unexpectedly observe that the asymmetric expression of *Hes6* genes on the left side is not conserved between chicken and quail embryos but it is conserved between chicken and mouse.

These results unveil the possibility that *Hes6* genes might be novel players in the genetic cascade that controls the establishment of left-right asymmetries in a class of vertebrates.

INTRODUCTION

In contrast to the symmetric external body plan, the internal organs such as the heart, lung, liver and digestive organs display highly conserved asymmetric orientations that are essential for their correct functioning. The asymmetric placement of the internal organs is a conserved feature of the vertebrate body. The failure to correctly pattern the left-right (LR) axis results in distinct classes of laterality defects, which is why this is an issue of considerable importance in biomedicine (reviewed in (Raya and Izpisua Belmonte 2006)).

In vertebrate embryos the specification of the body plan starts with the initial breaking symmetry of the embryo, after this the asymmetric information is transferred to the lateral plate mesoderm (LPM), and finally ends with the asymmetric morphogenesis of the internal organs (reviewed in (Raya and Izpisua Belmonte 2006). A number of developmental signalling pathways have been implicated in this complex process of LR asymmetry establishment. Notch signalling is such an example.

The Notch signalling pathway is a highly conserved cell signalling system present in most multicellular organisms. Identified initially in *Drosophila*, the Notch gene encodes a 300-kD single-pass transmembrane receptor. Both the Notch receptor and its ligands, Delta and Serrate (known as Jagged in mammals), are transmembrane proteins with large extracellular domains that consist primarily of epidermal growth factor (EGF)-like repeats (reviewed in (Artavanis-Tsakonas, Rand et al. 1999).

The signalling cascade appears to be very simple: binding of extracellular ligands to Notch receptors on neighbouring cells induces the proteolytic cleavage and release of the Notch intracellular domain (NICD).

NICD translocates to the nucleus, heterodimerizes with the transcription factor CSL (CBF-1 for humans, Suppressor of hairless for *Drosophila*, and LAG-1 for *Caenorhabditis elegans*, also known as RBP-J in the mouse), and recruits coactivators, including Mastermind-like proteins (MAM), to induce transcription of target genes (reviewed in (Artavanis-Tsakonas, Rand et al. 1999; Lai 2004; Bray 2006) (Fig. V.1). Without Notch activation, the CSL protein is part of a transcriptional repressor complex including N-CoR, SHARP and CtBP. However, upon interactions with NICD, the repressor complex is dissociated and CSL becomes part of an activator complex that includes NICD, MAM and p300/CBP, which drives transcription of previously repressed Notch target genes (reviewed in (Artavanis-Tsakonas, Rand et al. 1999; Lai 2004) (Fig. V.1).

Notch signalling has been implicated in LR patterning in vertebrates, mostly through the activation of *nodal* expression in the mouse node (Krebs, Iwai et al. 2003; Takeuchi, Lickert et al. 2007), in the *Xenopus* gastrocoel roof plate (GRP) (Sakano, Kato et al. 2010) and in the chicken Hensen's node (Raya, Kawakami et al. 2004). In the zebrafish Kupffer's vesicle (KV), Notch signalling activates the expression of *charon* (a negative regulator of Nodal activity) (Gourronc, Ahmad et al. 2007). In addition to its importance in the node region, it has also been shown that the Notch signalling pathway is required for the expression of *nodal* in the left LPM through Nodal activation from the node. This was observed in the node of the mouse (Krebs, Iwai et al. 2003; Raya, Kawakami et al. 2003; Raya, Kawakami et al. 2004; Takeuchi, Lickert et al. 2007), zebrafish (Raya, Kawakami et al. 2003; Hashimoto, Rebagliati et al. 2004; Gourronc, Ahmad et al. 2007; Hojo, Takashima et al. 2007), chicken (Raya, Kawakami et al. 2004) and *Xenopus* (Sakano, Kato et al. 2010) as well.

In the mouse embryo, the loss of perinodal expression of the *nodal* gene and the laterality defects observed in *delta-like1* mutant and *notch1/notch2* double-mutant, established that Notch signalling plays a significant and early role in regulating development of the LR axis in mammals (Krebs, Iwai et al. 2003).

In *Xenopus notch1* morphants (MO), the expression of *xnr1* (*Xenopus nodal* related gene) was decreased on both sides of the GRP, however still asymmetric, which led to several defects in the displacement of their internal organs, like for instance, the orientation of gut origin, gut coiling and heart looping. These data indicate that *Xenopus* Notch signalling promotes the expression of *xnr1* in the GRP and that this is essential for LR patterning in amphibians (Sakano, Kato et al. 2010). A recent study in *Xenopus* embryos showed that the transcription of selected Notch target genes in the LPM must be subsequently suppressed for maintenance of *pitx2* expression and LR asymmetry. Still, the role of Notch signalling in the LPM is poorly understood (Sakano, Kato et al. 2010)

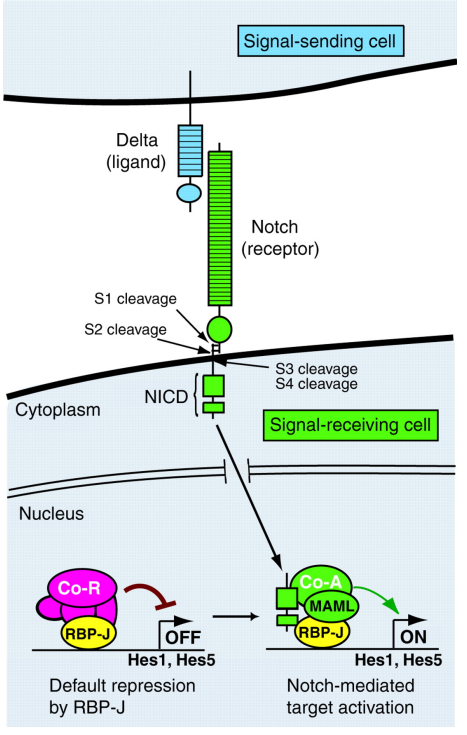

Figure V.1| The core pathway of Notch signalling. The newly synthesized Notch molecule is processed by a furin-like convertase at the S1 site into two fragments that remain associated to form the functional heterodimeric receptor. The first cleavage is at the S2 site by an extracellular protease of the ADAM (a disintegrin and metalloprotease) family. The truncated product is further processed at two endomembrane sites, S3 and S4, by the γ-secretase activity of Presenilins 1 and 2, which release the intracellular domain of Notch (NICD) from the plasma membrane. The NICD translocates to the nucleus and associates with the DNA-binding transcription factor RBP-J. As a result, RBP-J is converted from a transcriptional repressor to an activator. In this process, NICD, RBP-J and MAML assemble on target DNA and form a RBP-J-NICD-MAML ternary complex. This transcriptional activation complex is formed through displacement of the co-repressor complex and recruitment of the coactivators. Thus, Notch signalling activates the transcription of target genes, such as *Hes1* and *Hes5.* Hes factors then subsequently repress the transcription of proneural genes such as *Mash1*. From (Kageyama, Ohtsuka et al. 2007).

In zebrafish, the expression of *cyclops* and *spaw* (two Nodal-related genes) in the left LPM is regulated by Notch signalling, however these two genes appear to be controlled through different mechanisms. Overexpression of Notch randomized both, *cyclops* and *spaw* in the LPM, but only *cyclops* expression in the perinode region was increased (Raya, Kawakami et al. 2003; Gourronc, Ahmad et al. 2007). A recent study showed that a mutant *deltaD* (a homologue of DLL1) led to short cilia and a slow fluid flow velocity within the KV (Lopes, Lourenco et al. 2010). Interestingly, hyper-activation of Notch signalling by overexpression of NICD and *deltaD* increased the length of cilia through *foxj1a* (a marker of

KV motile cilia), demonstrating that Notch signalling can affect cilia length (Lopes, Lourenco et al. 2010). However, it was observed by others that in the mouse Dll1 null embryos, the leftward fluid flow at the node was normal (Raya, Kawakami et al. 2003). Therefore, it remains unclear whether the role of Notch signalling during ciliogenesis is conserved in other vertebrates.

In the chicken embryo it was also observed that Notch signalling plays an important role in LR asymmetry in the node. It can be understood as a transient and robust mechanism that acting as a sensor of extracellular Ca^{2+} generates directly an asymmetric expression of *nodal* and *dll1* in the node (Raya, Kawakami et al. 2004). These authors also observed that by inhibiting the H^+/K^+-ATPase pump in the chicken embryo, the asymmetric expression of *dll1* and *nodal* around the Hensen's node was inhibited, indicating that the activity of H^+/K^+-ATPase could be a responsible factor for the regulation of Notch signalling on the left side of Hensen's node.

The best characterized Notch targets belong to the Hairy-Enhancer of Split (HES) family of bHLH transcriptional repressors. These proteins are able to negatively regulate the expression of their respective genes (reviewed in (Kageyama, Ohtsuka et al. 2008) as well as negatively cross-regulate each other (Gajewski, Sieger et al. 2003).

Recently, it was reported the existence of two Hes6-like genes in chicken and *Xenopus* genomes, c*Hes6-1* and c*Hes6-2* and only one in the mouse and human, *Hes6* (Vilas-Boas and Henrique 2010). The same authors show that c*Hes6-1* is expressed during early embryonic development in the chicken embryo (between stages HH4 and HH11) starting in the epiblast and the Hensen's node. At stage HH5, the expression of c*Hes6-1* is also detected in the emerging head process.

During gastrulation, c*Hes6-1* is always expressed around Hensen's node and in the forming notochord. Other sites of c*Hes6-1* expression in early embryos (between HH6-HH9) include the neural folds and neural tube, the cranial placodes, the infundibulum, the prospective heart, the prospective eye, the olfactory pit, the otic vesicle, the tail bud and the rhombomeres. Later on, the expression is also found in the retina and in muscle fibres. Expression can also be detected in the lateral mesoderm flanking the regressing node in 5-somite embryos (late HH8), but only in the left side. This asymmetric expression continues throughout stage HH9 and HH10 and finally equalizes in both sides at stage HH11, suggesting that c*Hes6-1* may have a role in left-right asymmetry (Vilas-Boas and Henrique 2010). The authors also found that c*Hes6-1* expression was under the control of the Notch pathway. The inhibition of Notch signalling pathway with the highly specific γ-secretase inhibitor (LY411575) at 4 to 8-somite stage (HH8-HH9), strongly reduced the expression of c*Hes6-1* in the lateral mesoderm, meaning that c*Hes6-1* requires Notch signalling to be asymmetrically expressed in this region of the embryo (Vilas-Boas and Henrique 2010).

In this study, I have investigated whether or not c*Hes6-1* was under the LR asymmetry cascade in the chicken embryo. By inhibiting the first symmetry-breaking event known in the chicken, the H^+/K^+-ATPase ion pump. I could conclude that the asymmetric expression of *cHes6-1* is dependent on the H^+/K^+-ATPase exchanger activity. I could also observe that c*Hes6-1* asymmetric expression on the left side of the mesoderm lateral to the PS is under the control of the Nodal signalling pathway. Additionally, I found a conserved asymmetric expression of *Hes6* between

chicken and mouse but unexpectedly the asymmetric expression was not conserved in the quail.

V.1 RESULTS

V.1.1 c*Hes6-1* asymmetric expression is downstream of the H^+/K^+ATPase pump

In the chicken it was shown that left-right differences in the H^+/K^+ATPase activity are detected early in the embryo. This asymmetrically localized ion flux controls asymmetric gene expression and is thus far the first known symmetry-breaking event in the chicken embryo (Levin, Thorlin et al. 2002).

To investigate whether the asymmetric c*Hes6-1* expression was under the control of the H^+/K^+ATPase exchanger, I analysed the expression of c*Hes6-1* in embryos where the proton pump was inhibited. To block the H^+/K^+ATPase exchanger, I used beads soaked in omeprazole drug, which were placed on both sides of the primitive streak (PS) at stage $HH3^+$ in New cultures (Fig. 1A). In DMSO-control treated embryos, the expression of c*Hes6-1* was stronger on the left mesoderm lateral to the PS in 100% (n=62) of the cases, although the level of expression in this territory was higher in 62% of the cases (Figs. 1B, B') and lower in 38% of the cases (Figs. 1C, C'). In contrast, 40% (n=32) of omeprazole-treated embryos showed an increase of c*Hes6-1* expression on the right mesoderm lateral to the PS (Figs. 1D, D') and in 60% (n=19) of the cases, the asymmetries between the two sides were no longer evident (Figs. 1E, E').

These results indicate that c*Hes6-1* asymmetric expression in the chicken embryo is downstream of the H^+/K^+ATPase activity.

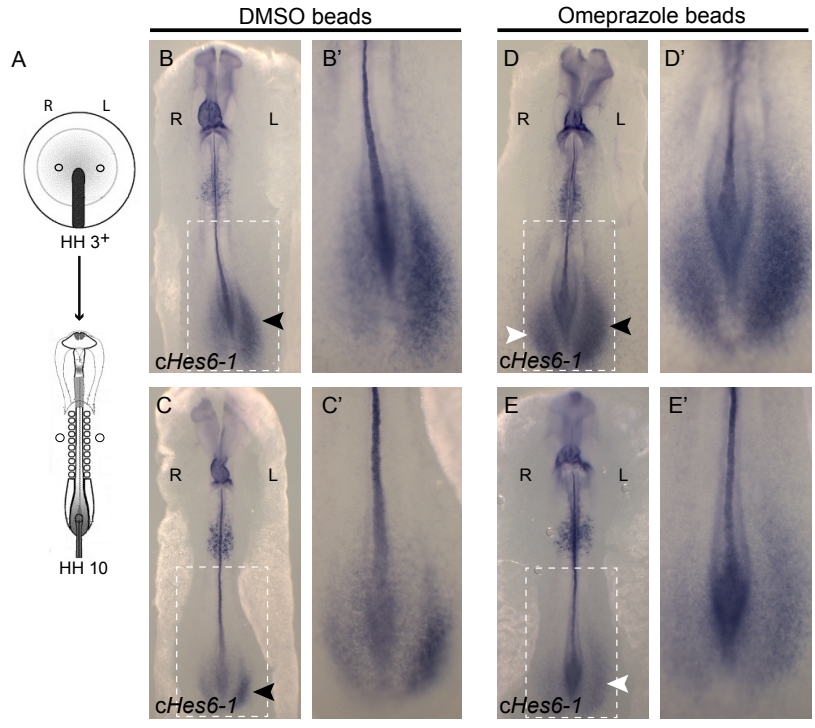

Figure 1| The H^+/K^+ATPase pump activity modulates the expression of c*Hes6-1*. (**A**) Schematic representation of the experiment. Beads were implanted on both sides of the PS at stage $HH3^+$ and the embryos were analysed at stage HH10. (**B-E'**) c*Hes6-1* expression at stage HH10 in embryos previously treated with DMSO (**B-C'**) or omeprazole (**D-E'**) beads at stage $HH3^+$. Boxes indicate the magnified region that is shown in panels on the right (**B', D', C', E'**). Black arrowheads indicate normal expression of c*Hes6-1*. White arrowheads indicate abnormal expression of c*Hes6-1*. L, left; R, Right.

V.1.2 c*Hes6-1* asymmetric expression requires Nodal signalling

Accordingly to Vilas-Boas *et al* (2010), the asymmetric expression pattern of c*Hes6-1* begins at stage HH9 on the left side of the mesoderm lateral to the PS and last until HH11. This is coincident with the expression pattern of *nodal* on the left LPM. The expression of *nodal* in the left LPM occurs sequentially in a wave-like fashion along the anterior-posterior axis and reaches the posterior end of the embryo at late stage HH8 (5 somites), coinciding with the onset of expression of c*Hes6-1* in this region. In addition, when *nodal* expression in the posterior lateral mesoderm is

extinguished at late HH10, asymmetric expression of c*Hes6-1* also starts to fade out. Both genes are asymmetrically expressed in close-related regions during approximately the same time-window. These observations lead us to question whether Nodal could induce the asymmetric expression of c*Hes6-1*.

To determine whether Nodal can regulate c*Hes6-1* asymmetric expression in the left mesoderm, beads soaked with Nodal protein were implanted on the right side of the embryos at stage HH8 (4-5 somites) at the level of the LPM, as schematically illustrated in Fig. 2A. Beads loaded with PBS were used as control. Bead-implanted embryos were re-incubated and allowed to develop until stage HH10 when they were collected, and examined by whole-mount *in situ* hybridization for c*Hes6-1* expression. Nodal application to the right LPM of stage HH8 embryos resulted in an appreciable upregulation of c*Hes6-1* expression (66%, n=15; Figs. 2C; 2C'). Control PBS beads implanted on the right side of embryos had no effect on c*Hes6-1* expression (100%, n= 16; Figs. 2B, B').

Thus, c*Hes6-1* appears to be positively regulated by Nodal signalling, which might indicate that Nodal is upstream to c*Hes6-1* and may be responsible for setting up left-right asymmetric expression of c*Hes6-1* in the chicken embryo.

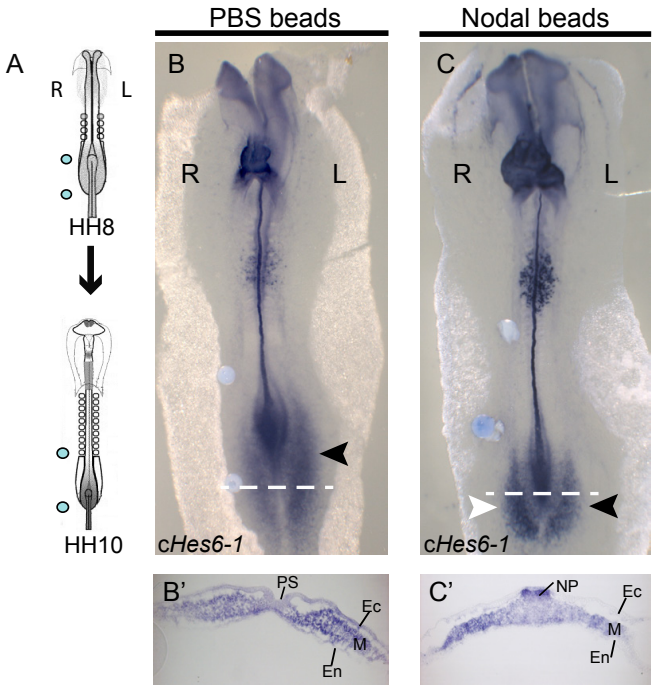

Figure 2| Nodal induces c*Hes6-1* expression. (**A**) Schematic representation of the experiment. Beads were implanted on the right sides of the embryo at stage HH8 and the embryos were analysed at stage HH10. (**B**) Control embryo showing the asymmetric expression of c*Hes6-1* on the left side at stage HH10. (**B'**) Transversal section of the embryo in (**B**). (**C**) Embryo implanted with beads loaded with Nodal protein on the right side, showing an increase in c*Hes6-1* expression on the left side. (**C'**) Transversal section of the embryo in (**C**). Black arrowheads point to the normal expression of c*Hes6-1* on the left side. White arrowhead point to the induced expression on the right side of the embryo. Ec-Ectoderm; En-Endoderm; M-Mesoderm; NP- Neural Plate; PS- Primitive Streak. L, left; R, Right.

V.1.3 c*Hes6-1* asymmetric expression seems to be conserved between chicken and mouse but not in quail embryos

Nodal genes exhibit a conserved asymmetric expression pattern in the left LPM that ranges from ascidians (HrNodal) (Morokuma, Ueno et al. 2002), zebrafish (*cyclops* and *southpaw*) (Lowe, Supp et al. 1996; Rebagliati, Toyama et al. 1998), *Xenopus* (*xnr1*) (Lowe, Supp et al. 1996), snail (*nodal*) (Grande and Patel 2009; Kuroda, Endo et al. 2009), rabbit (*nodal*) (Fischer,

Viebahn et al. 2002), chicken (*nodal*) (Levin, Johnson et al. 1995) and mouse (*nodal*) (Collignon, Varlet et al. 1996; Lowe, Supp et al. 1996).

According to the results presented here, the asymmetric expression of c*Hes6-1* gene on the left side of the posterior mesoderm lateral to the PS seems to be dependent on Nodal activity. Therefore we wondered if, like *nodal,* c*Hes6-1* asymmetric expression could also be conserved in other vertebrates, like quail and mouse. To explore the evolutionary conservation of the *Hes6* in other organisms I compared the distribution of *Hes6* transcripts in equivalent developmental stages of the quail and mouse embryos.

The results of the *in situ* hybridisation in quails show that c*hes6-1* gene was expressed in the neural tube, sinus rhomboidalis, pancreatic progenitors, heart and on both sides of the mesoderm lateral to the primitive streak (Figs. 3A-E) between 7 and 11-somite stage. Contrary to what was observed in the chicken embryo, c*hes6-1* was not asymmetrically expressed in the mesoderm lateral to the PS (4 embryos per stage, n=20; Figs. 3A-E).

The same analysis was performed in the mouse between E8.0-E8.5. The m*Hes6* (belonging to the *Hes6-1* subgroup) gene was expressed in the ectoderm, perspective forebrain, lateral plate mesoderm, visceral yolk sac and also in the neural ectoderm (Figs. 3F, G). Surprisingly, we could also notice that on the left side of the LPM m*Hes6* was strongly expressed when comparing with the opposite side (Figs. 3F, G). Regardless the fact that we only analysed three mouse embryos, we believe that *cHes6* asymmetric expression is conserved between chicken and mouse.

These results lead us to conclude that unexpectedly *Hes6* asymmetric expression in the lateral mesoderm in conserved between chicken and mouse but it is not conserved in the quail embryo.

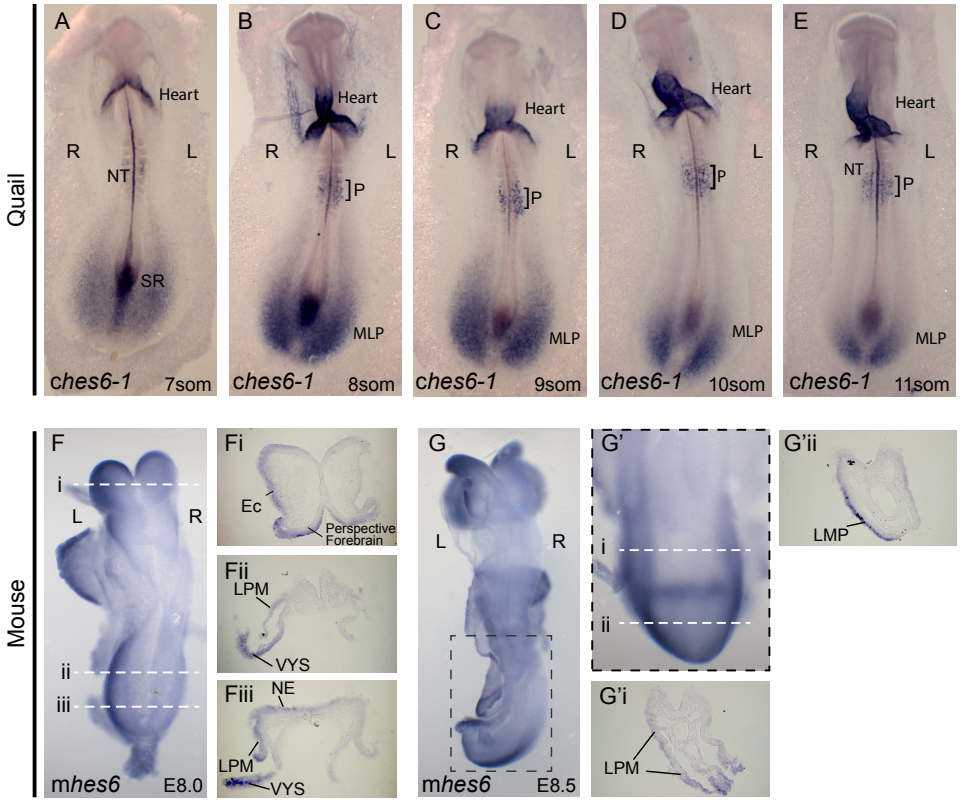

Figure 3| *hes6* expression pattern in different organisms. (**A-E**) Quail c*hes6-1* expression. (**F-G**) Mouse *hes6* expression. (**F**) Whole embryo showing the expression of m*hes6* at E8.0. (**Fi-Fiii**) Cross sections of the embryo show in (**F**). (**Fi**) Asymmetric expression of m*Hes6* at the left ectoderm of the head and perspective forebrain. (**Fii**) Asymmetric expression in the left LPM and VYS. (**Fiii**) m*Hes6* expression in the NE and asymmetrically on the left LPM and VYS. (**G**) Whole embryo showing the expression of m*Hes6* at E8.5. (**G'**) The boxes indicate the magnified region. (**Gi**) Transverse section showing the stronger expression of m*hes6* on the left Ectoderm and Mesothelium. (**Gii**) Transverse section showing the asymmetric expression of *mhes6* on the left side. Ec-Ectoderm; NT-Neural Tube; SR- Sinus Rhomboidalis; P- Pancreatic progenitors; MLP- Mesoderm Lateral to the Primitive streak; VYS- Visceral Yolk Sac; LPM- Lateral Plate Mesoderm; NE- Neural Ectoderm. L, Left; R, Right.

V.2 DISCUSSION

In this Chapter, I demonstrate that in the chicken embryo the novel asymmetrically expressed gene c*Hes6-1* (Vilas-Boas and Henrique 2010) is downstream of the ion exchanger H^+/K^+-ATPase and the Nodal signalling pathway. Surprisingly, the asymmetric localization of c*Hes6-1* in the mesoderm lateral to the primitive streak is not shared with the chicken closest related organism, the quail. Instead, it seems that this asymmetric expression is shared with the mouse *mHes6*.

Overall, these results uncover a new possible player in the left-right asymmetry cascade. Yet, why is this gene asymmetrically expressed in the mesoderm lateral to the primitive streak, or in other words, which asymmetric structure(s) will arise from it, is still to be addressed.

V.2.1 Asymmetric expression of c*Hes6-1* is H^+/K^+-ATPase pump dependent

In chicken, generation of the initial asymmetric signals requires a gradient of membrane potentials originated by differences in H^+/K^+-ATPase activity. This early difference across the midline organizer is translated into an asymmetric genetic cascade that creates left-right identity (Levin, Thorlin et al. 2002). The results presented in this chapter, reveal that the c*Hes6-1* asymmetric expression is dependent on the very early proton pump activity. One possible explanation, on how the proton pump might have a role in c*Hes6-1* asymmetric expression so late in the embryo, is perhaps through Nodal. It is known that *nodal* expression in the node is also dependent on the H^+/K^+-ATPase activity (Raya, Kawakami et al. 2004), and that perinode Nodal will induce itself later in the left LPM (Brennan, Norris

et al. 2002; Saijoh, Oki et al. 2003). Taking this into account, we propose that it is through Nodal signalling that the H^+/K^+-ATPase has an influence on c*Hes6-1* asymmetric expression.

V.2.2 Nodal signalling activates c*Hes6-1* on the left mesoderm lateral to the primitive streak

The asymmetric expression of *nodal* starts at stage HH7 in the anterior portion of the left LPM, and as the embryo develops this asymmetric expression extends posteriorly. At late stage HH8 (5-somite stage), *nodal* expression is present in the entire left LPM, after which, it starts to become more restricted to the posterior region, until it finally disappears at late stage HH10 (Levin, Johnson et al. 1995).

The emergence of c*Hes6-1* asymmetric expression is coincident with the arrival of *nodal* expression to the posterior region of the left LPM, and the disappearance of c*Hes6-1* asymmetric expression at late stage HH10 also correlates with the fading of *nodal* expression. These observations suggest a correlation between the expressions of both genes, which might imply that c*Hes6-1,* is a downstream target of Nodal signalling in the left mesoderm.

The results show that the exogenous application of Nodal in the right LPM rapidly induced c*Hes6-1* ectopic expression on that side, thus leading us to conclude that c*Hes6-1* requires Nodal signalling for its expression. This result is in agreement with previous results showing that *Hes6* expression is downstream of Nodal signalling in *Xenopus* early gastrula embryos (Murai, Vernon et al. 2007).

Interestingly, c*Hes6-1* asymmetric expression is only observed around the time that *nodal* reaches the posterior region of the LPM, and not before

that suggesting that a second signal must be present in the posterior LPM to cooperate with Nodal in the activation of c*Hes6-1* expression. Notch signalling is an excellent candidate for such a second signal, since Vilas-Boas et al, has demonstrated that the inhibition of Notch signalling in the chicken embryo, severely downregulated c*Hes6-1* expression in the mesoderm lateral to the primitive streak (Vilas-Boas and Henrique 2010). As a follow up of these results it would be fundamental to determine if the activation of c*Hes6-1* expression by Nodal is indeed dependent on Notch signalling. In addition, it would be important to find which ligands and receptors of the Notch pathway are expressed in the posterior LPM of the chicken embryo.

V.2.3 c*Hes6-1* asymmetric expression seems to be conserved between chicken and mouse but not in quail embryos

It has been clear that the establishment of left-right asymmetries is controlled by robust genetic and epigenetic mechanisms, some of which show a significant degree of evolutionary conservation, whereas others seem to be species-specific.

The results presented here, show that *Hes6* asymmetric expression is also present on the left side of the mesoderm in the mouse embryo. However and contrary to what would be expected, this is not true for the quail embryo, in which c*Hes6-1* expression was bilateral symmetric in the mesoderm lateral to the primitive streak. In an evolutionary perspective, this would be unlikely, because the chicken is closest related to the quail than it is with the mouse, given that chicken and quail belong to the bird class and mouse to the mammalian.

According to our results and knowing that *nodal* is also asymmetrically expressed in the left LPM of the quail (Zile, Kostetskii et al. 2000), it would be expected that Nodal would also induce asymmetrically the expression of c*Hes6-1*. We might consider that c*Hes6-1* asymmetric expression in the quail exists at a level other than mRNA (protein processing, translation, etc.) or that its expression levels are so subtle, that they are missed by *in situ* hybridisation. A similar situation might underlie the left-sided expression of *xnr1,* which is quite variable, being undetectable in up to 25% of the *Xenopus* embryos (Lohr, Danos et al. 1997; Levin 1998).

V.2.4 A fate map of the c*Hes6-1*-expressing region is needed

The transient and asymmetric expression of c*Hes6-1* raises the question of which asymmetric structure(s) arise from the lateral mesoderm region expressing this gene.

It is likely that the anterior tip of c*Hes6-1* asymmetric expression might contribute to intermediate mesoderm, and in this case, would contribute to the gonads, as it has been previously fate-mapped (Rodemer, Ihmer et al. 1986). It is thus possible that the transient and asymmetric c*Hes6-1* expression in the lateral mesoderm might contribute to gonad asymmetries in chickens. In the female chicken, the right gonad is developmentally retarded when compared to the left one (Mittwoch 1998; Guioli and Lovell-Badge 2007; Ishimaru, Komatsu et al. 2008; Rodriguez-Leon, Rodriguez Esteban et al. 2008). These gonad asymmetries are not restricted to females since there is a report where similar male gonads asymmetries were also reported during chicken development (Mittwoch 1998).

The more posterior region of c*Hes6-1* asymmetric expression might contribute to the lateral plate mesoderm (Sweetman, Wagstaff et al. 2008). This region has been fate-mapped among other organs, to give rise to the spleen, that it is asymmetrically positioned on the right side in the chicken embryo (Bellairs and Osmond 2005).

Whether chick c*Hes6-1* asymmetric expression in the mesoderm lateral to the primitive streak between HH8-HH11 embryos contributes to asymmetrically localizing the spleen, or to generate asymmetric gonads, will only be determined after careful fate mapping of this embryonic region.

Chapter VI

CONCLUSIONS and FUTURE DIRECTIONS

CONCLUSIONS

Although vertebrates are bilaterally symmetric externally, internal organs are positioned asymmetrically to allow for efficient packaging in the limited space of the body cavities and proper organ physiology. In humans, disruptions in asymmetric organ positioning, termed laterality defects, occur in 1:10000 live births (Aylsworth 2001; Peeters and Devriendt 2006; Sutherland and Ware 2009). These defects can manifest as a complete reversal along the left-right (LR) axis, termed *situs inversus,* which has only mild consequences, or isomerisms or heterotaxias along the entire axis that are often incompatible with life. Understanding the morphogenesis of the normal and malformed organs, therefore, might be of considerable clinical interest.

In spite of recent progresses, our knowledge of LR determination remains incomplete. For example, the mechanism by which the initial determination of LR polarity eventually results in the asymmetric expression of signalling molecules, and the mechanism by which *situs*-specific morphogenesis is performed, remains unknown.

The main objective of this thesis was to understand how the molecular and morphological asymmetries of the Hensen's node of the chicken embryo are generated, in particular, the role of the cell adhesion molecule N-cadherin in these processes.

A secondary objective was to understand the regulation of asymmetric gene expression in mesodermal tissues, in particular, of the Notch target c*Hes6-1*.

In this last Chapter, I will outline the main conclusions reached from the

experiments described in this thesis, and expose some future directions that should be considered to complete and improve our knowledge in left-right asymmetry patterning.

In Chapter III, I showed that:

- The same leftward cell movements that generate the asymmetric expression of *shh* and *fgf8* in the node and that are downstream of the H^+/K^+-ATPase pump (Gros, Feistel et al. 2009), also promote an asymmetric displacement of cells expressing *cdh2* to the node right side at stage HH5.

- Blocking N-cadherin function in the node using two different blocking antibodies, allowed the leftward cell movements to continue beyond stage HH4, which lead us to conclude that N-cadherin expression on the right side of the node is vital to end the leftward cell movements.

- As a consequence of the continuous displacement of cells towards the left side of the node in the absence of N-cadherin activity, the asymmetric expression of *fgf8* and *nodal* in the node were compromised and, consequently, originate an abnormal expression of the asymmetric genes *cer1* and *snai1* in the LPM, resulting in mispositioned hearts.

- Importantly, we were able to rescue the expression of *cer1* and *snai1* in the LPM and the position of the heart by blocking the Fgf signalling specifically on the left side of the node at stage HH5, in embryos where the function of N-cadherin was blocked.

- Premature asymmetric expression of N-cadherin on the right side of the node altered the typical leftward cell movement at stage HH4. Instead, the cells aggregate and start to adopt a cell displacement pattern typical of stage HH5, with the cells moving rostrally as a consequence of the rostral-caudal body axis extension.

- According to the rostral movements displaced by the overexpressing N-cadherin cells in the node at stage HH4, the asymmetric expression of *shh*, *fgf8* or *nodal* were not affected in the node. Consequently, the asymmetric expression of *cer1* on the left LPM or *snai1* on the right LPM, were also unaltered.

In this study, we conclude that N-cadherin is a key molecule responsible for finishing the leftward cell movements, and that this termination is an essential step in the establishment of LR asymmetry.

In Chapter IV, I showed that:

- Different levels of N-cadherin in the node at stage HH5 seem to preserve its asymmetric morphology by maintaining a higher number of cells on the right side.

- Different levels of N-cadherin in the node at stage HH5 seem to have a role in sorting-out cells from the left and from the right sides.

All together, these results suggest that different levels of N-cadherin in the Hensen's node preserves the LR morphological and molecular identity of this embryonic region.

In Chapter V, I showed that:

- The expression of c*Hes6-1*, a Notch target belonging to the Hairy-Enhancer of Split (HES) is downstream of the H^+/K^+ATPase pump.
- c*Hes6-1* seems to be positively regulated by Nodal signalling, which might indicate that Nodal is upstream to c*Hes6-1* and may be responsible for setting up left-right asymmetric expression of c*Hes6-1* in the chicken embryo.
- c*Hes6-1* asymmetric expression seems to be conserved between chicken and mouse but not in quail embryos.

These results unveil *Hes6* genes as possible new players in the genetic cascade that controls the establishment of left-right asymmetries in chicken and mouse embryos.

FUTURE DIRECTIONS

VI.1 What directs cell movements towards the left side of the node during stage HH4?

Based on the observation that during stage HH4 the movement of the node's cells is always done towards the left side, we can hypothesize that maybe, this could be due to a chemoattractant located on the left or a chemorepellent located on the right side of the node. It is known that cell movement requires precise guidance signals to instruct the cells how to reach their final destination. These signals can be physical, chemical, diffusible, or non-diffusible, and are detected by receptor proteins located on the cell membrane that subsequently transmit them via signalling cascades, to the interior of the cell (Alberts and Lewis 2002). The distances that the cells move can vary widely from a few microns to centimetres, which why obviously, the signals that guide these movements must also vary considerably (Affolter and Weijer 2005).

There are evidences showing that *fgf4* acts as a chemoattractant in gastrulating chicken embryos (Yang, Dormann et al. 2002), however, its expression on the right side of the node at stage HH4 (Shamim and Mason 1999), excludes it as a player in directing node's cells movements. On the other hand, *fgf8* was demonstrated to repulse cells from the primitive streak causing them to move away in gastrulating chicken embryos (Yang, Dormann et al. 2002). Again, *fgf8* cannot be a serious candidate to push the right side cells towards the left side, as it is not expressed in the node region at stage HH4 (Boettger, Wittler et al. 1999). In addition to this, the asymmetric expression of *fgf8* in later stages in the node is also dependent

on the leftward movements (Gros, Feistel et al. 2009). We could also look for other Fgf members of the signalling pathway that could be asymmetrically expressed on the right or on the left side of the node at stage HH4, and that could act as a chemoattractants or chemorepellents, respectively.

Another candidate could be a gene belonging to the Wnt family. It has been shown that Wnt signalling plays a major role in cell migration with different Wnt family members displaying a diversity of signal transduction and physiological function in chick, mouse and *Drosophila*. An example of this, is the involvement of different Wnt family members in axon guidance in the chick optic tectum (Wnt3) (Schmitt, Shi et al. 2006), in the mouse spinal cord (Wnt4) (Lyuksyutova, Lu et al. 2003) and in *Drosophila* nervous system development (Wnt5) (Yoshikawa, McKinnon et al. 2003).

Recently, it was demonstrated that Wnt3a plays a crucial role in guiding cardiac progenitor cells through a RhoA-dependent mechanism, which involved a negative chemotaxis in the chicken embryo (Yue, Wagstaff et al. 2008). In addition to this, it was also shown that Wnt3a inhibited and Wnt5a promoted the migration of paraxial and lateral mesoderm precursors cells as they leave the primitive streak of the chicken embryo (Sweetman, Wagstaff et al. 2008). Taking these findings into account, we could investigate if there is a Wnt gene asymmetrically expressed on the right side of Hensen's node at stage HH4. According to Geisha (*Gallus* expression *in situ* hybridisation analysis) web tool, *wnt3a* seems to be a good candidate, since there is the possibility that it could be expressed asymmetrically on the node at stage HH4, in contrast to *wnt5a* that is not expressed in the node at this stage. If this hypothesis proves to be true, to answer the question of whether or not Wnt3a is the chemorepellent that forces the leftward movements of the node's cells,

two experiments could be performed:

- Inhibit Wnt3a on the right side of the node with one of its pharmacological inhibitors SFRP1/2 (Galli, Barnes et al. 2006) and see if the leftward cell movements are abolished at stage HH4:

- Implant pellets of RatB1a fibroblasts expressing Wnt3a on the left side of the node, and see if these cells are able to move away from the node.

On the other hand, we might think that maybe the counterclockwise cell movements displayed in the node, can be caused by its surrounding tissues and not by intrinsic signals or forces.

To test this hypothesis, we could label the left or right sides of the node with a lipophilic dye, rotate it 180° at stage HH3^{+} (prior to the onset of leftward cell migration) and finally, analyse the cell movements in the node from stage HH4 until stage HH6. If for instance, the left-sided labelled cells (now on the right side) still migrate to the left side of the node, this result would mean that, there is an intrinsic cell-side information to drive the leftward cell movement. If not, and the cells couldn't migrate to the left side, then this would lead us to assume that the leftward cell movements are induced by the surrounding tissues.

Finding out what is the driving force that produces the asymmetric displacement of the cells in the node towards the left side, would be a key challenge and a major progress in the left-right field.

VI.2 What is inhibiting *fgf8* expression in the rostral region of the node?

The results reveal that blocking N-cadherin function promotes the continuous displacement of cells from the right to the left side of the node. Taking this type of movement into account, it would be expected to see *fgf8*-expressing cells around the entire node. However, we never saw this type of expression, instead *fgf8* expression was restricted only to the left and to the right side, but never in the anteriormost region of the node. We hypothesize that maybe, something must be inhibiting *fgf8* expression in the cells that are crossing the anterior region of the node. It should be interesting to see, if in the absence of N-cadherin function, Fgf8 protein is still present in the anterior portion of the node, and more importantly, determine what could be inhibiting *fgf8* expression.

VI.3 Find out what causes the asymmetric morphology of the node

I have shown that N-cadherin is important to maintain the asymmetric structure of the node at stage HH5. However, what makes the node asymmetric in the first place, is still unknown. The most complete analysis of Hensen's node morphology, was only done from stage HH4 onwards (Dathe, Gamel et al. 2002). New studies are needed to characterize node's morphology starting at earlier stages, so that we can understand what changes it undergoes before it gets asymmetric.

Beside cell shape and size, cell orientation should be studied and for that a 3D cell reconstruction would help to understand in the node context, how are cells oriented over a period ranging from HH3 to HH6.

VI.4 Investigate the functional relevance of asymmetric levels of N-cadherin in the node.

Evidence for the role of different levels of cadherin in morphogenesis *in vivo* has only been reported in the *Drosophila* egg chamber. In this case, differential expression of DE-cadherin on the follicle and nursing cells positions the oocyte (Friedlander, Mege et al. 1989; Godt and Tepass 1998). Until know, whether a similar cell sorting process mediated by different levels of cadherin operates during development in vertebrates was unknown.

Our data suggest that different levels of N-cadherin prevents cell mixing in the node, a therefore a thorough investigation on the role of different levels of N-cadherin in promoting cell sorting should be investigated.

To answer this question and see if indeed, different levels of N-cadherin in the node promote cell sorting, two different approaches could be used:

- replace a left-side host (low N-cadherin levels) by a right-side donor (high N-cadherin levels), or the other way around,
- replace a right-side host by a left-side donor.

With these manipulations, we would equalize the endogenous levels of N-cadherin in the node, creating nodes with both, low-levels of N-cadherin (two left sides) or high levels of N-cadherin (two right sides). To distinguish the left from the right sides, and to know which one is the donor, or the host, the perspective node region should be electroporated at stage $HH3^{+}$ with nuclear GPF or mCherry and then allow these embryos to growth until stage HH5. At this stage, the right side of the node of a host mCherry labelled-embryo should be replaced by the left side of a node taken from a

GFP donor embryo, thus creating a double left-sided node, both with low levels of N-cadherin. Using the same strategy, we should create a double right-sided node. If indeed, different levels of N-cadherin are important to sort out the cells in the node, with this experiments, we should expect to see cell mixing in the node.

VI.5 Is the activation of c*Hes6-1* expression by Nodal dependent on the Notch signalling pathway?

We have shown that Nodal can activate the expression of c*Hes6-1* in the mesoderm lateral to the primitive streak. Vilas-Boas et al, has already demonstrated that c*Hes6-1* expression was severely downregulated after Notch signalling inhibition (Vilas-Boas and Henrique 2010).

As a follow up, it would be fundamental to determine if the activation of c*Hes6-1* expression by Nodal is dependent or not on Notch signalling. To address this question, Nodal soaked beads could be ectopically implanted on the right side of the embryo at stage HH8, at the same time that Notch signalling would be pharmacologically inhibited. We could then analyze the expression of c*Hes6-1* by *in situ* hybridization. The results of this experiment would allow us to determine the signals needed to activate c*Hes6-1* expression and to refine the position this new player in the left-right patterning cascade.

In addition, it should also be important to find which ligands and receptors of the Notch pathway are expressed in the posterior lateral plate mesoderm of the chicken embryo. To assess this, the RNA from the mesoderm lateral to the primitive streak from stages HH8-HH11 chicken embryos would be obtained to produce cDNA. After this, amplification by PCR with specific primers should reveal which ligands and receptors are

being expressed in the same territory and at the same time as c*Hes6-1.* This information would allow us to infer with more detail, how Notch signalling regulates c*Hes6-1* asymmetric expression in the chicken embryo.

VI.6 Fate mapping c*Hes6-1*-expressing region

The transient and asymmetric expression of c*Hes6-1* raises the question of which asymmetric structure(s) arise(s) from the lateral mesoderm region expressing this gene.

For that purpose, we could apply small crystals of vital dye in the c*Hes6*-expressing mesoderm region and then follow marked cells to uncover which tissue or organ will they contribute to. One of the advantages of using the dyes is that they only mark the progeny of labelled cells but not to their neighbour cells. The other advantage is that they are less invasive and technically quite easy to apply. However, we could face one obstacle, that is the fact that the labelled cells and their descendants can be traced for up to no more than 3 days before the signal becomes diluted by cell division becoming too weak to be detected. Furthermore, we cannot guarantee that by using the dye crystals, the tissues above (ectoderm) and below (endoderm) the mesoderm will not be labelled as well.

We could also label the desired population of cells by using the new developed photo-switchable Cyan Fluorescent Protein transgenic chickens to photoconvert specific cells and determine their fate at later stages. However, this option has also similar disadvantages as the crystals. Once again, we could face the "life-time" problem of photoconverted cells, and the difficulty to reach the mesodermal cells without photoconverting the other two layers (ectoderm and/or endoderm).

Another method that we could use is the classical chick-quail chimeras. The fact that quail cells can be distinguished from chick cells because of the staining properties of their nuclei (Le Douarin 1974), would overcome the limited "life-time" of crystal dyes, and would allow specific labelling of mesoderm cells. However, the fact that c*Hes6-1* is not asymmetrically expressed in the quail embryo, could mean that the fate of this territory may not be exactly the same between the quail and the chick. As an alternative to the chick-quail chimeras, I could use transgenic GFP-chicken embryos to graft the *cHes6-1*-expressing region to a normal host embryo. This permanent labelling will allows us to determine the fate of these cells in a chicken context.

REFERENCES

REFERENCES

Affolter, M. and C. J. Weijer (2005). "Signaling to cytoskeletal dynamics during chemotaxis." Dev Cell **9**(1): 19-34.

Afzelius, B. A. (1976). "A human syndrome caused by immotile cilia." Science **193**(4250): 317-9.

Anastasiadis, P. Z. (2007). "p120-ctn: A nexus for contextual signaling via Rho GTPases." Biochim Biophys Acta **1773**(1): 34-46.

Artavanis-Tsakonas, S., M. D. Rand, et al. (1999). "Notch signaling: cell fate control and signal integration in development." Science **284**(5415): 770-6.

Asano, K., O. Kubo, et al. (2000). "Expression of cadherin and CSF dissemination in malignant astrocytic tumors." Neurosurg Rev **23**(1): 39-44.

Aw, S. and M. Levin (2009). "Is left-right asymmetry a form of planar cell polarity?" Development **136**(3): 355-66.

Aylsworth, A. S. (2001). "Clinical aspects of defects in the determination of laterality." Am J Med Genet **101**(4): 345-55.

Becker, S. F., R. Langhe, et al. (2012). "Giving the right tug for migration: cadherins in tissue movements." Arch Biochem Biophys **524**(1): 30-42.

Bellairs, R. (1986). "The primitive streak." Anat Embryol (Berl) **174**(1): 1-14.

Bellairs, R., Osmond, M (2005). "The Atlas of Chick Development". Academic Press.

Bellomo, D., A. Lander, et al. (1996). "Cell proliferation in mammalian gastrulation: the ventral node and notochord are relatively quiescent." Dev Dyn **205**(4): 471-85.

Bertocchini, F. and C. D. Stern (2002). "The hypoblast of the chick embryo positions the primitive streak by antagonizing nodal signaling." Dev Cell **3**(5): 735-44.

Berx, G. and F. Van Roy (2001). "The E-cadherin/catenin complex: an important gatekeeper in breast cancer tumorigenesis and malignant progression." Breast Cancer Res **3**(5): 289-93.

Birchmeier, W. (1995). "E-cadherin as a tumor (invasion) suppressor gene." Bioessays **17**(2): 97-9.

Bodenstein, L. and C. D. Stern (2005). "Formation of the chick primitive streak as studied in computer simulations." J Theor Biol **233**(2): 253-69.

Boettger, T., L. Wittler, et al. (1999). "FGF8 functions in the specification of the right body side of the chick." Curr Biol **9**(5): 277-80.

Bolos, V., H. Peinado, et al. (2003). "The transcription factor Slug represses E-cadherin expression and induces epithelial to mesenchymal transitions: a comparison with Snail and E47 repressors." J Cell Sci **116**(Pt 3): 499-511.

Brand-Saberi, B., A. J. Gamel, et al. (1996). "N-cadherin is involved in myoblast migration and muscle differentiation in the avian limb bud." Dev Biol **178**(1): 160-73.

Bray, S. J. (2006). "Notch signalling: a simple pathway becomes complex." Nat Rev Mol Cell Biol **7**(9): 678-89.

Brennan, J., D. P. Norris, et al. (2002). "Nodal activity in the node governs left-right asymmetry." Genes Dev **16**(18): 2339-44.

Britz-Cunningham, S. H., M. M. Shah, et al. (1995). "Mutations of the Connexin43 gap-junction gene in patients with heart malformations and defects of laterality." N Engl J Med **332**(20): 1323-9.

Brizuela, B. J., O. Wessely, et al. (2001). "Overexpression of the Xenopus tight-junction protein claudin causes randomization of the left-right body axis." Dev Biol **230**(2): 217-29.

Bronner-Fraser, M., J. J. Wolf, et al. (1992). "Effects of antibodies against N-cadherin and N-CAM on the cranial neural crest and neural tube." Dev Biol **153**(2): 291-301.

Brown, N. A. and L. Wolpert (1990). "The development of handedness in left/right asymmetry." Development **109**(1): 1-9.

Bunney, T. D., A. H. De Boer, et al. (2003). "Fusicoccin signaling reveals 14-3-3 protein function as a novel step in left-right patterning during amphibian embryogenesis." Development **130**(20): 4847-58.

Campione, M., H. Steinbeisser, et al. (1999). "The homeobox gene Pitx2: mediator of asymmetric left-right signaling in vertebrate heart and gut looping." Development **126**(6): 1225-34.

Cartwright, J. H., O. Piro, et al. (2004). "Fluid-dynamical basis of the embryonic development of left-right asymmetry in vertebrates." Proc Natl Acad Sci U S A **101**(19): 7234-9.

Castro Alves, C., E. Rosivatz, et al. (2007). "Slug is overexpressed in gastric carcinomas and may act synergistically with SIP1 and Snail in the down-regulation of E-cadherin." J Pathol **211**(5): 507-15.

Catala, M., M. A. Teillet, et al. (1996). "A spinal cord fate map in the avian embryo: while regressing, Hensen's node lays down the notochord and floor plate thus joining the spinal cord lateral walls." Development **122**(9): 2599-610.

Charrier, J. B., F. Lapointe, et al. (2002). "Dual origin of the floor plate in the avian embryo." Development **129**(20): 4785-96.

Chen, Y. and A. F. Schier (2001). "The zebrafish Nodal signal Squint functions as a morphogen." Nature **411**(6837): 607-10.

Christophorou, N. A., M. Mende, et al. (2010). "Pax2 coordinates epithelial morphogenesis and cell fate in the inner ear." Dev Biol **345**(2): 180-90.

Cinnamon, Y., R. Ben-Yair, et al. (2006). "Differential effects of N-cadherin-mediated adhesion on the development of myotomal waves." Development **133**(6): 1101-12.

Collignon, J., I. Varlet, et al. (1996). "Relationship between asymmetric nodal expression and the direction of embryonic turning." Nature **381**(6578): 155-8.

Cortes, F., D. Daggett, et al. (2003). "Cadherin-mediated differential cell adhesion controls slow muscle cell migration in the developing zebrafish myotome." Dev Cell **5**(6): 865-76.

Crossley, P. H., G. Minowada, et al. (1996). "Roles for FGF8 in the induction, initiation, and maintenance of chick limb development." Cell **84**(1): 127-36.

Cui, C., C. D. Little, et al. (2009). "Rotation of organizer tissue contributes to left-right asymmetry." Anat Rec (Hoboken) **292**(4): 557-61.

Danos, M. C. and H. J. Yost (1995). "Linkage of cardiac left-right asymmetry and dorsal-anterior development in Xenopus." Development **121**(5): 1467-74.

Darnell, D. K. and G. C. Schoenwolf (2000). "The chick embryo as a model system for analyzing mechanisms of development." Methods Mol Biol **135**: 25-9.

Dathe, V., A. Gamel, et al. (2002). "Morphological left-right asymmetry of Hensen's node precedes the asymmetric expression of Shh and Fgf8 in the chick embryo." Anat Embryol (Berl) **205**(5-6): 343-54.

Davis, N. M., N. A. Kurpios, et al. (2008). "The chirality of gut rotation derives from left-right asymmetric changes in the architecture of the dorsal mesentery." Dev Cell **15**(1): 134-45.

de Campos-Baptista, M. I., N. G. Holtzman, et al. (2008). "Nodal signaling promotes the speed and directional movement of cardiomyocytes in zebrafish." Dev Dyn **237**(12): 3624-33.

Delise, A. M. and R. S. Tuan (2002). "Analysis of N-cadherin function in limb mesenchymal chondrogenesis in vitro." Dev Dyn **225**(2): 195-204.

Derycke, L. D. and M. E. Bracke (2004). "N-cadherin in the spotlight of cell-cell adhesion, differentiation, embryogenesis, invasion and signalling." Int J Dev Biol **48**(5-6): 463-76.

Duboc, V., E. Rottinger, et al. (2005). "Left-right asymmetry in the sea urchin embryo is regulated by nodal signaling on the right side." Dev Cell **9**(1): 147-58.

Esser, A. T., K. C. Smith, et al. (2006). "Mathematical model of morphogen electrophoresis through gap junctions." Dev Dyn **235**(8): 2144-59.

Essner, J. J., J. D. Amack, et al. (2005). "Kupffer's vesicle is a ciliated organ of asymmetry in the zebrafish embryo that initiates left-right development of the brain, heart and gut." Development **132**(6): 1247-60.

Essner, J. J., W. W. Branford, et al. (2000). "Mesendoderm and left-right brain, heart and gut development are differentially regulated by pitx2 isoforms." Development **127**(5): 1081-93.

Essner, J. J., K. J. Vogan, et al. (2002). "Conserved function for embryonic nodal cilia." Nature **418**(6893): 37-8.

Fischer, A., C. Viebahn, et al. (2002). "FGF8 acts as a right determinant during establishment of the left-right axis in the rabbit." Curr Biol **12**(21): 1807-16.

Fliegauf, M., T. Benzing, et al. (2007). "When cilia go bad: cilia defects and ciliopathies." Nat Rev Mol Cell Biol **8**(11): 880-93.

Frankel, J. (1991). "Intracellular handedness in ciliates." Ciba Found Symp **162**: 73-88; discussion 88-93.

Friedl, P. and D. Gilmour (2009). "Collective cell migration in morphogenesis, regeneration and cancer." Nat Rev Mol Cell Biol **10**(7): 445-57.

Friedlander, D. R., R. M. Mege, et al. (1989). "Cell sorting-out is modulated by both the specificity and amount of different cell adhesion molecules (CAMs) expressed on cell surfaces." Proc Natl Acad Sci U S A **86**(18): 7043-7.

Fujimori, T. and M. Takeichi (1993). "Disruption of epithelial cell-cell adhesion by exogenous expression of a mutated nonfunctional N-cadherin." Mol Biol Cell **4**(1): 37-47.

Fujinaga, M. (1997). "Development of sidedness of asymmetric body structures in vertebrates." Int J Dev Biol **41**(2): 153-86.

Fukumoto, T., I. P. Kema, et al. (2005). "Serotonin signaling is a very early step in patterning of the left-right axis in chick and frog embryos." Curr Biol **15**(9): 794-803.

Gage, P. J., H. Suh, et al. (1999). "Dosage requirement of Pitx2 for development of multiple organs." Development **126**(20): 4643-51.

Gajewski, M., D. Sieger, et al. (2003). "Anterior and posterior waves of cyclic her1 gene expression are differentially regulated in the presomitic mesoderm of zebrafish." Development **130**(18): 4269-78.

Galli, L. M., T. Barnes, et al. (2006). "Differential inhibition of Wnt-3a by Sfrp-1, Sfrp-2, and Sfrp-3." Dev Dyn **235**(3): 681-90.

Ganzler-Odenthal, S. I. and C. Redies (1998). "Blocking N-cadherin function disrupts the epithelial structure of differentiating neural tissue in the embryonic chicken brain." J Neurosci **18**(14): 5415-25.

Garcia-Castro, M. I., E. Vielmetter, et al. (2000). "N-Cadherin, a cell adhesion molecule involved in establishment of embryonic left-right asymmetry." Science **288**(5468): 1047-51.

Gartner, A., E. F. Fornasiero, et al. (2012). "N-cadherin specifies first asymmetry in developing neurons." EMBO J **31**(8): 1893-903.

George-Weinstein, M., J. Gerhart, et al. (1997). "N-cadherin promotes the commitment and differentiation of skeletal muscle precursor cells." Dev Biol **185**(1): 14-24.

Gerhart, J., M. Danilchik, et al. (1989). "Cortical rotation of the Xenopus egg: consequences for the anteroposterior pattern of embryonic dorsal development." Development **107 Suppl**: 37-51.

Godt, D. and U. Tepass (1998). "Drosophila oocyte localization is mediated by differential cadherin-based adhesion." Nature **395**(6700): 387-91.

Gonzalez-Reyes, A. and D. St Johnston (1998). "The Drosophila AP axis is polarised by the cadherin-mediated positioning of the oocyte." Development **125**(18): 3635-44.

Gourronc, F., N. Ahmad, et al. (2007). "Nodal activity around Kupffer's vesicle depends on the T-box transcription factors Notail and Spadetail and on Notch signaling." Dev Dyn **236**(8): 2131-46.

Grabowski, C. T. (1957). "The induction of secondary embryos in the early chick blastoderm by grafts of Hensen's node." Am J Anat **101**(1): 101-33.

Granata, A. and N. A. Quaderi (2003). "The Opitz syndrome gene MID1 is essential for establishing asymmetric gene expression in Hensen's node." Dev Biol **258**(2): 397-405.

Granata, A. and N. A. Quaderi (2005). "Asymmetric expression of Gli transcription factors in Hensen's node." Gene Expr Patterns **5**(4): 529-31.

Grande, C. and N. H. Patel (2009). "Nodal signalling is involved in left-right asymmetry in snails." Nature **457**(7232): 1007-11.

Gros, J., K. Feistel, et al. (2009). "Cell movements at Hensen's node establish left/right asymmetric gene expression in the chick." Science **324**(5929): 941-4.

Guioli, S. and R. Lovell-Badge (2007). "PITX2 controls asymmetric gonadal development in both sexes of the chick and can rescue the degeneration of the right ovary." Development **134**(23): 4199-208.

Gumbiner, B., B. Stevenson, et al. (1988). "The role of the cell adhesion molecule uvomorulin in the formation and maintenance of the epithelial junctional complex." J Cell Biol **107**(4): 1575-87.

Gumbiner, B. M. (1992). "Epithelial morphogenesis." Cell **69**(3): 385-7.

Gumbiner, B. M. (2000). "Regulation of cadherin adhesive activity." J Cell Biol **148**(3): 399-404.

Gumbiner, B. M. (2005). "Regulation of cadherin-mediated adhesion in morphogenesis." Nat Rev Mol Cell Biol **6**(8): 622-34.

Hajra, K. M., D. Y. Chen, et al. (2002). "The SLUG zinc-finger protein represses E-cadherin in breast cancer." Cancer Res **62**(6): 1613-8.

Halbleib, J. M. and W. J. Nelson (2006). "Cadherins in development: cell adhesion, sorting, and tissue morphogenesis." Genes Dev **20**(23): 3199-214.

Hamada, H. (2008). "Breakthroughs and future challenges in left-right patterning." Dev Growth Differ **50 Suppl 1**: S71-8.

Hamada, H., C. Meno, et al. (2002). "Establishment of vertebrate left-right asymmetry." Nat Rev Genet **3**(2): 103-13.

Hamburger, V. and H. L. Hamilton (1992). "A series of normal stages in the development of the chick embryo. 1951." Dev Dyn **195**(4): 231-72.

Hanahan, D. (1983). "Studies on transformation of Escherichia coli with plasmids." J Mol Biol **166**(4): 557-80.

Hashimoto, H., M. Rebagliati, et al. (2004). "The Cerberus/Dan-family protein Charon is a negative regulator of Nodal signaling during left-right patterning in zebrafish." Development **131**(8): 1741-53.

Hatler, J. M., J. J. Essner, et al. (2009). "A gap junction connexin is required in the vertebrate left-right organizer." Dev Biol **336**(2): 183-91.

Hatta, K., S. Takagi, et al. (1987). "Spatial and temporal expression pattern of N-cadherin cell adhesion molecules correlated with morphogenetic processes of chicken embryos." Dev Biol **120**(1): 215-27.

Hatta, K., A. Nose, et al. (1988). "Cloning and expression of cDNA encoding a neural calcium-dependent cell adhesion molecule: its identity in the cadherin gene family." J Cell Biol **106**(3): 873-81.
Hatta, K. and M. Takeichi (1986). "Expression of N-cadherin adhesion molecules associated with early morphogenetic events in chick development." Nature **320**(6061): 447-9.

Hatta, K., A. Nose, et al. (1988). "Cloning and expression of cDNA encoding a neural calcium-dependent cell adhesion molecule: its identity in the cadherin gene family." J Cell Biol **106**(3): 873-81.

Henrique, D., J. Adam, et al. (1995). "Expression of a Delta homologue in prospective neurons in the chick." Nature **375**(6534): 787-90.

Hermiston, M. L., M. H. Wong, et al. (1996). "Forced expression of E-cadherin in the mouse intestinal epithelium slows cell migration and provides evidence for nonautonomous regulation of cell fate in a self-renewing system." Genes Dev **10**(8): 985-96.

Hirokawa, N., Y. Tanaka, et al. (2012). "Cilia, KIF3 molecular motor and nodal flow." Curr Opin Cell Biol **24**(1): 31-9.

Hollyday, M., J. A. McMahon, et al. (1995). "Wnt expression patterns in chick embryo nervous system." Mech Dev **52**(1): 9-25.

Hirokawa, N., Y. Tanaka, et al. (2006). "Nodal flow and the generation of left-right asymmetry." Cell **125**(1): 33-45.

Hojo, M., S. Takashima, et al. (2007). "Right-elevated expression of charon is regulated by fluid flow in medaka Kupffer's vesicle." Dev Growth Differ **49**(5): 395-405.

Huber, M. A., N. Kraut, et al. (2005). "Molecular requirements for epithelial-mesenchymal transition during tumor progression." Curr Opin Cell Biol **17**(5): 548-58.

Imai, K. S., M. Levine, et al. (2006). "Regulatory blueprint for a chordate embryo." Science **312**(5777): 1183-7.

Isaac, A., M. G. Sargent, et al. (1997). "Control of vertebrate left-right asymmetry by a snail-related zinc finger gene." Science **275**(5304): 1301-4.

Ishimaru, Y., T. Komatsu, et al. (2008). "Mechanism of asymmetric ovarian development in chick embryos." Development **135**(4): 677-85.

Itoh, K., K. Yoshioka, et al. (1999). "An essential part for Rho-associated kinase in the transcellular invasion of tumor cells." Nat Med **5**(2): 221-5.
Kageyama, R., T. Ohtsuka, et al. (2007). "The Hes gene family: repressors and oscillators that orchestrate embryogenesis." Development **134**(7): 1243-51.

Kageyama, R., T. Ohtsuka, et al. (2008). "Roles of Hes genes in neural development." Dev Growth Differ **50 Suppl 1**: S97-103.

Kashima, T., J. Kawaguchi, et al. (1999). "Anomalous cadherin expression in osteosarcoma. Possible relationships to metastasis and morphogenesis." Am J Pathol **155**(5): 1549-55.

Kashima, T., K. Nakamura, et al. (2003). "Overexpression of cadherins suppresses pulmonary metastasis of osteosarcoma in vivo." Int J Cancer **104**(2): 147-54.

Keller, R. (2002). "Shaping the vertebrate body plan by polarized embryonic cell movements." Science **298**(5600): 1950-4.

Kelly, K. A., Y. Wei, et al. (2002). "Cell death along the embryo midline regulates left-right sidedness." Dev Dyn **224**(2): 238-44.

Khaner, O. (1993). "Axis determination in the avian embryo." Curr Top Dev Biol **28**: 155-80.

Kikuchi, A., S. Kishida, et al. (2006). "Regulation of Wnt signaling by protein-protein interaction and post-translational modifications." Exp Mol Med **38**(1): 1-10.

Kim, J. B., S. Islam, et al. (2000). "N-Cadherin extracellular repeat 4 mediates epithelial to mesenchymal transition and increased motility." J Cell Biol **151**(6): 1193-206.

Kitamura, K., H. Miura, et al. (1999). "Mouse Pitx2 deficiency leads to anomalies of the ventral body wall, heart, extra- and periocular mesoderm and right pulmonary isomerism." Development **126**(24): 5749-58.

Knezevic, V., R. De Santo, et al. (1998). "Continuing organizer function during chick tail development." Development **125**(10): 1791-801.

Kobielak, A. and E. Fuchs (2004). "Alpha-catenin: at the junction of intercellular adhesion and actin dynamics." Nat Rev Mol Cell Biol **5**(8): 614-25.

Krebs, L. T., N. Iwai, et al. (2003). "Notch signaling regulates left-right asymmetry determination by inducing Nodal expression." Genes Dev **17**(10): 1207-12.

Kuroda, R., B. Endo, et al. (2009). "Chiral blastomere arrangement dictates zygotic left-right asymmetry pathway in snails." Nature **462**(7274): 790-4.

Kurpios, N. A., M. Ibanes, et al. (2008). "The direction of gut looping is established by changes in the extracellular matrix and in cell:cell adhesion." Proc Natl Acad Sci U S A **105**(25): 8499-506.

Kurpios, N. A., L. MacNeil, et al. (2009). "The Pea3 Ets transcription factor regulates differentiation of multipotent progenitor cells during mammary gland development." Dev Biol **325**(1): 106-21.

Lai, E. C. (2004). "Notch signaling: control of cell communication and cell fate." Development **131**(5): 965-73.

Le Douarin, N. M. (1974). "Cell recognition based on natural morphological nuclear markers." Med Biol **52**(5): 281-319.

Lemaire, L. and M. Kessel (1997). "Gastrulation and homeobox genes in chick embryos." Mech Dev **67**(1): 3-16.

Lettice, L., J. Hecksher-Sorensen, et al. (2001). "The role of Bapx1 (Nkx3.2) in the development and evolution of the axial skeleton." J Anat **199**(Pt 1-2): 181-7.

Levin, M. (2004). "The embryonic origins of left-right asymmetry." Crit Rev Oral Biol Med **15**(4): 197-206.

Levin, M. (2007). "Gap junctional communication in morphogenesis." Prog Biophys Mol Biol **94**(1-2): 186-206.

Levin, M., R. L. Johnson, et al. (1995). "A molecular pathway determining left-right asymmetry in chick embryogenesis." Cell **82**(5): 803-14.

Levin, M. (1998). "Left-right asymmetry and the chick embryo." Semin Cell Dev Biol **9**(1): 67-76.

Levin, M. and M. Mercola (1998). "Evolutionary conservation of mechanisms upstream of asymmetric Nodal expression: reconciling chick and Xenopus." Dev Genet **23**(3): 185-93.

Levin, M. and M. Mercola (1998). "Gap junctions are involved in the early generation of left-right asymmetry." Dev Biol **203**(1): 90-105.

Levin, M. and N. Nascone (1997). "Two molecular models of initial left-right asymmetry generation." Med Hypotheses **49**(5): 429-35.

Levin, M., S. Pagan, et al. (1997). "Left/right patterning signals and the independent regulation of different aspects of situs in the chick embryo." Dev Biol **189**(1): 57-67.

Levin, M. (2005). "Left-right asymmetry in embryonic development: a comprehensive review." Mech Dev **122**(1): 3-25.
Levin, M. and A. R. Palmer (2007). "Left-right patterning from the inside out: widespread evidence for intracellular control." Bioessays **29**(3): 271-87.

Levin, M., T. Thorlin, et al. (2002). "Asymmetries in H+/K+-ATPase and cell membrane potentials comprise a very early step in left-right patterning." Cell **111**(1): 77-89.

Li, G. and M. Herlyn (2000). "Dynamics of intercellular communication during melanoma development." Mol Med Today **6**(4): 163-9.

Linask, K. K. (1992). "N-cadherin localization in early heart development and polar expression of Na+,K(+)-ATPase, and integrin during pericardial coelom formation and epithelialization of the differentiating myocardium." Dev Biol **151**(1): 213-24.

Linask, K. K., K. A. Knudsen, et al. (1997). "N-cadherin-catenin interaction: necessary component of cardiac cell compartmentalization during early vertebrate heart development." Dev Biol **185**(2): 148-64.

Linask, K. K. and J. W. Lash (1993). "Early heart development: dynamics of endocardial cell sorting suggests a common origin with cardiomyocytes." Dev Dyn **196**(1): 62-9.

Logan, M., S. M. Pagan-Westphal, et al. (1998). "The transcription factor Pitx2 mediates situs-specific morphogenesis in response to left-right asymmetric signals." Cell **94**(3): 307-17.

Lohr, J. L., M. C. Danos, et al. (1997). "Left-right asymmetry of a nodal-related gene is regulated by dorsoanterior midline structures during Xenopus development." Development **124**(8): 1465-72.

Lopes, S. S., R. Lourenco, et al. (2010). "Notch signalling regulates left-right asymmetry through ciliary length control." Development **137**(21): 3625-32.

Lourenço, R. and L. Saúde (2010). "Symmetry OUT, Asymmetry IN." Symmetry **2**(2): 1033-1054.
Lowe, L. A., D. M. Supp, et al. (1996). "Conserved left-right asymmetry of nodal expression and alterations in murine situs inversus." Nature **381**(6578): 158-61.

Lyuksyutova, A. I., C. C. Lu, et al. (2003). "Anterior-posterior guidance of commissural axons by Wnt-frizzled signaling." Science **302**(5652): 1984-8.

Makrigiannakis, A., G. Coukos, et al. (1999). "N-cadherin-mediated human granulosa cell adhesion prevents apoptosis: a role in follicular atresia and luteolysis?" Am J Pathol **154**(5): 1391-406.

Manner, J. (2001). "Does an equivalent of the "ventral node" exist in chick embryos? A scanning electron microscopic study." Anat Embryol (Berl) **203**(6): 481-90.

Marin, F. and M. A. Nieto (2004). "Expression of chicken slug and snail in mesenchymal components of the developing central nervous system." Dev Dyn **230**(1): 144-8.

Marjoram, L. and C. Wright (2011). "Rapid differential transport of Nodal and Lefty on sulfated proteoglycan-rich extracellular matrix regulates left-right asymmetry in Xenopus." Development **138**(3): 475-85.

Maroto, M., R. A. Bone, et al. (2012). "Somitogenesis." Development **139**(14): 2453-6.

Matsunaga, M., K. Hatta, et al. (1988). "Role of N-cadherin cell adhesion molecules in the histogenesis of neural retina." Neuron **1**(4): 289-95.

Matsunami, H. and M. Takeichi (1995). "Fetal brain subdivisions defined by R- and E-cadherin expressions: evidence for the role of cadherin activity in region-specific, cell-cell adhesion." Dev Biol **172**(2): 466-78.

McKay, M. M. and D. K. Morrison (2007). "Integrating signals from RTKs to ERK/MAPK." Oncogene **26**(22): 3113-21.

Meno, C., Y. Saijoh, et al. (1996). "Left-right asymmetric expression of the TGF beta-family member lefty in mouse embryos." Nature **381**(6578): 151-5.

Meno, C., A. Shimono, et al. (1998). "lefty-1 is required for left-right determination as a regulator of lefty-2 and nodal." Cell **94**(3): 287-97.

Meno, C., J. Takeuchi, et al. (2001). "Diffusion of nodal signaling activity in the absence of the feedback inhibitor Lefty2." Dev Cell **1**(1): 127-38.

Mercola, M. and M. Levin (2001). "Left-right asymmetry determination in vertebrates." Annu Rev Cell Dev Biol **17**: 779-805.

Mittwoch, U. (1998). "Phenotypic manifestations during the development of the dominant and default gonads in mammals and birds." J Exp Zool **281**(5): 466-71.

Mohammadi, M., G. McMahon, et al. (1997). "Structures of the tyrosine kinase domain of fibroblast growth factor receptor in complex with inhibitors." Science **276**(5314): 955-60.

Monier-Gavelle, F. and J. L. Duband (1995). "Control of N-cadherin-mediated intercellular adhesion in migrating neural crest cells in vitro." J Cell Sci **108 (Pt 12)**: 3839-53.

Monsoro-Burq, A. and N. Le Douarin (2000). "Left-right asymmetry in BMP4 signalling pathway during chick gastrulation." Mech Dev **97**(1-2): 105-8.

Montell, D. J. (2003). "Border-cell migration: the race is on." Nat Rev Mol Cell Biol **4**(1): 13-24.

Morokuma, J., M. Ueno, et al. (2002). "HrNodal, the ascidian nodal-related gene, is expressed in the left side of the epidermis, and lies upstream of HrPitx." Dev Genes Evol **212**(9): 439-46.

Murai, K., A. E. Vernon, et al. (2007). "Hes6 is required for MyoD induction during gastrulation." Dev Biol **312**(1): 61-76.

Murray, S. A. and T. Gridley (2006). "Snail family genes are required for left-right asymmetry determination, but not neural crest formation, in mice." Proc Natl Acad Sci U S A **103**(27): 10300-4.

Nagafuchi, A. and M. Takeichi (1989). "Transmembrane control of cadherin-mediated cell adhesion: a 94 kDa protein functionally associated with a specific region of the cytoplasmic domain of E-cadherin." Cell Regul **1**(1): 37-44.

Nakagawa, S. and M. Takeichi (1997). "N-cadherin is crucial for heart formation in the chick embryo." Dev Growth Differ **39**(4): 451-5.

Nakagawa, S. and M. Takeichi (1998). "Neural crest emigration from the neural tube depends on regulated cadherin expression." Development **125**(15): 2963-71.

Nakamura, T., N. Mine, et al. (2006). "Generation of robust left-right asymmetry in the mouse embryo requires a self-enhancement and lateral-inhibition system." Dev Cell **11**(4): 495-504.

Nakaya, Y., E. W. Sukowati, et al. (2008). "RhoA and microtubule dynamics control cell-basement membrane interaction in EMT during gastrulation." Nat Cell Biol **10**(7): 765-75.

Nieman, M. T., R. S. Prudoff, et al. (1999). "N-cadherin promotes motility in human breast cancer cells regardless of their E-cadherin expression." J Cell Biol **147**(3): 631-44.

Niessen, C. M., D. Leckband, et al. (2011). "Tissue organization by cadherin adhesion molecules: dynamic molecular and cellular mechanisms of morphogenetic regulation." Physiol Rev **91**(2): 691-731.

Ninomiya, H., R. David, et al. (2012). "Cadherin-dependent differential cell adhesion in Xenopus causes cell sorting in vitro but not in the embryo." J Cell Sci **125**(Pt 8): 1877-83.

Nonaka, S., H. Shiratori, et al. (2002). "Determination of left-right patterning of the mouse embryo by artificial nodal flow." Nature **418**(6893): 96-9.

Nonaka, S., Y. Tanaka, et al. (1998). "Randomization of left-right asymmetry due to loss of nodal cilia generating leftward flow of extraembryonic fluid in mice lacking KIF3B motor protein." Cell **95**(6): 829-37.

Nuessle, J. M., K. Giehl, et al. (2011). "TGFbeta1 suppresses vascular smooth muscle cell motility by expression of N-cadherin." Biol Chem **392**(5): 461-74.

Ohuchi, H., S. Kimura, et al. (2000). "Involvement of fibroblast growth factor (FGF)18-FGF8 signaling in specification of left-right asymmetry and brain and limb development of the chick embryo." Mech Dev **95**(1-2): 55-66.

Okada, Y., S. Nonaka, et al. (1999). "Abnormal nodal flow precedes situs inversus in iv and inv mice." Mol Cell **4**(4): 459-68.

Ong, L. L., N. Kim, et al. (1998). "Trabecular myocytes of the embryonic heart require N-cadherin for migratory unit identity." Dev Biol **193**(1): 1-9.

Pagan-Westphal, S. M. and C. J. Tabin (1998). "The transfer of left-right positional information during chick embryogenesis." Cell **93**(1): 25-35.

Patel, I. S., P. Madan, et al. (2003). "Cadherin switching in ovarian cancer progression." Int J Cancer **106**(2): 172-7.

Patel, K., A. Isaac, et al. (1999). "Nodal signalling and the roles of the transcription factors SnR and Pitx2 in vertebrate left-right asymmetry." Curr Biol **9**(11): 609-12.

Petzoldt, A. G., J. B. Coutelis, et al. (2012). "DE-Cadherin regulates unconventional Myosin ID and Myosin IC in Drosophila left-right asymmetry establishment." Development **139**(10): 1874-84.

Piedra, M. E. and M. A. Ros (2002). "BMP signaling positively regulates Nodal expression during left right specification in the chick embryo." Development **129**(14): 3431-40.

Plageman, T. F., Jr., A. L. Zacharias, et al. (2011). "Shroom3 and a Pitx2-N-cadherin pathway function cooperatively to generate asymmetric cell shape changes during gut morphogenesis." Dev Biol **357**(1): 227-34.

Potthoff, S., F. Entschladen, et al. (2007). "N-cadherin engagement provides a dominant stop signal for the migration of MDA-MB-468 breast carcinoma cells." Breast Cancer Res Treat **105**(3): 287-95.

Psychoyos, D. and C. D. Stern (1996). "Restoration of the organizer after radical ablation of Hensen's node and the anterior primitive streak in the chick embryo." Development **122**(10): 3263-73.

Psychoyos, D. and C. D. Stern (1996). "Fates and migratory routes of primitive streak cells in the chick embryo." Development **122**(5): 1523-34.

Qiu, D., S. M. Cheng, et al. (2005). "Localization and loss-of-function implicates ciliary proteins in early, cytoplasmic roles in left-right asymmetry." Dev Dyn **234**(1): 176-89.

Rand, M. D., A. Lindblom, et al. (1997). "Calcium binding to tandem repeats of EGF-like modules. Expression and characterization of the EGF-like modules of human Notch-1 implicated in receptor-ligand interactions." Protein Sci **6**(10): 2059-71.

Rao, Z., P. Handford, et al. (1995). "The structure of a Ca(2+)-binding epidermal growth factor-like domain: its role in protein-protein interactions." Cell **82**(1): 131-41.

Raya, A. and J. C. Izpisua Belmonte (2006). "Left-right asymmetry in the vertebrate embryo: from early information to higher-level integration." Nat Rev Genet **7**(4): 283-93.

Raya, A., Y. Kawakami, et al. (2003). "Notch activity induces Nodal expression and mediates the establishment of left-right asymmetry in vertebrate embryos." Genes Dev **17**(10): 1213-8.

Raya, A., Y. Kawakami, et al. (2004). "Notch activity acts as a sensor for extracellular calcium during vertebrate left-right determination." Nature **427**(6970): 121-8.

Rebagliati, M. R., R. Toyama, et al. (1998). "Zebrafish nodal-related genes are implicated in axial patterning and establishing left-right asymmetry." Dev Biol **199**(2): 261-72.

Rembold, M., F. Loosli, et al. (2006). "Individual cell migration serves as the driving force for optic vesicle evagination." Science **313**(5790): 1130-4.

Riddle, R. D., R. L. Johnson, et al. (1993). Sonic hedgehog mediates the polarizing activity of the ZPA. Cell. **75:** 1401-16.

Rimm, D. L., E. R. Koslov, et al. (1995). "Alpha 1(E)-catenin is an actin-binding and -bundling protein mediating the attachment of F-actin to the membrane adhesion complex." Proc Natl Acad Sci U S A **92**(19): 8813-7.

Rodemer, E. S., A. Ihmer, et al. (1986). "Gonadal development of the chick embryo following microsurgically caused agenesis of the mesonephros and using interspecific quail-chick chimaeras." J Embryol Exp Morphol **98**: 269-85.

Rodriguez Esteban, C., J. Capdevila, et al. (1999). "The novel Cer-like protein Caronte mediates the establishment of embryonic left-right asymmetry." Nature **401**(6750): 243-51.

Rodriguez-Leon, J., C. Rodriguez Esteban, et al. (2008). "Pitx2 regulates gonad morphogenesis." Proc Natl Acad Sci U S A **105**(32): 11242-7.

Rohr, S., C. Otten, et al. (2008). "Asymmetric involution of the myocardial field drives heart tube formation in zebrafish." Circ Res **102**(2): e12-9.

Rosenquist, G. C. (1972). "Endoderm movements in the chick embryo between the early short streak and head process stages." J Exp Zool **180**(1): 95-103.

Rosenquist, G. C. (1983). "The chorda center in Hensen's node of the chick embryo." Anat Rec **207**(2): 349-55.

Ryan, A. K., B. Blumberg, et al. (1998). "Pitx2 determines left-right asymmetry of internal organs in vertebrates." Nature **394**(6693): 545-51.

Saijoh, Y., S. Oki, et al. (2003). "Left-right patterning of the mouse lateral plate requires nodal produced in the node." Dev Biol **256**(1): 160-72.

Sakano, D., A. Kato, et al. (2010). "BCL6 canalizes Notch-dependent transcription, excluding Mastermind-like1 from selected target genes during left-right patterning." Dev Cell **18**(3): 450-62.

Sanders, E. J., M. K. Khare, et al. (1986). "An experimental and morphological analysis of the tail bud mesenchyme of the chick embryo." Anat Embryol (Berl) **174**(2): 179-85.

Sanders, E. J., M. Varedi, et al. (1993). "Cell proliferation in the gastrulating chick embryo: a study using BrdU incorporation and PCNA localization." Development **118**(2): 389-99.

Sarmah, B., A. J. Latimer, et al. (2005). "Inositol polyphosphates regulate zebrafish left-right asymmetry." Dev Cell **9**(1): 133-45.

Sato, T., M. Takahoko, et al. (2006). "HuC:Kaede, a useful tool to label neural morphologies in networks in vivo." Genesis **44**(3): 136-42.

Sauka-Spengler, T. and M. Bronner-Fraser (2008). "A gene regulatory network orchestrates neural crest formation." Nat Rev Mol Cell Biol **9**(7): 557-68.

Sausedo, R. A. and G. C. Schoenwolf (1993). "Cell behaviors underlying notochord formation and extension in avian embryos: quantitative and immunocytochemical studies." Anat Rec **237**(1): 58-70.

Schmitt, A. M., J. Shi, et al. (2006). "Wnt-Ryk signalling mediates medial-lateral retinotectal topographic mapping." Nature **439**(7072): 31-7.

Schlange, T., H. H. Arnold, et al. (2002). "BMP2 is a positive regulator of Nodal signaling during left-right axis formation in the chicken embryo." Development **129**(14): 3421-9.

Schlueter, J. and T. Brand (2007). "Left-right axis development: examples of similar and divergent strategies to generate asymmetric morphogenesis in chick and mouse embryos." Cytogenet Genome Res **117**(1-4): 256-67.

Schneider, A., T. Mijalski, et al. (1999). "The homeobox gene NKX3.2 is a target of left-right signalling and is expressed on opposite sides in chick and mouse embryos." Curr Biol **9**(16): 911-4.

Schoenwolf, G. C. and I. S. Alvarez (1989). "Roles of neuroepithelial cell rearrangement and division in shaping of the avian neural plate." Development **106**(3): 427-39.

Schweickert, A., M. Campione, et al. (2000). "Pitx2 isoforms: involvement of Pitx2c but not Pitx2a or Pitx2b in vertebrate left-right asymmetry." Mech Dev **90**(1): 41-51.

Sefton, M., S. Sanchez, et al. (1998). "Conserved and divergent roles for members of the Snail family of transcription factors in the chick and mouse embryo." Development **125**(16): 3111-21.

Selleck, M. A. and C. D. Stern (1991). "Fate mapping and cell lineage analysis of Hensen's node in the chick embryo." Development **112**(2): 615-26.

Shamim, H. and I. Mason (1999). "Expression of Fgf4 during early development of the chick embryo." Mech Dev **85**(1-2): 189-92.

Shimeld, S. M. and M. Levin (2006). "Evidence for the regulation of left-right asymmetry in Ciona intestinalis by ion flux." Dev Dyn **235**(6): 1543-53.

Shiratori, H., R. Sakuma, et al. (2001). "Two-step regulation of left-right asymmetric expression of Pitx2: initiation by nodal signaling and maintenance by Nkx2." Mol Cell **7**(1): 137-49.

Shiratori, H., K. Yashiro, et al. (2006). "Conserved regulation and role of Pitx2 in situs-specific morphogenesis of visceral organs." Development **133**(15): 3015-25.

Shoval, I., A. Ludwig, et al. (2007). "Antagonistic roles of full-length N-cadherin and its soluble BMP cleavage product in neural crest delamination." Development **134**(3): 491-501.

Skaper, S. D., S. E. Moore, et al. (2001). "Cell signalling cascades regulating neuronal growth-promoting and inhibitory cues." Prog Neurobiol **65**(6): 593-608.

Skromne, I. and C. D. Stern (2001). "Interactions between Wnt and Vg1 signalling pathways initiate primitive streak formation in the chick embryo." Development **128**(15): 2915-27.

Solnica-Krezel, L. (2005). "Conserved patterns of cell movements during vertebrate gastrulation." Curr Biol **15**(6): R213-28.

Song, H., J. Hu, et al. (2010). "Planar cell polarity breaks bilateral symmetry by controlling ciliary positioning." Nature **466**(7304): 378-82.

Spratt, N. T., Jr. (1958). "Analysis of the organizer center in the early chick embryo. IV. Some differential enzyme activities of node center cells." J Exp Zool **138**(1): 51-79.

Steinberg, M. S. and M. Takeichi (1994). "Experimental specification of cell sorting, tissue spreading, and specific spatial patterning by quantitative differences in cadherin expression." Proc Natl Acad Sci U S A **91**(1): 206-9.

Stemmler, M., A. Beelmann, et al. (2007). "Improving parenting practices in order to prevent child behavior problems: a study on parent training as part of the EFFEKT program." Int J Hyg Environ Health **210**(5): 563-70.

Stemple, D. L. (2005). "Structure and function of the notochord: an essential organ for chordate development." Development **132**(11): 2503-12.

Stern, C. D. (2004). "The chick embryo--past, present and future as a model system in developmental biology." Mech Dev **121**(9): 1011-3.

Sulik, K., D. B. Dehart, et al. (1994). "Morphogenesis of the murine node and notochordal plate." Dev Dyn **201**(3): 260-78.

Sutherland, M. J. and S. M. Ware (2009). "Disorders of left-right asymmetry: heterotaxy and situs inversus." Am J Med Genet C Semin Med Genet **151C**(4): 307-17.

Sweetman, D., L. Wagstaff, et al. (2008). "The migration of paraxial and lateral plate mesoderm cells emerging from the late primitive streak is controlled by different Wnt signals." BMC Dev Biol **8**: 63.

Takeichi, M. (1988). "The cadherins: cell-cell adhesion molecules controlling animal morphogenesis." Development **102**(4): 639-55.

Takeichi, M. (1995). "Morphogenetic roles of classic cadherins." Curr Opin Cell Biol **7**(5): 619-27.

Takeuchi, J. K., H. Lickert, et al. (2007). "Baf60c is a nuclear Notch signaling component required for the establishment of left-right asymmetry." Proc Natl Acad Sci U S A **104**(3): 846-51.

Tanaka, H., W. Shan, et al. (2000). "Molecular modification of N-cadherin in response to synaptic activity." Neuron **25**(1): 93-107.

Tanaka, Y., Y. Okada, et al. (2005). "FGF-induced vesicular release of Sonic hedgehog and retinoic acid in leftward nodal flow is critical for left-right determination." Nature **435**(7039): 172-7.

Tavares, A. T., S. Andrade, et al. (2007). "Cerberus is a feedback inhibitor of Nodal asymmetric signaling in the chick embryo." Development **134**(11): 2051-60.

Tepass, U., D. Godt, et al. (2002). "Cell sorting in animal development: signalling and adhesive mechanisms in the formation of tissue boundaries." Curr Opin Genet Dev **12**(5): 572-82.

Thiery, J. P. (2002). "Epithelial-mesenchymal transitions in tumour progression." Nat Rev Cancer **2**(6): 442-54.

Tomita, K., A. van Bokhoven, et al. (2000). "Cadherin switching in human prostate cancer progression." Cancer Res **60**(13): 3650-4.

Townes, P. L. and J. Holtfreter (1955). "Directed movements and selective adhesion of embryonic amphibian cells." Journal of Experimental Zoology **128**(1): 53-120.

Troyanovsky, S. (2005). "Cadherin dimers in cell-cell adhesion." Eur J Cell Biol **84**(2-3): 225-33.

Tsikolia, N., S. Schroder, et al. (2012). "Paraxial left-sided nodal expression and the start of left-right patterning in the early chick embryo." Differentiation **84**(5): 380-91.

Tsung, S. D., I. L. Ning, et al. (1965). "[Studies on the Inductive Action of the Hensen's Node Following Its Transplantation in Ovo to the Early Chick

Blastoderm. Ii. Regionally Specific Induction of the Node Region of Different Ages]." Shi Yan Sheng Wu Xue Bao **10**: 69-83.

Uehata, M., T. Ishizaki, et al. (1997). "Calcium sensitization of smooth muscle mediated by a Rho-associated protein kinase in hypertension." Nature **389**(6654): 990-4.

Utton, M. A., B. Eickholt, et al. (2001). "Soluble N-cadherin stimulates fibroblast growth factor receptor dependent neurite outgrowth and N-cadherin and the fibroblast growth factor receptor co-cluster in cells." J Neurochem **76**(5): 1421-30.

Vasiev, B., A. Balter, et al. (2010). "Modeling gastrulation in the chick embryo: formation of the primitive streak." PLoS One **5**(5): e10571.

Vilas-Boas, F. and D. Henrique (2010). "HES6-1 and HES6-2 function through different mechanisms during neuronal differentiation." PLoS One **5**(12): e15459.

Vleminckx, K., L. Vakaet, Jr., et al. (1991). "Genetic manipulation of E-cadherin expression by epithelial tumor cells reveals an invasion suppressor role." Cell **66**(1): 107-19.

Wang, G., A. B. Cadwallader, et al. (2011). "The Rho kinase Rock2b establishes anteroposterior asymmetry of the ciliated Kupffer's vesicle in zebrafish." Development **138**(1): 45-54.

Wang, Y. and J. Nathans (2007). "Tissue/planar cell polarity in vertebrates: new insights and new questions." Development **134**(4): 647-58.

Warga, R. M. and D. A. Kane (2007). "A role for N-cadherin in mesodermal morphogenesis during gastrulation." Dev Biol **310**(2): 211-25.

Wheelock, M. J., Y. Shintani, et al. (2008). "Cadherin switching." J Cell Sci **121**(Pt 6): 727-35.

Williams, E. J., G. Williams, et al. (2001). "Identification of an N-cadherin motif that can interact with the fibroblast growth factor receptor and is required for axonal growth." J Biol Chem **276**(47): 43879-86.

Williams, G., E. J. Williams, et al. (2002). "Dimeric versions of two short N-cadherin binding motifs (HAVDI and INPISG) function as N-cadherin agonists." J Biol Chem **277**(6): 4361-7.

Wolszon, L. R., V. Rehder, et al. (1994). "Calcium wave fronts that cross gap junctions may signal neuronal death during development." J Neurosci **14**(6): 3437-48.

Xiao, K., R. G. Oas, et al. (2007). "Role of p120-catenin in cadherin trafficking." Biochim Biophys Acta **1773**(1): 8-16.

Yajima, H., S. Yoneitamura, et al. (1999). "Role of N-cadherin in the sorting-out of mesenchymal cells and in the positional identity along the proximodistal axis of the chick limb bud." Dev Dyn **216**(3): 274-84.

Yamamoto, M., N. Mine, et al. (2003). "Nodal signaling induces the midline barrier by activating Nodal expression in the lateral plate." Development **130**(9): 1795-804.

Yang, X., D. Dormann, et al. (2002). "Cell movement patterns during gastrulation in the chick are controlled by positive and negative chemotaxis mediated by FGF4 and FGF8." Dev Cell **3**(3): 425-37.

Yap, A. S., W. M. Brieher, et al. (1997). "Molecular and functional analysis of cadherin-based adherens junctions." Annu Rev Cell Dev Biol **13**: 119-46.

Yin, Y., F. Bangs, et al. (2009). "The Talpid3 gene (KIAA0586) encodes a centrosomal protein that is essential for primary cilia formation." Development **136**(4): 655-64.

Yokouchi, Y., K. J. Vogan, et al. (1999). "Antagonistic signaling by Caronte, a novel Cerberus-related gene, establishes left-right asymmetric gene expression." Cell **98**(5): 573-83.

Yoshioka, H., C. Meno, et al. (1998). "Pitx2, a bicoid-type homeobox gene, is involved in a lefty-signaling pathway in determination of left-right asymmetry." Cell **94**(3): 299-305.

Yoshikawa, S., R. D. McKinnon, et al. (2003). "Wnt-mediated axon guidance via the Drosophila Derailed receptor." Nature **422**(6932): 583-8.

Yost, H. J. (1991). "Development of the left-right axis in amphibians." Ciba Found Symp **162**: 165-76; discussion 176-81.

Yuan, S. and G. C. Schoenwolf (1998). "De novo induction of the organizer and formation of the primitive streak in an experimental model of notochord reconstitution in avian embryos." Development **125**(2): 201-13.

Yue, Q., L. Wagstaff, et al. (2008). "Wnt3a-mediated chemorepulsion controls movement patterns of cardiac progenitors and requires RhoA function." Development **135**(6): 1029-37.

Zhang, Y. and M. Levin (2009). "Left-right asymmetry in the chick embryo requires core planar cell polarity protein Vangl2." Genesis **47**(11): 719-28.

Zhu, L., M. J. Marvin, et al. (1999). "Cerberus regulates left-right asymmetry of the embryonic head and heart." Curr Biol **9**(17): 931-8.

Zile, M. H., I. Kostetskii, et al. (2000). "Retinoid signaling is required to complete the vertebrate cardiac left/right asymmetry pathway." Dev Biol **223**(2): 323-38.